UNIVERSITÄT KOBLENZ · LANDAU

unikorn AG Rechnernetze

HOCHSCHULE KOBLENZ UNIVERSITY OF APPLIED SCIENCES

Wireless communication on the factory floor supporting agile production

by
Eike Lyczkowski

Approved Dissertation thesis for the partial fulfilment of the requirements for a Doctor of Natural Sciences (Dr. rer. nat.)
Fachbereich 4: Informatik
University of Koblenz-Landau

Chair of PhD Board:	Prof. Dr. Ralf Lämmel, University of Koblenz
Chair of PhD Commission:	Prof. Dr. Susan Williams, University of Koblenz
Examiner and Supervisor:	Prof. Dr. Hannes Frey, University of Koblenz
Examiner and Supervisor:	Prof. Dr. Wolfgang Kiess, University of Applied Sciences Koblenz

Date of the doctoral viva: 14.09.2023

Abstract

The trends of industry 4.0 and the further enhancements toward an ever changing factory lead to more mobility and flexibility on the factory floor. With that higher need of mobility and flexibility the requirements on wireless communication rise. A key requirement in that setting is the demand for wireless Ultra-Reliability and Low Latency Communication (URLLC). Example use cases therefore are cooperative Automated Guided Vehicles (AGVs) and mobile robotics in general.
Working along that setting this thesis provides insights regarding the whole network stack. Thereby, the focus is always on industrial applications. Starting on the physical layer, extensive measurements from $2\,\mathrm{GHz}$ to $6\,\mathrm{GHz}$ on the factory floor are performed. The raw data is published and analyzed. Based on that data an improved Saleh-Valenzuela (SV) model is provided. As ad-hoc networks are highly depended on node mobility, the mobility of AGVs is modeled. Additionally, Nodal Encounter Patterns (NEPs) are recorded and analyzed. A method to record NEP is illustrated.
The performance by means of latency and reliability are key parameters from an application perspective. Thus, measurements of those two parameters in factory environments are performed using Wireless Local Area Network (WLAN) (IEEE 802.11n), private Long Term Evolution (pLTE) and 5G. This showed auto-correlated latency values. Hence, a method to construct confidence intervals based on auto-correlated data containing rare events is developed.
Subsequently, four performance improvements for wireless networks on the factory floor are proposed. Of those optimization three cover ad-hoc networks, two deal with safety relevant communication, one orchestrates the usage of two orthogonal networks and lastly one optimizes the usage of information within cellular networks.
Finally, this thesis is concluded by an outlook toward open research questions. This includes open questions remaining in the context of industry 4.0 and further the ones around 6G. Along the research topics of 6G the two most relevant topics concern the ideas of a network of networks and overcoming best-effort IP.

Kurzfassung

Die Entwicklungen im Fabrikumfeld gehen über Industrie 4.0 weiter in Richtung der laufend wandelbaren Fabrik. In dieser Entwicklung steigt die Mobilität und Autonomie der einzelnen Teilnehmer und dadurch die Anforderungen an die drahtlose Kommunikation. Entscheidend ist dabei die Anforderung nach hoch-verlässlicher Kommunikation mit geringer Latenz, die Anwendungsfälle wie kooperative fahrerlose Transportsysteme (FTS) oder mobile Robotik im Allgemeinen stellen.
Um dieser Entwicklung zu begegnen, befasst sich diese Arbeit mit Themen entlang des gesamten Netzwerkstacks. Dabei liegt der Fokus immer auf einer industriellen Umgebung. Unten im ISO/OSI Referenzmodell beginnend, werden daher die Ausbreitungsbedingungen von Funkkanälen im Bereich zwischen $2\,\mathrm{GHz}$ und $6\,\mathrm{GHz}$ untersucht. Da Netze auch von der Mobilität ihrer Teilnehmer abhängen wird die Mobilität von FTS untersucht und modelliert. Neben der reinen Mobilität wird auch die gegenseitige Sichtbarkeit von Teilnehmern in ad-hoc Netzen betrachtet. Hierfür werden diese Sichtbarkeiten aufgezeichnet, analysiert und die Rohdaten sowie die Aufzeichnungsmethodik dargelegt.
Da die Leistungsfähigkeit von Netzen für die Parameter Latenz und Verlässlichkeit aus Sicht der Anwendungfälle relevante Eigenschaften darstellen, werden die Leistungsfähigkeit von WLAN (IEEE 802.11n), privatem LTE und 5G im Fabrikumfeld emprische evaluiert. Da die Latenzen in diesen Messungen autokorreliert sind, wurde eine Methode entwicklet, um Konfidenzintervall bei autokorrelierten Daten, die seltene Ereignisse enthalten, konstruieren zu können.
Schließlich finden sich in dieser Arbeit noch vier Möglichkeiten die Leistungsfähigkeit von drahtlosen Netzen in der Produktion zu optimieren. Dabei enthalten sind drei Optimierungen für ad-hoc Netze, zwei befassen sich mit sicherheitsrelevanter Kommunikation, eine befasst mit der zeitgleichen Nutzung unterschiedlicher Netze und eine befasst sich mit der effizienten Nutzung von Informationen aus Zellfunknetzen.
Die Arbeit schließt mit einem Ausblick auf offene Forschungsfragen. Das beinhaltetdie drahtlose Kommunikation in Industrie 4.0 Szenarien und auch 6G. Bei 6G sind aus Sicht industrieller Anwendungen vor Allem die Punkte vollständig deterministischer Kommunikation und einem Netze der Netze relevant.

Acknowledgments

During the time of my doctorate, I am indebted to people who encouraged, supported and guided me on my way to this thesis. I would like to thank those people.
Firstly, I would like to thank my supervisors Wolfgang Kiess and Hannes Frey. Wolfgang Kiess especially for already defining the collaboration between him and my employer SEW-EURODRIVE and the opportunity to participate in his working group and further to provide close supervision throughout the entire time. Getting feedback on research work that all other co-authors always loved for its details and insights is of highest value. Hannes Frey for the openness to supervise this thesis although I already started working, another professor already being involved and me being employed by a company and for all the insights provided. Cooperation between three institutions is supposed to be challenging but worked perfectly smooth thanks to all participants.
At SEW-EURODRIVE I want to thank my present and past associates. Especially, Christian Sauer for always having the time to discuss any question that came up and the research work we did together. Further, my colleagues Frank, Thomas, Robin, Max, Yannick, Michael and Zhidong. I am glad to have worked with excellent students who co-authored some papers. Thanks to Nils Brödner, Konrad Junkes, Felix Reichert and Tobias Weber. Of course, I want to thanks SEW-EURODRIVE for providing an environment that enabled this work.
Further, I want to thank Yudhistir Ramjatan for proofreading many papers and this thesis in particular and thereby providing the views of a native speaker.
Finally, thanks to my wife Caro for providing support and encouragement throughout this journey. Especially for doing so during the lasts month of writing while being on the way of bringing our son into this world.

Contents

List of Figures

List of Tables

List of Abbreviations

3GPP 3rd Generation Partnership Project
ABG Alpha Beta Gamma (model)
ACK Acknowledge
AF Application Function
AGV Automated Guided Vehicle
AMF Access and Mobility Management Function
AODV Ad hoc On-Demand Distance Vector Routing
AP Access Point
APDP Average Power Delay Profile
API Application Programming Interface
AQOR ad-hoc QoS on demand routing
AR Augmented Reality
AUSF Authentication Server Function
BS Base Station
BER Bit Error Rate
BLER Block Error Rate
CA Carrier Aggregation
CCDF Complementary Cumulative Distribution Function
CHEN Chen-Heinzelman protocol
CI Close-in
CP Control Plane
CSI Channel State Information
CDF Cumulative Distribution Function
CQI Channel Quality Indicator
CRC Cyclic Redundancy Check
DC Dual Connectivity
DN Data Network
DTN Delay Tolerant Network
DSR Dynamic Source Routing
eMBB enhanced Mobile Broadband
EPC Evolved Packet Core
FA Forward Algorithm
FBNM Flooding-based Network Monitoring
FDD Frequency Division Duplex
HARQ Hybrid Automatic Repeat reQuest
HMI Human Machine Interface
IoT Internet of Things
IP Internet Protocol
ISM Industrial Scientific and Medical
KPI Key Performance Indicator
LAN Local Area Network

LDPC Low-Density Parity-Check
LED Light Emitting Diode
LLC-PF Low-Latency Communications Proportional Fair
LOS Line-of-Sight
LRC Low Range Communication
LRE Limited Relative Error
LTE Long Term Evolution
MBB Moving Block Bootstrapping
MCS Modulation and Coding Scheme
MEC Mobile Edge Computing
MES Manufacturing Execution System
MIMO Multiple Input Multiple Output
MMIMO Massive Multiple Input Multiple Output
MQTT Message Queuing Telemetry Transport
MANET Mobile Ad-hoc NETwork
MSN Mobile Sensor Network
MPC Multi-Path Component
mMTC massive Machine-Type Communication
NACK Negative Acknowledge
NEF Network Exposure Function
NFC Near Field Communication
NFV Network Function Virtualization
NLOS non Line-of-Sight
NPN Non-Public-Network
NRF Network Repository Function
NSSF Network Slice Selection Function
NTP Network Time Protocol
NEP Nodal Encounter Pattern
NGMN Next Generation Mobile Networks Alliance
NR New Radio
PCF Policy Control Function
pLTE private Long Term Evolution
PD Packet Duplication
PER Packet Error Rate
PEPF Pre-emptive Proportional Fair
P2P Peer-to-Peer
PC Production Cell
PD Packet Duplication
PDP Power-Delay-Profile
PDF Probability Density Function
PoC Proof-of-Concept
OFDMA Orthogonal Frequency Division Multiple Access
QoS Quality of Service

RAN Radio Access Network
RAT Radio Access Technology
RMSE Root Mean Squared Error
RWPM Random Way-Point Model
RRC Radio Ressource Control
RS Reference Signal
RTAD Real-Time Alarm Dissemination
RTT Round-Trip-Time
SA Stand-Alone
SCMA Sparse Code Multiple Access
SCP Service Communication Proxy
SG Signal Generation
SNR Signal-to-Noise-Ratio
SMF Session Management Function
SLAM Simultaneous Localization and Mapping
SDN Software-Defined Networking
SV Saleh-Valenzuela
SDWSN Software-Defined Wireless Sensor Network
SSB Synchronization Signal Block
TCP Transmission Control Protocol
TDD Time Division Duplex
TSN Time-Sensitive Networking
TTI Transmit Time Interval
UCLA User Centric Latency Aware Schedule
UDM Unified Data Management
UE User Equipment
URLLC Ultra-Reliability and Low Latency Communication
UDP User Datagram Protocol
UP User Plane
UPF User Plane Function
V2V Vehicle to Vehicle
VDMA German association for mechanical and plant engineering
VLC Visible Light Communication
VNA Vector Network Analyzer
VR Virtual Reality
WiFi Wireless Fidelity
WLAN Wireless Local Area Network
WSN Wireless Sensor Network

1 Introduction

Wireless communication in industrial applications emerges with the production processes becoming more agile. Thereby, this general trend covers terms like industry 4.0, smart factory or intelligent plants [230]. This is synonym to a high product variety and lot sizes down to lot size one [237] and leads to more mobility as well as a higher flexibility on the factory floor. Thus, new demands for wireless communication systems are defined by different institutions [19, 1, 2, 20, 76] and discussed in many research articles [78, 94, 154, 245, 84, 75]. In addition , wireless communication is needed along the complete production process including all production steps and participants, so the complete value chain is connected [19, 154].
A typical scheme, that describes the structure on the factory floor is the matrix production [154]. Within this production scheme independent production cells (PC) that are able to perform one production step are interconnected by intra-logistic functions. The intra-logistic functions are implemented by Automated Guided Vehicles (AGVs). Typically a central controller orchestrates the AGVs. The matrix production scheme is illustrated in Fig. 1 which shows two possible paths a product may travel on the factory floor. This scheme illustrates the need for further autonomy and flexibility of production functions, because of the loose coupling between the elements and the high variety of productions process enabled.

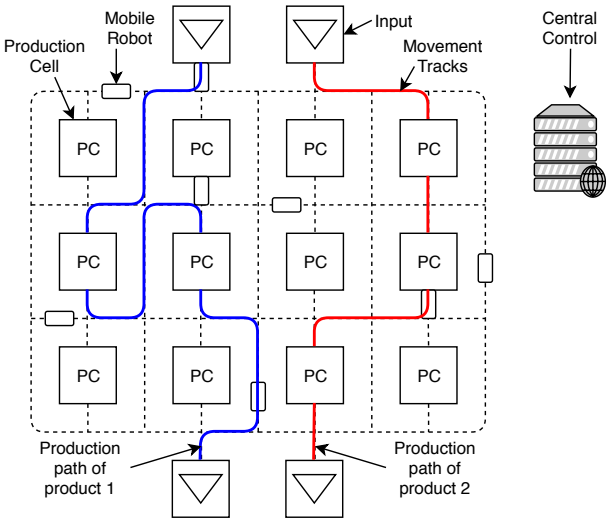

Figure 1: Scheme of a matrix production

Not only are requirements for wireless communications emerging in terms of latency, reliability, throughput and the number of connected devices, but also there is a lack of research articles describing aspects of industrial environments. The newly emerging requirements are based on use cases like the ones under the umbrella of cloud robotics [129], more specific cloud Simultaneous Localization and Mapping (SLAM) [85], use cases with a need for real-time video transmissions like Augmented Reality (AR)

and Virtual Reality (VR), Human Machine Interface (HMI) [102] or safety use cases that employ wireless links [211, 155].
Factory floors have typical characteristics. Those include many conductive structures, lots of mobility or changing environments. A precise description of propagation conditions is needed for working with wireless technologies [159]. Further, it is currently stated that industrial environments and the propagation conditions are extremely scenario specific [207]. Thus, there is a demand for additional evaluations on these characteristics.
Presently, there are many communication technologies available that are used in factories [154, 84, 245] and need to be orchestrated [160]. Those technologies are, but are not limited to WLAN, Long Term Evolution (LTE), 5G, Bluetooth, Zigbee, VLC, Radar and Near Field Communication (NFC). This is due to the variety of use cases and the scarcity of spectrum [155, 154].
So, the overall challenges for wireless communications in factory environments have different dimensions:

- Challenging and changing propagation environments
- Scarce resources on the air interface
- Wide variety of communication technologies

In this context, with 5G the first cellular communication standard is established that is partly developed and standardized to satisfy requirements from industry [173]. 5G features three service classes and the most relevant one for this work is URLLC. URLLC in 5G aims to provide highly-reliable low-latency communication on the air interface. Thus, it is a key enabler for future use cases. However, URLLC is not limited to 5G networks that are typically referenced in such cases. 5G aims for a reliability of $99.999\,\%$ with a latency of $1\,\mathrm{ms}$ [7].
Wireless URLLC networks have some inherent challenges: As they are ultra reliable, lost packets as service degrading events per definition are rare events and thus proper statistical analysis methods are needed. Additionally, this is complicated by the auto-correlated nature of these networks [156]. The reliability needs to be achieved on top of a statistical medium that behaves highly scenario specific on the factory floor [159, 207]. Besides the propagation, the movement of nodes differs significantly from other scenarios [199].
Thus, to overall contextualize this work from a high level perspective, the following statement applies: In modern applications in industrial contexts, new challenges arise due to new use cases, the volatile and scenario specific propagation environments, mobility patterns and the wireless URLLC requirements.
Hence, this thesis describes those constraints and proposes new solutions.

1.1 Main research questions and thesis structure

The previous Section outlined the general context of this thesis and motivated why there are open research questions around wireless URLLC in industrial environments. This Section briefly illustrates the structure of the thesis and lists the most prominent research

question for each Section. Throughout the whole thesis there is a focus on empirical evaluations present.
The related work section provides a high level view on use cases and their requirements to provide a broad overview on the challenges for wireless URLLC. Further, the related work elaborates in propagation conditions and channel modeling. The channel modeling is discussed for two kinds of models. Those are path-loss models and the Saleh-Valenzuela (SV) model. Subsequently, communication technologies and standards are surveyed. For 5G an in-depth section on its radio part is provided because it is the key technology for wireless URLLC. The state of research on statistical analysis with a tight focus on autocorrelated systems with rare events in empirical data is reviewed as well.
Section 3 is the first Section to discuss research questions and splits them into two parts. The first part is concerned with channel modeling and discusses the two key questions:

- What is a suitable channel model and what are its parameters?
- How to fit the Saleh-Valenzuela (SV) model to measurements of Power-Delay-Profiles (PDPs) and can the fitting be optimized?

Both of those topics are approached by an extensive measurement campaign and comparing the results to current work.
The second part of this Section elaborates on the mobility patterns of AGVs on the one hand and on nodal encounters on the other hand. An encounter here means that two nodes are able to communicate with each other.

- How to statistically describe AGV mobility on the factory floor?
- How to acquire and gain insights from Nodal Encounter Patterns (NEPs) from an AGV fleet?

Both questions are also discussed based on measurements from running factories.
Section 4 discusses Key Performance Indicators (KPIs) of wireless communication technologies on the factory floor. This is equivalent to asking:

- What are the KPIs for state of the art wireless communication technologies?

The question is answered empirically for WLAN (in terms of IEEE 802.11 b/g/n), private Long Term Evolution (pLTE) and 5G on the factory floor.
In Section 4.1 a new method to analyze measurement data from wireless URLLC networks is provided. The data analyzed in this Section are latency measurements and the research question discussed is:

- How to analyze auto-correlated empirical latency data from wireless URLLC networks to determine a relative error and confidence intervals?

Although rare event analysis is generally well investigated, a new method for the analysis was developed because the characteristics of data used in this thesis being empirical, auto-correlated and containing rare events is unique.
Section 5 asks how to optimize wireless URLLC in industrial environments. Thereby, the questions:

- How to disseminate real-time alarm in an environment where network coverage cannot be guaranteed?
- Can the mobility of AGVs be adapted to improve network coverage and subsequently their overall performance?

- How can the overhead in safe communication protocols using wireless links be minimized?
- Can redundant communication links with orthogonal wireless technologies be orchestrated to optimize communication KPIs?

are discussed. The performance improvements have different focuses. The light-weight dissemination of alarms aims for reducing bandwidth usage while keeping the ability to fulfill real-time requirements. The optimization is achieved by an improved protocol. The approach of optimizing networking protocols is used by the last two research questions as well. Thereby, reliability is enhanced and bandwidth usage is reduced. The second question that deals with controlling AGV mobility addresses the complete application of an AGV fleet and its performance.
Lastly, a conclusion around those questions is drawn including a discussion on the feasibility of use cases combined with the examinations from previous sections.

1.2 Contributions

Within this thesis, contributions regarding different focus areas of industrial wireless URLLCs are provided. Most of them have been published in peer-reviewed conferences, conference workshops or journals. Additionally, some contributions are part of the white paper on the usage of 5G in the mechanical and plant engineering industries published by the German association for mechanical and plant engineering (VDMA) [229] and the use case examples therein. For all published papers where the author of this thesis is not the main author a short statement on the individual contribution is provided.
A short paper (Work-in-Progess) motivating this thesis and providing an overview on communication technologies and challenges in industrial environments is available at:

- E. Lyczkowski et al. “Wireless Communication in Industrial Applications”. In: *24th IEEE International Conference on Emerging Technologies and Factory Automation (ETFA)*. 2019

Analyses of the performance of the wireless technologies WLAN, pLTE and 5G by means of latency and reliability are presented in:

- Eike Lyczkowski et al. “Performance of private LTE on the factory floor”. In: *International Conference on Communications Workshops (ICC Workshops)*. 2020
- Eike Lyczkowski et al. “Performance of a 5G NPN in industry: statistical analysis and application to black channel protocols”. In: *26th IEEE International Conference on Emerging Technologies and Factory Automation (ETFA)*. 2021

Those two works also contain an application of the results to use cases and propose a new statistical analysis method. The measurements used in both works were acquired on factory floors using a network architecture that is similar to the network architecture of AGVs.
Algorithmic optimizations for communications in industrial environments have been published in:

- Eike Lyczkowski et al. “Avoiding keep-alive messages by exposing 5G channel

state information to applications". In: *26th IEEE International Conference on Emerging Technologies and Factory Automation (ETFA)*. 2021
- Christian Sauer et al. "Real-time Alarm Dissemination in Mobile Industrial Networks". In: *In Proceedings of IEEE International Conference on Industrial Technology (ICIT)*. 2021
- Christian Sauer et al. "Testing AGV Mobility Control Method for MANET Coverage Optimization using Procedural Generation". In: *ACM 24th International Conference on Modeling, Analysis and Simulation of Wireless and Mobile Systems (MSWiM)*. 2021

For the work on *real-time alarm dissemination* [203] the author of this work provided the analysis on the complexity of the compared approaches, provided data from measurements from cellular networks and participated in the writing and results discussion. In this work a new ad-hoc network protocol is developed that provides minimal overhead and complexity by means of number of messages and message size and still adheres to real-time requirements.
For the work on *testing an AGV mobility control method* [204] the author of this thesis performed some statistical analysis and participated in the results discussion as well as the writing process. The outcome of this work is an adaptive mobility control method for AGVs to improve network coverage and thereby improve AGV fleet performance.
Describing and modeling factory environments was done from two view points. Firstly, node behavior in factories by nodal encounter patterns and movements of mobile nodes:

- Christian Sauer, Marco Schmidt, and Eike Lyczkowski. "On Ad Hoc Communication in Industrial Environments". In: *Applied Sciences* 10.24 (2020)
- Christian Sauer, Eike Lyczkowski, and Marco Schmidt. "Mobility Models for the Industrial Peer-to-Peer Context Based on Empirical Investigation". In: *IEEE Annual International Symposium on Personal, Indoor, and Mobile Radio Communications (PIMRC)*. 2021

For the work on *ad-hoc communication in industrial environments* [200] the author of this thesis participated in the discussion of the results, the writing process and supported the mathematical work. The work records and analyses NEPs and provides the raw data as well as the tool for recording the NEPs.
For the work on *mobility models for industrial peer-to-peer contexts* [199] this author supported the statistical analysis, the discussion on the results and the writing process. The outcome is a improved speed selection algorithm for AGVs on the factory floor based on empirical evaluations. The navigation graph of an AGV fleet is also illustrated.
Secondly, describing and modeling of the physical layer is presented in the works:

- Eike Lyczkowski et al. "Power delay profile analysis of industrial channels at 2.1, 2.6, 3.8 and 5.1 GHz". In: *IEEE Annual International Symposium on Personal, Indoor, and Mobile Radio Communications (PIMRC)*. 2021
- Eike Lyczkowski et al. "Power decay behavior of the Saleh-Valenzuela model for industrial environments from 2 to 6 GHz". In: *IEEE Wireless Communications and Networking Conference (WCNC)*. 2022

Both papers are based on the same measurement campaign that measured over 6000

PDPs on a factory floor during production. Signal strength are recorded, too. From those measurements path loss models are fitted, the behavior of multipath components is discussed and the complete SV model is fitted and the model optimized.
Lastly, one paper discusses the orchestration of redundant wireless links in a mixture of infrastructure-based and ad-hoc networks:

- Eike Lyczkowski et al. "SDN controlled visible light communication clusters for AGVs". In: *European Conference on Networks and Communications (EuCNC)*. 2021

The wireless technologies used are WLAN and VLC to optimize the KPIs latency and reliability in the use case of AGVs cooperatively transporting goods. The two wireless technologies are orchestrated in the fashion of a Software-Defined Wireless Sensor Network (SDWSN).
In addition, there are contributions to the white paper consisting of two parts, as there is a main part of the white paper itself:

- VDMA and Fraunhofer IIS. *5G im Maschinen- und Anlagenabu*. Tech. rep. VDMA - German association for mechanical and plant engineering, 2019

and to the use cases therein. The white paper describes usage scenarios and architectures for 5G in the industrial context and is a guideline to companies that plan to use 5G in production environments. Appended to the white paper a collection of use cases is published. Within the use cases the author was the representative of SEW-EURODRIVE:

- AGCO - FENDT et al. *5G im Maschinen- und Anlagenabu - Use Case Remoteanwendungen*. Tech. rep. VDMA - German association for mechanical and plant engineering, 2019
- HAHN GROUP, SEW-EURODRIVE, and Fraunhofer IIS. *5G im Maschinen- und Anlagenabu - Use Case Human Machine Interface*. Tech. rep. VDMA - German association for mechanical and plant engineering, 2019
- KION GROUP/STILL, SEW-EURODRIVE, and Fraunhofer IIS. *5G im Maschinen- und Anlagenabu - Use Case Ortung und Kommunikation in der Logistik*. Tech. rep. VDMA - German association for mechanical and plant engineering, 2019

2 Related Work

Research and development are driven by new requirements. Thus, use cases defining new requirements for wireless communication are examined in the first subsection. Afterwards wireless communication technologies are surveyed that are of interest for industrial use cases with a strong focus on 5G URLLC. This section discusses the communication paradigms of ad-hoc and infrastructure based networks and software defined networking. A dedicated discussion on the analysis of measurements from URLLC networks is needed, as that data has unique properties and thus the statistical analysis needs attention.

Hereinafter, a set of Key Performance Indicators (KPIs) of wireless networks are used for characterizing the networks. Thus, they are defined for this thesis and those definitions are compared to research literature:

Latency is the one-way transmission delay measured at the application layer from source to destination node. Those nodes are typically one wireless and one stationary node in infrastructure based networks or two wireless nodes in an ad-hoc network. This definition is in line with the 3rd Generation Partnership Project (3GPP) definition [7, 2], research literature [116, 184, 218], with the latter one using the 3GPP definition and the majority of network operators represented by Next Generation Mobile Networks Alliance (NGMN) [175].

Reliability is defined as the probability of transferring a data packet of a certain size within a given latency. This is equal to the number of successfully sent packets divided by the number of all sent packets. A packet is only considered successfully sent if it is transferred within the given latency [175, 229]. This definition is as well in line with 3GPP, most of the research literature and NGMN [7, 76, 38, 175].

Throughput is the amount of data transferred per time. The overhead added to the communication by higher layers is not considered for the throughput.

Jitter is the time deviation from the intended packet arrival time [229, 1].

2.1 Use cases and requirements

In this chapter, use cases and the relation to their requirements are examined. As this work focuses on an industrial context, the use cases here focus on industrial use cases within Non-Public-Networks (NPNs). To provide a comprehensive overview, this chapter is structured into two subsections. Subsection 2.1.1 provides a simple view on the relation from a use case to its requirements with examples and Subsection 2.1.2 contains an overview on use cases and groups them.

2.1.1 Requirements related to their use case

To provide an impression on the requirements of URLLC and to understand where they are derived from, in the following the relation of use case and communication requirement is illustrated in two ways. There is a multitude of methods available to do this and such methods are not in the focus of this thesis. Hence, the two examples used here aim at illustrating the relation of use case and requirement in a simple, understandable way.

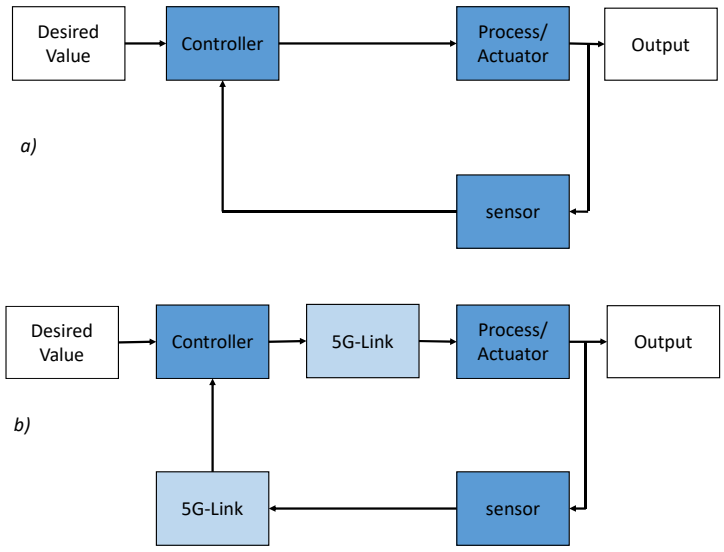

Figure 2: Closed-loop controls with and without a 5G-link

Firstly, in a simple control theory based approach for closed-loop controls and secondly, for the remote navigation of an AGV [215, 85].

Closed-loop controls can be found in many examples like motion control, temperature control in process automation or mobile robots [1, 19, 154]. In these cases the typical control theory approaches as used in everyday engineering apply and a wide range of methods is available [110]. As this thesis focuses on the wireless communication aspects in the following, only an exemplary way to derive requirements is illustrated, but no controller design. In wireless networks digital controllers are used [176]. By the usage of 5G or other wireless networks the control system becomes a wireless networked control system.

In Fig. 2 two closed-loop controls are illustrated. Closed-loop a) is a standard closed-loop and b) includes two 5G-links and thus is a networked control system. These links are additional functional blocks and have an impact on the complete networked control system due to the latency they introduce. The effect of that latency is a reduction in system-performance and a destabilization of the control-system [225, 135]. Thus, the age of information is an important metric in wireless network control systems [135].

A key characteristic of a digital control is its sampling frequency $f_{sampling}$ [176]. This characteristic is of high importance for determining the maximum latency $T_{latency}$ that is tolerated in a communication link.

The lower limit for the sampling frequency $f_{sampling}$ is defined by the Nyquist-Shannon sampling theorem that states

$$f_{sampling} > 2 \cdot f_{max} \tag{1}$$

with f_{max} being the highest frequency of the process [193].

For the sake of simplicity to determine the maximum latency *sampling time scheduling methodology* is applied with one closed-loop-control only [225, 68]. This method provides a simple way of determining the maximum latency for a networked control system. So the requirement

$$T_{delay} \leq \frac{1}{f_{sampling}} \tag{2}$$

applies with T_{delay} being the sum of all delays, containing processing times and network latency. Those are represented by the functional blocks *5G-Link* and *Controller* in Fig. 2. If the processing time $T_{processing}$ of the controller is small in relation to the network latency

$$T_{processing} \leq \frac{T_{delay}}{10} \tag{3}$$

it may be neglected [225, 68].
A closed-loop control contains two communication links, both are marked as *5G-Link* in Fig. 2. Thus the delay T_{delay} can be determined with

$$T_{delay} = T_{processing} + 2 \cdot T_{latency} \tag{4}$$

$T_{latency}$ here is the one-way latency from controller to actuator or from sensor to controller and we assume that these latencies are equally long. Thus, the maximum latency for each message can be calculated with

$$T_{latency} \leq (\frac{1}{f_{sampling}} - T_{processing}) \cdot \frac{1}{2} \tag{5}$$

From the sensor to the controller state information is transferred, while from the controller to the actuator desired values are transferred. Thus, the communication payload is not necessarily symmetrical.
The packet size of the transmission depends on the values that need to be transmitted. In the examples of temperature control, filling tanks or simple speed control of an electric drive only one floating point parameter has to be transferred. Hence, such closed-loop controls are called one parameter control-systems. If a video-stream is included far greater packets have to be transferred. This can happen for example in case of mobile robots and their cooperation [1, 215, 102, 85].
In automation regularly the term *cycle time* is used. That term defines the time period within which all periodic actions have to be performed once. This includes processing all sensor values and determining new actuator values. So, the sampling time can be directly mapped to automation requirements based on the cycle time [20, 19].
A low-demand motion control or a high-demand factory automation use case [19, 20, 1] exhibits a highest frequency of $f_{max} = 200\,\mathrm{Hz}$. As motion control works with fast controllers the processing time $T_{processing}$ is assumed to be insignificant. So with Equation (5) the maximum latency can be calculated:

$$T_{Latency} \leq (\frac{1}{2 \cdot f_{max}} - T_{processing}) \cdot \frac{1}{2} \tag{6}$$

$$T_{Latency} \leq (\frac{1}{2 \cdot 200\,\mathrm{Hz}}) \cdot \frac{1}{2} \tag{7}$$

leading to $T_{Latency} \leq 1.25\,\mathrm{ms}$. This illustrates the applicability for wireless URLLC networks in automation as in 5G a one-way latency of $1\,\mathrm{ms}$ is envisioned [15, 7]. For further details on networked control systems refer to [110, 225, 68].

Remote navigation is another example where requirements for a wireless URLLC use case can be derived from. The example to derive requirements is the usage of a cloud based SLAM. Thereby, the algorithm for navigating an AGV runs in a cloud or edge device instead of having the necessary computing power on the AGV [215, 39, 45, 129]. The example here is similar to [85].

In this set-up all safety functions that an AGV has to employ are still performed locally on the AGV itself. So, the requirements for the wireless communication link are derived in a way that safety stops due to errors in the navigation system are avoided. The relevant parameters of the AGV are

$$\begin{aligned} v_{max} &= 2\,\frac{\mathrm{m}}{\mathrm{s}} \\ s_{stop} &= 0.67\,\mathrm{m} \\ t_{delayInternal} &= 0.01\,\mathrm{s} \\ f_{SLAM} &= 15\,\mathrm{Hz} \end{aligned} \tag{8}$$

with v_{max} the maximum speed of the AGV, s_{stop} its stopping distance, $t_{delayInternal}$ the internal delay and f_{SLAM} the frequency of the SLAM algorithm. If we allow an extra space of $0.03\,\mathrm{m}$ around the safety field that the navigation uses for maneuvering a latency of $30\,\mathrm{ms}$ is needed in case of negligible processing times. To provide reliability requirements in terms of Packet Error Rate (PER) an assumption regarding tolerable packet loss and its effects is needed. A harsh worst case assumption is that each packet loss may lead to an unnecessary safety stop. Thereby, one safety stop per $8\,\mathrm{h}$ may be tolerable. This results in a PER of $2.3 \cdot 10^{-6}$ [85]. The data rate for this use case can be determined based on the distance and intensity values of the laser scanner that is used in AGV navigation. The laser scanner provides a 2D point-cloud with each point having the aforementioned distance and intensity value. Assuming $360°$ view and a point per $0.5°$ results in an uplink data rate of $\approx 50\,\mathrm{kbps}$ [85].

These two examples illustrate different ways to determine requirements and there are other methods available [110, 176, 222, 225, 68, 211]. Additionally, it is obvious that by varying application parameters only slightly, significantly different requirements emerge.

2.1.2 Use cases

Use cases can be grouped by the vertical domain (branch of industry) they originate from. So, the use cases can be grouped by automation [19, 1, 94, 103, 211], automotive [2, 78, 94], logistics [1, 161, 103], health care [19, 81], public safety [2, 1, 81], public transport [1, 2], energy [1], agriculture [81, 1, 2], retail [19, 81, 2, 1] and media and entertainment [81, 2].

Table 1: Requirements overview surveyed from the cited reference

branch of industry	Use case description	Reliability	Latency	Data-rate
Automation	Mobile robots	99.9999%	1 ms	$\leq$150 kbytes
[19]	Motion control	99.9999%	1 ms	$\leq$50 bytes
Automotive	Remote driving	99.999%	2 ms	20 Mbps
[2, 78, 94]	Sensor sharing	90%	10 ms	25 Mbps
Logistics [1, 161]	Continuous traceability	99.9%	10 ms	none
Health care [81, 19]	Cloud robotic assisted living	99.9999%	1 ms	$\leq$ 250 bytes
Public safety	High resolution streaming	none	20 ms	10 Mbps
[2, 1, 81]	Helmet with AR	99.9%	10 ms	$\geq$20 Mbps
Public transport	Passenger internet access	99.9%	$\leq$10 s	$\geq$0.2 Mbps
[1, 2]	Real time surveillance	99.99%	none	20 Mbps
Energy [1]	Primary frequency control	high	50 ms	100 bytes
	Load control	99.9999%	50 ms	not specified
Agriculture	Autonomous vehicles	99.9999%	2 ms	$\leq$ 50 Mbps
[81, 1, 2]	In field AR support	99.9%	10 ms	$\geq$ 20 Mbps
Retail [19,	AR/VR shopping	99.9%	10 ms	$\geq$20 Mbps
81, 2, 1]	Automated warehouse	$\leq$99.9999%	10 ms	$\leq$250 bytes
Media [81, 2]	High quality streaming	none	$\leq$ 10 s	10 Mbps

Table 1 provides an overview on example use cases. All in all those use cases illustrate the challenging requirements for wireless networks. As this work focuses on an industrial context around factory automation, we take a closer look at use cases from this domain.

There are different use case collections available [19, 20, 1] as well as the collection that is appended to [229]. The key use cases that are referenced later in this work are summarized in Table 2.

In the following on the factory floor a matrix production scheme is assumed. In a matrix production independent Production Cells (PCs) are interconnected by intra-logistic functions. Thereby, each product may travel a different path on the factory floor producing a different outcome. Envisioned are lot-sizes done to the lot-size one. This structure of a factory floor adheres to trends that can be summarized under the terms of industry 4.0, smart factories or factories of the future and provides high flexibility [20, 237, 230, 20]. For an increased flexibility an increased mobility is needed. This reflects in a wide variety in AGV use case [1, 19, 154]. In addition, mobile control panels with and without safety functions are envisioned [102, 1].

AGV use cases can be divided into standard operation, cooperative driving, remote operation and use cases concerning a robot-arm mounted to the AGV.

The standard operation of AGVs has the lowest demands as in this case the AGVs perform the single operation, like drive to a certain way-point autonomously. Thus, in this case only control information is transferred with relaxed requirements [154, 1] in accordance to the VDA5050 standard for AGV communication [228]. This is the most

Table 2: Use cases referred to in the following and the references detailing them

Use case family	**scenario**	**latency**	**reliability**	**packet size / data rate**
AGV	standard operation [1]	$\leq 500\,\mathrm{ms}$	10^{-6}	$\leq 250\,\mathrm{byte}$
AGV	cooperative driving [1]	$10\,\mathrm{ms}$	10^{-6}	$\leq 250\,\mathrm{byte}$
AGV	remote [85]	$3\,\mathrm{ms}$	$2.3 \cdot 10^{-6}$	$1400\,\mathrm{byte}$
AGV	robotic [1]	$1\,\mathrm{ms}$	10^{-6}	$\leq 250\,\mathrm{byte}$
Mobile control panels	without safety and AR [102]	$< 10\,\mathrm{ms}$	10^{-3}	$> 20\,\mathrm{Mbps}$
Mobile control panels	with safety [211]	$< 8\,\mathrm{ms}$	10^{-6}	unknown

used variant today and is implemented by WLAN. Thus, those implementations have to tolerate even worse latency and worse reliability [157] than required according to [1]. In case of cooperative driving the AGVs have to exchange information on their positions because in cooperative driving AGVs have to precisely keep their formation. Here the risk of collisions or more general of losing the formation exists. In the case goods being transported by several AGVs minimizing the deviation in the formation minimizes the stresses on the transported good. This is equivalent to minimizing the latency and enhancing the reliability.
Remote operation is always the case when edge or cloud computing are used for the operation of the AGVs. In these cases parts of the processing power are not present on the AGV but in the cloud or edge [215, 85, 39, 45, 129].
The last case of a mobile robot mounted to an AGV depends extremely on the question where the processing is placed and whether cooperation between robot and worker takes place. Anyway, the robot mounted to the AGV has to adjust to changes in the environment that emerge due to changing the location.
Mobile control panel use cases can be differentiated by being safety relevant or not. If they are safety related they fall under the category of black channel use cases [211]. For mobile control panels a wide variety of scenarios exists and the three examples of fitting a machine via a mobile panel, monitoring a machine or the same examples employing AR are presented in [102].
For fitting the machine to a new product, process parameters and a video from the tools perspective need to be transmitted in real time, while in the monitoring case only the process data is needed. Of course, in both cases AR may be used as well to display additional information [102].
The black channel paradigm is always used if reliable communication on top of an unreliable communication system is needed [82]. Because reliable communication cannot be guaranteed in such scenarios, black channel protocols detect communication errors and notify applications about communication errors. This paradigm is employed by different protocols that adhere to the IEC 61784 standard [115] and those protocols are then called black channel protocols. Safety relevant is any use case where a human may be harmed if the communication fails. As those protocols work on top of unreliable communication systems they have to detect at least the following errors [60, 30, 155]:

- data corruption
- unintended repetition
- incorrect sequence
- packet loss
- unacceptable delay
- packet / data insertion
- masquerading
- wrong addressing
- revolving memory failure within switches

This introduces the requirement that at least the following measures are part of each black channel protocol:

- Sequence number
- Time-out / connection loss detection by cyclic messages
- Connection ID
- Data integrity assurance

If one of the aforementioned communications errors is detected, the system using the black channel performs a safety stop. The parameter of the time-out thereby is important, as it defines how many cyclic messages may be lost. If the time-out is set sufficiently slower then the cycle time of the cyclic messages several consecutive message losses may be tolerated [155]. In the following each safety stop resulting from a communication error instead of an event in the application is called a false positive.
Regarding the security aspects of black channel protocols Perschern et al. [187] illustrate how to enhance security of such protocols. Anyway, security attacks towards black channel mostly cause communication errors. Thus, such an attack degrades the system performance instead of its security [106]. An usage example for electric drives is presented in [141].
As black channels themselfs have no requirements this use case is not part of Table 2. Performance evaluations in wireless systems work with timeouts of $150 - 250\,\mathrm{ms}$ [182, 104] while both these works perform protocol performance comparisons among User Datagram Protocol (UDP), Transmission Control Protocol (TCP) and Message Queuing Telemetry Transport (MQTT). Although the test setups in both works provide a rather optimal environment, in short evaluation times already safe state transitions occur [182, 104]. Being able to communicate safely via wireless systems is mandatory [182] and thus further improvements are needed in this context.

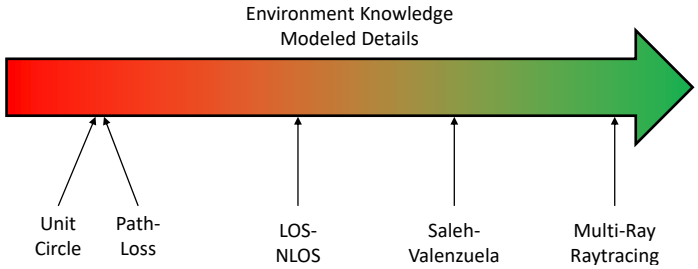

Figure 3: Overview on details of channel models [201]

2.2 Propagation and channel modeling

The proper description of wireless channels is mandatory for research in the context of wireless communications. Each environment has significant different properties by means of the channel behavior [234].
Channel models can be distinguished by the properties and details they describe as well as the frequencies [234, 201]. Generally, the more details a channel model provides the more detailed input is needed in terms of knowledge of the environment and measurement data to parameterize it. Fig. 3 shows some models and sorts them according to details and knowledge needed. The unit circle thereby just evaluates the distance between two nodes to decide whether they can communicate while multi-ray raytracing evaluates modeled 3D environments and the single rays / MPCs therein.
Additionally, single parameters of channels my be evaluated, like coherence bandwidth or delay spread. In the following the channel models and parameters are described. Measurement results of previous work are compared to this work and discussed in the context of the measurement results in Section 3. This chapter only contains a broad overview on parameters and measurement results.

2.2.1 Path-loss models

Most widely performed are path loss measurements and fitting path loss models. A path loss model describes the attenuation over distance and adds the noise by using a random variable. Such models are in contrast to more general ones like QuaDRiGa [57], WINNER / WINNER 2 / WINNER+, IMT-Advanced [234]. Generally, there is a wide range of different models. Hence, only a subset of models is discussed here. The choice of models is based on the usage for modeling scenarios on the factory floor:

- free space
- log distance
- Close-in (CI) model
- ABG-model

Here, the free space model is the most fundamental one and uses the logarithmic expression of the Friis equation [71, 32] resulting in the formula:

$$P_R(dBm) = P_t(dBm) + K(dB) - 10nlog_{10}(\frac{d}{d_0}) \tag{9}$$

with d being the distance in $meters$, d_0 the reference distance, K the path-loss at the reference distance and P_t the send power in dBm. The path loss exponent is $n = 2$ always. This model is only accurate in the Line-of-Sight (LOS) case and does not include noise.
The CI model is described by:

$$PL_{CI}(f, d) = FSPL(f, 1\,\mathrm{m}) + 10nlog_{10}(d) + \chi_\sigma \tag{10}$$

with

$$FSPL(f, 1\,\mathrm{m}) = 20log_{10}(\frac{4\pi f}{c}) \tag{11}$$

The CI model is an all frequency model [217], as the initial path-loss term $FSPL(f, 1\,\mathrm{m})$ illustrates. χ_σ describes the noise and typically adheres to the standard normal distribution. Obviously, this model is also based on the Friis equation but includes noise, a frequency dependent initial path loss and the path loss exponent is adjusted to the environment [217].
The log-distance path loss / log-normal shadowing model has only a small difference to the CI-model as only the initial path loss term differs:

$$PL(d) = PL(d_0) + 10n \cdot log_{10}\left(\frac{d}{d_0}\right) + \chi_\sigma \tag{12}$$

Anyway, both models are regularly used [70, 71, 69, 217, 25, 108].
The multi-wall-floor model only adds the attenuation that is due to floors and walls to the model by summing them up and is otherwise identical to the log distance model described in Eq. 12 [71].
The ABG model is an all frequency model described by [217, 207]:

$$PL_{ABG}(f, d) = 10\alpha log_{10}(\frac{d}{d_0}) + \beta + 10\gamma log_{10}(\frac{f}{f_0}) + \chi_\sigma \tag{13}$$

This model is significantly easier to use since [217] provided closed form equations to perform the fitting by minimizing the mean squared error. This model has the specialty that the parameters β and γ have no physical representation [217]. Thereby, the parameters α, β and γ can be chosen in a way that the ABG model becomes identical to the CI model.
Closely related general path loss models including their parameters may be found in e.g. [216, 234, 70, 71, 221].
All these models have in common that they consist at least of:

- initial path loss
- path loss
- noise / fading

Jaeckel et al. [118] has industry scenario parameters as well. Thereby the QuaDriGa model [57] is used, but the parameters path loss and noise are described similar to the aforementioned models, althoug the QuaDriGa model contains more details [118, 57].

Table 3: Parameters of the ABG-model

Source	path loss (α)	β	γ	σ
Schmieder et al. [207] LOS	2.27	27.29	1.94	1.62
Schmieder et al. [207] NLOS	3.02	28.35	1.78	1.61
TR 38.901 LOS [5]	2.15	31.84	1.90	4.30
TR 38.901 NLOS [5]	3.57	18.60	2.00	7.20
Jaeckel et al. [118] LOS	1.83	36.30	1.95	1.63
Jaeckel et al. [118] NLOS	2.41	29.10	2.54	3.58

An overview on industry scenario parameters for the ABG model is illustrated in Tab. 3. Schmieder et al. [207] state that industrial propagation conditions are highly scenario specific and the high variances in the values from Tab. 3 facilitates that statement. The path loss denoted as α describes the intensity of the path loss over distance in an identical manner as n in the other models.
For the one-slope model and the ITU model results from industrial measurements can be found in [70, 71]. In many cases in those measurements the results for the path loss coefficient are $n \approx 3$ and once $n = 4.2$. These are large path loss values. Adegoke et al.[25] has way lower path loss exponents with $n < 2$ in their measurements and fitting. Thereby, the log-normal path loss model is used.
The deviation in the measurement results and the seemingly high deviation between scenarios motivates further measurements and model fitting as well as a discussion on the differences.

2.2.2 Channel parameters

Besides channel models single parameters of a propagation channel can describe a property and have an influence on the communication system. Typically, thereby the parameters

- delay spread [26, 130, 170, 74, 108, 72]
- coherence time [226]
- coherence bandwidth [74, 226, 170]
- angular spread [207]
- K-factor [46, 221, 55, 28, 140, 23]

are used. In some cases the parameters are viewed as time variant [46] or as stationary random variable for one scenario [207].
The root mean square **delay spread** is defined by:

$$\tau_{rms} = \sqrt{\frac{\int (t-D)^2 p(t) dt}{\int p(t) dt}} \tag{14}$$

and is a measure of the width of a channel impulse response of a wireless channel [72] or its PDP. The difference of channel impulse response and PDP lies in the channel

impulse response including information on phase while the PDP only describes power over time. Thereby, Eq. 14 needs the power values on a linear scale.
The delay spread generally is larger if more reflections appear and if longer distances are possible for a signal to travel. Thus, it can be expected that in industrial scenarios the delay spread is larger than in other scenarios. In addition, a larger delay spread leads to a higher Bit Error Rate (BER) [72] and thus, behaves equivalent to more noise.
The values of the delay spread vary widely along current measurements. At $3.7\,\mathrm{GHz}$ mean delay spreads of $20.3\,\mathrm{ns}$ and $37.4\,\mathrm{ns}$ for LOS and non Line-of-Sight (NLOS) ,respectively [207], or $30\,\mathrm{ns}$ and $80\,\mathrm{ns}$ at $2.37\,\mathrm{GHz}$ and $5.4\,\mathrm{GHz}$ independent of LOS or NLOS are available from measurement campaigns [118]. The 3GPP channel model in [5] provides no complete parameter set for indoor factories and no values for the delay spread. Alone these values motivate further investigations on this topic, although value for outdoor scenarios and offices are available e.g. in [108, 5, 74, 130, 234].
The **coherence time** describes the time duration within which a wireless channel behaves stationary. To define an order of magnitude for that duration the coherence time T_c may be calculated by [226]:

$$T_c = \frac{1}{4D_s} \tag{15}$$

with D_s the Doppler shift of the channel. Obviously, Eq. 15 assumes at least one node of the communication is moving. The coherence time is relevant to determine the frequencies for channel measurements or to assign them the attribute of being fast or slow fading [226].
The **coherence bandwidth** has a similar definition as the coherence time. The coherence bandwidth describes the bandwidth within which the channel behaves similarly. Thereby, the coherence bandwidth can be determined by [74]:

$$B_c = \frac{1}{\alpha \cdot \tau_r ms} \tag{16}$$

with $\alpha \leq \pi^2$ [74, 87]. Thereby, Fleury [87] introduces the coherence level. The coherence bandwidth is for example relevant for PD because in case of PD over Carrier Aggregation (CA) the minimum distance between the frequencies to send the duplicated packets may be determined. In many current applications uncorrelated channels for PD are assumed, so channels outside each others coherence bandwidth [192, 191, 92].
The **angular spread** describes the distribution of the angles of arrival and the receive power of each angle [207].
The **k-factor** describes the ratio of the LOS and NLOS components powers in communications with LOS propagation [223, 58]. In LOS propagation the fading is Ricean distributed and the k-faktor thus is based on the Ricean distribution [223]. The k-factor can be calculated by [46]:

$$K = 10log_{10}(\frac{r^2}{2\sigma^2})[dB] \tag{17}$$

with r^2 representing the LOS or specular component and $2\sigma^2$ the NLOS or diffuse components. Anyway, the k-factor is often determined by fitting signal strength values to

a Riciean distribution and extracting the k-factor therefrom [55]. Mostly, the k-factor is used as a constant value within one scenario but in cases like Vehicle to Vehicle (V2V) communication the k-factor is time varying [46]. If the k-factor shrinks below $0\,\mathrm{dB}$ the fading characteristics change from Ricean to Rayleigh [136].
Typical values for outdoor scenarios are $6 - 30\,\mathrm{dB}$ while for industrial and indoor scenarios smaller values are measured [58]. For an automotive assembly factory values of $k = 3.3\,\mathrm{dB}$ at $2.2\,\mathrm{GHz}$ and and $k = 3.2$ at $5.4\,\mathrm{GHz}$ were measured [58]. At $2.45\,\mathrm{GHz}$ a k-factor of $1\,\mathrm{dB}$ can as well be found in industrial environments with a relativley large $\tau_{rms} = 77\,\mathrm{ns}$ [136]. Those values are in contrast to [55] who finds a negative k-factor for an indoor environment and thus, Rayleigh fading. In Tanghe et al. [221] along the frequencies $0.9, 2.4$ and $5.2\,\mathrm{GHz}$ k-factors of ≈ 12 are measured in an industrial environment.
The wide spread measurement results with the statement of highly scenario specific result in industrial applications [207] motivate further investigations.

2.2.3 Saleh-Valenzuela model

The SV model was first proposed by [197], mainly inspired by [227] and is designed to model channel impulse responses of wireless channels by the usage of weighted Dirac-impulses. The SV model is widely used and popular for describing the stochastic properties of MPCs and by means of their arrival and amplitude [165]. Due to its popularity in modeling channel impulse responses, the model is used therefore in this work.
The SV model assumes that MPCs arrive clustered [165, 197, 29] and the first one thereof represent the LOS component. The original model assumes that the power of the clusters as well as the power within the clusters decays linearly on a logarithmic scale (dB) [197]. The mathematical description of a channel impulse response is [197, 29]:

$$\begin{aligned} h(\tau) &= \sum_{l=1}^{L}\sum_{k=1}^{K_l} \beta_{k,l} e^{(j\phi_{kl})} \delta(\tau - T_l - \tau_{kl}) \\ &= \sum_{l=1}^{L}\sum_{k=1}^{K_l} (\overline{\beta_{11}^2} e^{-T_l/\Gamma} e^{-\tau_{kl}/\gamma})^{\frac{1}{2}} e^{j\phi_{kl}} \delta(\tau - T_l - \tau_{kl}) \end{aligned} \tag{18}$$

with L the number of clusters and K_l the number of MPCs in the cluster l. Gain and phase of MPC k and cluster l are $\beta_k l$ and $\Phi_k l$, respectively [29, 197]. The energy decay time is described by Γ and γ for clusters and MPCs, respectively [165]. The arrival times of cluster l is T_l and the arrival time of MPC k in cluster l is τ_{kl}.
The equivalency in Eq. 18 is proofed in [165] and is not trivial. From Eq. 18 the expression for a PDP in dB can be derived [29]:

$$PDP(\tau) = \sum_{l=1}^{L}\sum_{k=1}^{K_l} \Big[10log_{10}\overline{\beta_{11}^2} - \frac{T_l}{\Gamma}(10log_{10}e) - \frac{\tau_{kl}}{\gamma}(10log_{10}e) \Big] \delta(\tau - T_l - \tau_{kl}) \tag{19}$$

The power of the first ray in the first cluster in dB is defined by the minuend while the power of k^{th} ray in the l^{th} cluster are calculated by the use of the inter- and intra-cluster decay. Those are the first and second subtrahend. As the information on the phase is missing and only power over time information remains, Ep. 19 describes PDPs instead of channel impulse responses described by Eq. 18.
So, to fully describe the SV model the decay factors and the arrival rates must be extracted from measurement data.
Extracting the parameters for the SV model from measurement data includes some challenges. Firstly, the peak in PDPs must be identified. This is typically performed by visual inspection [127, 29]. Anyway, an algorithmic method was proposed by [238] that is not regularly used due to its complexity. The PDPs are normalized for the analysis by setting the first peak to $0\,\mathrm{dB}$ and $\tau = 0\,\mathrm{s}$ for the first MPC [29].
Secondly, for the arrival rate two methods are common [66]: Either the mean value of the arrival times is calculated and the assumption is made that the underlying process is a Poisson process or a distribution fitting is performed. This Poisson process can be explained by assuming one resolvable MPC is introduced by one scatterer and that the

positions of the scatterers are the result from a spatial Poisson process. This assumption still holds true when the number of scatterers is large and reflection on several scatterers per MPC are assumed [165].
Thirdly, there are the inter and intra-cluster power decay. The original SV model assumes a linear decay on the logarithmic scale [197] while an exponential decay in measurements in an industrial environment was found Ai et al. [29].

2.3 Communication standards and technologies

Within this work different communication technologies, standards and paradigms are discussed. Thus, all the ones that are used in the following are introduced with varying focus according to later usage. A brief overview is provided before the more detailed subsections:
Today, predominantly WLANs in the sense of solutions of the IEEE 802.11 family are used on the factory floor [154, 157]. Hence, WLAN is often the performance base line in industry focused research work [182, 104, 153] and it is a typical infrastructure based wireless network. Other examples of infrastructure based networks are all cellular technologies, that get an increasing attention in the context of factory automation [31, 38, 154]. Such solutions are the counterpart to the family of ad-hoc networks that enable communication along nodes without relying on any deployed infrastructure. So, ad-hoc networks only employ Peer-to-Peer (P2P) communications to form a network [96]. Generally, the need of and interest in wireless technologies on the factory floor gain importance [90], regardless of the used technology. Thereby, many new use cases and requirements emerge and especially AGVs have high wireless communication requirements that cannot be fulfilled with current wireless communication solutions [84, 245].
Due to the further digitization of factories the need to collect data increases and leads to investigations into Wireless Sensor Network (WSN) to enable a lightweight data collection.
Paradigms to orchestrate the communication networks gain more attention with Software-Defined Networking (SDN) being highly relevant [93]. Thereby, SDN aims to separate control plane and data plane in networks to enable better network management and flexibility.
This all takes place in a context where bandwidth on the air interface is a sparse resource and leads to employing many different technologies and frequency ranges [154].

2.3.1 Ad-Hoc networks

Ad-hoc networks can be classified into the subcategories:

- Mobile Ad-hoc NETwork (MANET)
- Delay Tolerant Network (DTN)
- Wireless Sensor Network (WSN) and its variant Mobile Sensor Network (MSN)

MANETs describe ad-hoc networks with mobile clients and AGVs are a typical example of mobile clients in this case. The mobility in MANETs leads to a time dependence of the network topology and thus the routing challenge in a MANET is more complex than in a static ad-hoc network [189]. For MANETs and their simulation it is extremely important to understand the mobility of the nodes in the network [169]. Modeling mobility when simulating and evaluating MANETs are of high importance and three variants are typically used [199]

- mobility traces
- mobility models
- Nodal Encounter Pattern (NEP)

Mobility traces consist of node positions that have been previously recorded and have the advantage to recreate the reality precisely but are limited to the recorded duration. Mobility models describe the statistical properties of node mobility and thus have the advantage to provide an arbitrary run-time for simulations. NEP describe solely which nodes are able to communicate with each other in a time dependent manner.
For many use cases mobility traces, models and NEP are available but with a lack in industrial scenarios [199]. This leads to the usage of typical models like the Random Way-Point Model (RWPM) or the Manhattan model [33, 22, 162].
The first time DTNs were proposed was in the context of interplanetary space-probe communication [83] but they were also used in contexts with only sparsely spread nodes [124].
WSNs are a kind of network that is proposed in various literature, sometimes as an ad-hoc and sometimes as an infrastructure based network [1, 242, 36]. Thereby, mostly an optimization towards low cost low energy solutions is present [137]. Although Arvind et al. [36] discuss the usage of WSN in industry, the focus on energy efficiency is dominant. MSNs are an special case of WSN including mobility [188].
An typical approach to optimize ad-hoc networks is clustering to enable scaleability, mobility and reduce energy consumption, to improve route life span, reduce overhead or for load balancing [21].
Surveys on ad-hoc and routing exist in [44, 107]. A metric to describe the overhead of ad-hoc routing protocols is the complexity of the number of messages sent compared to the number of nodes n [203, 44]. The same accounts for message size and storage needed per node. Low complexity routing and communication algorithms for MANETs that are designed for their specialized purposes provide a complexity for the number of messages of $\mathcal{O}(n)$ with a message size complexity of $\mathcal{O}(1)$ and storage complexities of at least $\mathcal{O}(n)$ if the algorithm determines the network state [44, 203].
Generally, any communication technology that enables P2P communication can be used for ad-hoc networks. This includes the 802.11 family, cellular technologies from LTE Release 12 on (sidelink mode one and two) and Release 14 on (sidelink mode three and four) [167], VLC [160, 178], Bluetooth, ZigBee and Radar [154].

2.3.2 Software defined networking

Software-Defined Networking (SDN) describes an approach that aims at separating control plane and data plane in networks [109] and thereby simplifying usage, monitoring and network management [190]. Due to separating control and data plane and no longer integrating both into one device it becomes possible to define forwarding / routing rules based on network wide knowledge [109]. One or a few controllers control the forwarding rules and supply the rules for other network devices [73]. This makes the network directly programmable [27]. Generally, the usage of SDN degrades the raw performance indicators of networks due to the overhead this paradigm introduces, but the improved orchestration of the network provides an overall improved network performance [93].
By introducing the paradigm SDWSN, SDN was brought to the factory floor [137] and

is relatively new to the industrial domain [27]. Thereby, the literature survey by Kobo et al. [137] focuses on typical WSN parameters instead of latency and reliability that are the key parameters in this work. Anyway, SDN can be used on top of industrial real-time communication technologies [27].
SDN is a paradigm that can be used in the industrial domain but further examinations are needed. A lack of investigation is especially present for implemented solutions and their empirical evaluation [137].

2.3.3 WiFi / WLAN

Currently the variants of the IEEE 802.11 family (Wireless Fidelity (WiFi)) are predominantly used on the factory floor [154, 84, 119] with still mainly WiFi 4 alias IEEE 802.11n. In the following the term WiFi is used as synonym for WLANs adhering to the IEEE 802.11 standard.
WiFi generally has the drawback of having a non-deterministic behavior and thereby having longer latencies of $> 50\,\mathrm{ms}$ [153]. Additionally, WiFi uses the Industrial Scientific and Medical (ISM) band that is completely allocated in most factories [154] and thus WLAN cannot solve any bandwidth problems [160].
The evolution from IEEE 802.11a to IEEE 802.11ac mainly focuses on enhancing the bandwidth by enabling higher Modulation and Coding Scheme (MCS), wider channels and introducing the usage of Multiple Input Multiple Output (MIMO) in WiFi 4 [134]. Although there is a mechanism to use contention free channel access in current WiFi standards this feature remains nearly unused [134].
A possible enhancement of the performance of WiFi is illustrated by [153] by employing two independent links via two different Access Points (APs).
Due to WiFi being the most used wireless technology on the factory floor it serves as performance base line. Lucas-Estan et al. [153] illustrate within a factory alike set up that a mean latency $> 120\,\mathrm{ms}$ easily appears. Even if using two redundant links, still $\approx 60\,\%$ of the packets have a latency above $120\,\mathrm{ms}$.

2.3.4 5G and cellular

5G has to fulfill a wide set of use cases spanning from smart phones in public networks to applications on the factory floor. Thus, 5G has three generic service types:

1. enhanced Mobile Broadband (eMBB)
2. massive Machine-Type Communication (mMTC)
3. Ultra-Reliability and Low Latency Communication (URLLC)

Hereby, each service-type prioritizes the KPI differently [7]. KPIs in cellular networks are throughput, latency and reliability.

- eMBB is the service that is optimized for high throughput in data-hungry applications, like video streaming
- mMTC is the service designed for IoT applications with massive amounts of devices, that send small data-packets in a sporadic manner
- URLLC is optimized towards low latency and high reliability for use cases like autonomous driving or factory automation. So, 5G is the first cellular technology

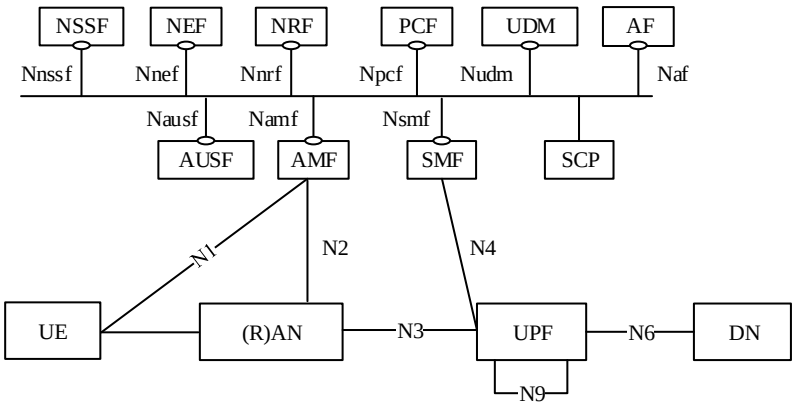

Figure 4: Overall 5G architecture including the core network [8]

that is partly designed for use cases in the context of industry [173]

In this section two different parts of the 5G network are examined. There are the core network and the Radio Access Network (RAN). Although the core network experienced major, revolutionary changes [220] by shifting towards a software oriented architecture the main latency reductions and reliability enhancements take place in the RAN. Therefore, firstly the 5G core network is examined and the most relevant characteristics are surveyed briefly and afterwards the RAN of 5G is discussed in detail.

Fig. 4 illustrates the overall 5G architecture as it is standardized [8] with a focus on the core network and its function. Thereby, the building blocks in the figure are:

- Application Function (AF)
- Authentication Server Function (AUSF)
- Access and Mobility Management Function (AMF)
- Data Network (DN)
- Network Exposure Function (NEF)
- Network Repository Function (NRF)
- Network Slice Selection Function (NSSF)
- Policy Control Function (PCF)
- Session Management Function (SMF)
- Unified Data Management (UDM)
- User Equipment (UE)
- User Plane Function (UPF)
- Radio Access Network (RAN)
- Service Communication Proxy (SCP)

and illustrate the service oriented architecture by enabling the on-demand orchestration of the network functions [24].

The network functions in the 5G core network are completely virtualized and this adheres to the paradigm of Network Function Virtualization (NFV) [177, 8]. In addition, this enables to employ the paradigm of Software-Defined Networking (SDN) that is en-

visioned for the 5G core and already tested for performance with positive results [24]. Much of the research examining the effects of SDN in the core network add an extra SDN controller into the core network and is based on the openFlow protocol [177]. Thereby, the network functions are decoupled from the hardware enabling higher flexibility [177], aiming to be stateless [8]. Also, Mobile Edge Computing (MEC) will be used for applications using 5G [213] as well as the 5G core itself [88]. Thereby, MEC brings UPFs closer to the user and reduce latency [88].
This newly designed core network, that is a significant change to the previous core network from LTE [220], is needed to cope with the wide variety of use cases proposed for 5G [177]. Inside the core network trade-offs between capacity and latency, storage and link load as well as memory and data rate have to be made [177].
Furthermore, the 5G network has a split between the Control Plane (CP) and User Plane (UP). The UP transmits the user data and thus includes routing functionalities and enforces the Quality of Service (QoS) policies. The CP contains all the functions managing the network like e.g. authentication, mobility management or network exposure. The UP and CP are decoupled and the information exchange between them is minimized.
The remainder of this section focuses on improvements for URLLC that are taking place in the RAN. Mainly Release 15 of the 5G standard is discussed. 5G as any other cellular technology is standardized in releases with a new one approximately delivered each 18 months.
The improvements of 5G RAN, that is also called New Radio (NR), compared to LTE RAN can be structured by reducing latency, enhancing reliability or providing more bandwidth.
Latency, reliability and throughput on the air interface are limited by a fundamental trade-off [214, 218]. Improving one of these three performance indicators degrades the other two, as long as parameters like processing times, resources and antenna gain are constant. If for example resources are reserved for low latency transmissions, throughput will be harmed because those resources can not be used for other transmissions. But if for example processing times are reduced, the latency will be reduced without harming reliability and throughput. Thus, there are two different kinds of improvements towards latency:

- Those affecting other KPIs
- Those not affecting other KPIs

Another aspect of resource usage of the RAN needs to be considered. The radio interface works with resources in the dimensions

- Time
- Frequency
- Space

It splits the resources into blocks for different users. The resource assignment for each user is done by a scheduler [132]. In the following a resource refers to a part of time and frequency within the range of one Base Station (BS).
Firstly, enhancements reducing latency are examined:

Transmit Time Interval:
The Transmit Time Interval (TTI) is defined as the shortest resource that can be scheduled. It defines the shortest block in time that can be assigned for a transmission. The LTE standard is optimized for mobile broadband and thus works with the relatively long TTI of $1\,\mathrm{ms}$. This length is good for throughput as the relation of overhead and information is well balanced.
Assuming a new transmission arrives directly at the beginning of a new TTI. In this case the transmission has to wait at least for one complete TTI. This illustrates, why $1\,\mathrm{ms}$ is too long for URLLC applications and why it has to be shortened [183, 121, 184, 239, 147, 133, 132, 180, 91, 179].
While latency is reduced the relation of transmitted information and overhead gets worse. Hence, it is not optimal to work with a shorter TTI in general. It is better to adapt the TTI and therefore the overhead for each use case [147].
Thus 3GPP agreed to use a flexible TTI [3, 15, 6]. TTI-lengths of $1\,\mathrm{ms}$ or shorter are possible. A TTI with a length of $1\,\mathrm{ms}$ consists of 7 or 14 symbols and can be divided into mini-slots that are at least 2 symbols long [3, 6]. So, a mini-slot equals $0.125\,\mathrm{ms}$ [15].
Trials and simulations with reduced TTIs between $0.14\,\mathrm{ms}$ and $0.25\,\mathrm{ms}$ report latencies of $0.4\,\mathrm{ms}$ to $3.3\,\mathrm{ms}$ [38, 184, 179]. Thereby, different scenarios and assumption about the 5G network are included. Field tests with a TTI of $0.25\,\mathrm{ms}$ show that a latency of $1\,\mathrm{ms}$ can be achieved [116, 117] in favorable channel conditions. Thereby, the channel conditions must be good enough, such that a packet fits into one transport block. Thus, a signal to noise ratio of $-3.1\,\mathrm{db}$ is needed to achieve a reliability of 10^{-5} with a latency of $1\,\mathrm{ms}$ for a $32\,\mathrm{byte}$ packet [117].
Scheduling:
A scheduler is an algorithm running at the base station to allocate resources to UEs [132]. The scheduler controls the resource usage and thereby the network performance of each UE.
Schedulers are generally designed to optimize a specific metric like throughput. In case of 5G, only optimizing for throughput is not sufficient, because 5G networks need to handle different kinds of services. So, further metrics must be considered depending on the service type. In the following, schedulers with a focus on latency and QoS fulfilment are of interest.
Besides the optimization metric, schedulers can be distinguished according to whether they are able to

- interrupt ongoing transmissions
- assign resources in a periodic manner

Thereby, interrupting ongoing transmissions has the advantage of reducing latency, however at the cost of corrupting another transmission. Schedulers that are able to interrupt transmissions are called **pre-emptive**, while other schedulers are called **non-pre-emptive**. Within 5G, pre-emptive scheduling is a standardized option [3, 6, 4].
The second characteristic, which is the ability to assign resources in a periodic manner, reduces latency and the signaling overhead for periodic occurring transmissions. For example, if a new packet arrives every $200\,\mathrm{ms}$ for the next $2\,\mathrm{s}$, all those packets can be

scheduled at once. This operation is called **semi-persistent scheduling** [3, 15, 6].
Commercially used schedulers are proprietary and thus not available. Therefore, schedulers from research literature are examined to understand the principles offering the highest gain with respect to latency [133, 132, 147, 180].
Three schedulers of interest remain, because they perform best in already tested scenarios, but have not been compared yet:

- Pre-emptive Proportional Fair (PEPF) [180]
- User Centric Latency Aware Schedule (UCLA) [147]
- Low-Latency Communications Proportional Fair (LLC-PF) [133]

Among those, the only pre-emptive scheduler is PEPF that aims to maintain high throughput for eMBB and to reduce latency for URLLC. While PEPF does not cope with corrupted messages, signal space diversity and an improved hybrid automatic repeat request process can be applied to increase the number of decoded messages [239, 183].
PEPF generally works with the assumption that eMBB traffic is scheduled with longer TTI than URLLC, so the complete eMBB transmission is never corrupted [180]. The longer TTI for eMBB is due to the high data rate in combination with less demands on latency.
The key characteristic of the other two scheduler is that they take all queued packets into account for scheduling and plan the schedule until the last packet is sent. So, not only the resources of the following TTI are taken into account, but all following TTIs, that are needed to send all queued packets [132, 147]. This optimizes the number of packets meeting their QoS requirements. Additionally, UCLA works with variable TTI lengths [147]. This reduces the overhead and improves eMBB throughput without harming URLLC traffic.
Overall, 5G enables a new variety in schedulers especially with the concepts of pre-emption and semi-persistent scheduling.
Radio Access:
In a cellular network the radio resources are managed by the Base Station (BS). If an UE wants to send data and the BS is not aware of it, the UE has to access the radio resources without prior knowledge of the BS. For this purpose different radio access protocols are used. The process of radio access adds onto latency.
The main difference between such protocols is which packets can collide. Hereby, collided packets usually can not be decoded at the receiver. Due to the nature of wireless networks, collisions occur in every radio access protocol. These protocols are distinguished if the packets carrying the user-data can collide or not. If the user-data packets can not collide, a radio access protocol is called *collision-free*, else it is called *contention-based* [205, 212]. This definition is not in line with the definition by 3GPP, as they call protocols collision-free if no collision at all can occur. This is only possible with two constraints of which one cannot hold true in cellular networks. Firstly, the BS has to assign resources to UEs without knowing whether they want to send data or not [15, 6]. Secondly, the BS has to be aware of the UEs presence. New UEs entering a BS need some contention based access.
In research literature three different radio access protocols are compared. The LTE radio

Figure 5: radio access in 5G

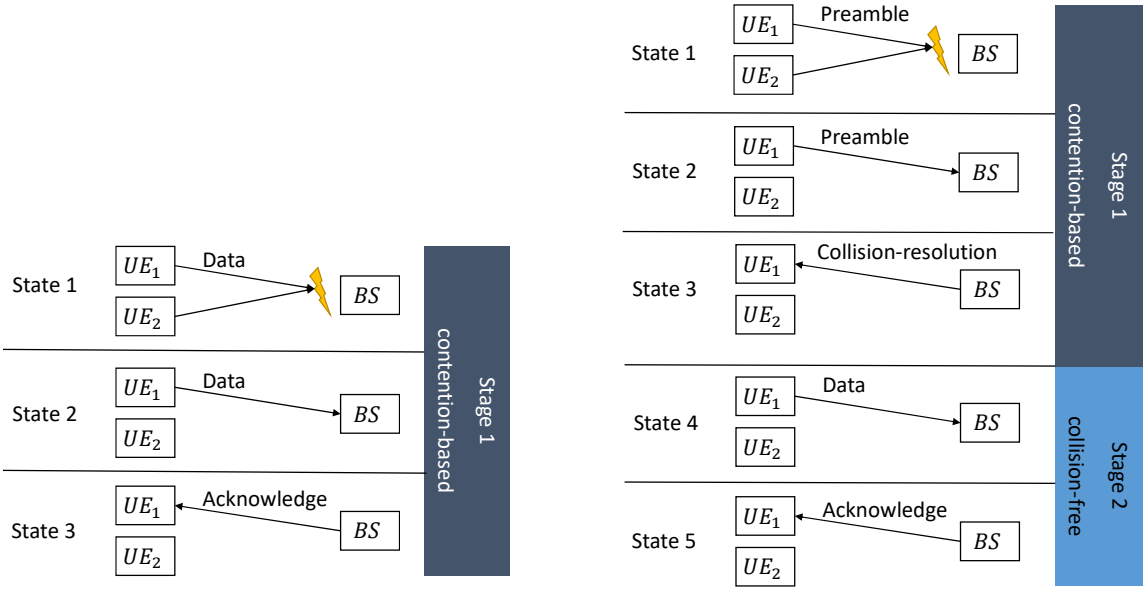

(a) Contention-based radio access

(b) Collision-free radio access

access protocol, referred to as a "three stage protocol", a so called "two stage protocol", that is identical to Fig. 5b, and a contention-based "one-stage protocol" that is identical to Fig. 5a [205, 61, 52].

In Fig. 5a contention-based "one-stage" radio access is illustrated. Three states of the radio access are shown. At state 1 two packets collide, so the BS cannot decode any packet. State 2 shows a data-transmission without a collision. State 3 shows the acknowledgment for the received data from State 2.

In Fig. 5b "two-stage" collision-free radio access is shown. In a collision-free radio access protocol the transmissions carrying user data can not collide, but the transmissions used for signaling can collide. This is an advantage because the signaling messages are way smaller than the user data messages. The message used for signaling is called preamble in 3GPP systems [16, 15] and contains the request for resources to send data. In state 1 a collision is shown, but the collided packets contain only the control data for the random access. As both UEs do not receive a collision resolution message (called random access response [16, 15]) they have to send the preamble again. In state 3 the BS sends the collision resolution message that carries the information when to send the data, called scheduling grant. This is followed by the data transmission (state 4) and an acknowledgment (state 5). If no collisions occur the procedure is shorter in both protocols.

Up to 3GPP Release 14, LTE exclusively utilizes a collision-free radio access protocol [61, 205, 11]. Starting with Release 15, an additional radio access protocol with no scheduling grant (contention-based) for a transmission is standardized for URLLC [6, 3].

In the collision-free protocols in LTE and 5G two additional messages are exchanged compared to Fig. 5b due to another collision resolution mechanism [11, 16, 205, 61].
As each stage of a radio access protocol adds overhead, the one-stage protocol is the most light-weight protocol, but degrades fast by means of throughput if the load increases. Generally contention-based protocols outperform collision-free protocols for low load by means of latency and reliability. The load at which the three stage-protocol begins to perform better depends on the scenario, although suitable loads for contention-based access occur more likely in an Internet of Things (IoT) or mMTC scenario than in an URLLC scenario [205, 61, 212, 52]. Thereby, in an IoT or mMTC scenario devices send sporadic small messages, that can cope with longer latencies.
To improve performance in such cases with Release 15 contention-based radio access is introduced in addition to collision-free access [6, 3, 4].
For further optimization in radio access Chen et al. [65] propose to reserve some of the random access resources exclusively for URLLC traffic. Depending on traffic load URLLC should be allowed to use the random access resources for URLLC and eMBB. Regardless which of those two variants is used, the performance is improved compared to no resource reservation for the URLLC traffic. Standardization enables to reserve random access resources for URLLC traffic with Release 15 [15].
Hybrid Automatic Repeat Request:
Messages that are sent over an unreliable channel like a wireless link may be corrupted. Thus some redundant information is added to each message, so the receiver can check the messages for consistency and correct some errors. If the message is that corrupt that the receiver cannot correct all errors, it will not send an Acknowledge (ACK) or will send a Negative Acknowledge (NACK) and the message or parts of it will be resent. This mechanism is called Hybrid Automatic Repeat reQuest (HARQ)).
So, HARQ improves the reliability of a single message and improves spectral efficiency at the cost of higher device complexity, more processing and higher latency. Therefore, HARQ exploits diversity in the time domain [163]. Re-sending messages has a huge impact on latency.
The time needed between sending a message and sending it again due to a NACK is called the HARQ RTT and is measured in the number of TTIs [54, 132]. Thus, TTI and HARQ RTT correlate directly. The HARQ RTT in LTE is 8ms or $8 \cdot TTI$ [146].
To improve the HARQ process, different parameters can be varied:

- TTI length
- retransmission scheme itself
- retransmission timing

The TTI has already been discussed above. The retransmission scheme can have three different designs.

- LTE-like solution: resending of messages only after NACK or time interval with no feedback
- The BLIND-scheme: resending the same message until a ACK is received
- The HYBRID-scheme: after a time interval the message is resent until a ACK is received

Among those three, the HYBRID solution is preferable, as in 80% of the cases it uses the same resources as the LTE-like solution but still performs better in terms of latency than the LTE-solution [54]. The time interval when the HYBRID scheme starts to resend the message is given in number of TTIs.
The retransmission can happen as fast as possible of after a static time interval reducing the degree of flexibility. [163]. 3GPP states that the UE has to indicate with which HARQ RTTs it is able to deal with and sets no other boundaries for the RTT [7]. With the only boundary being the capability of the UE, the HARQ RTT was realized with $0.75\,\mathrm{ms}$ to $1\,\mathrm{ms}$ in field tests. Thereby, the HYBRID retransmission scheme was used [116, 117]. The exact HARQ process is described in [10, 16] and in standardization a HARQ process in sub-slot dimension (so within $1\,\mathrm{ms}$) is enabled [145].
Multiple Access Schemes:
3GPP mandates Orthogonal Frequency Division Multiple Access (OFDMA) as multiple access scheme for 5G URLLC [15, 13], and promising field tests for URLLC took place using OFDMA achieving latencies of $\approx 1\,\mathrm{ms}$. Both field tests were conducted using a frame structure close to 5G numerology, took place in Yokohama, Japan and were performed by NTT Docomo [116, 117].
In research literature work on different multiple access schemes can be found, but due to the performance of OFDMA combined with its low computational complexity it is still favored for URLLC [52, 79]. Anyway, in other usage scenarios with an eMBB focus Sparse Code Multiple Access (SCMA) can be favored [239, 52].
In a further field test that tested polar code, massive MIMO, filtered OFDMA and non-orthogonal access schemes with several static UEs, SCMA improved throughput by 90% compared to OFDMA in an eMBB scenario [235, 77]. Hence, multiple access schemes are not further examined due to the consensus for URLLC and because there are no changes in comparison to LTE.
Duplex:
The duplexing mode describes how the link is used for uplink and downlink: in a Time Division Duplex (TDD) system the communication link is divided into time slots that can either be used for uplink or downlink. In a Frequency Division Duplex (FDD) system two different links with different carrier frequencies are used. One for uplink and one for downlink. The duplexing mode is not of high importance as all mentioned concepts work in TDD and FDD as well [179]. In full duplex uplink and downlink take place at the same time using the same frequency. Thus full duplex has the advantage of improving resource usage by the factor 2, which is good for resource usage but does not effect latency.
For the 5G RAN TDD and FDD are standardized [6, 7, 18].
Now, improvements towards reliability are discussed. These, of course are as well limited by the fundamental trade-off between the KPIs.
The most important concept to improve reliability is diversity: channels with different characteristics are used for the same message and hereby differences in fading, interference and errors are exploited [192, 191, 172, 125, 122, 112]. The concept of diversity was first discussed in [53].

Within the dimension that can achieve diversity, time is the most problematic as it always enlarges latency, because packets are sent successively. HARQ illustrates this and is an example of using time diversity to improve latency. Diversity in the frequency domain describes the usage of different frequencies for the same message and diversity in space can, for example, be achieved by two different BS receiving the same message. Similarly, different Radio Access Technology (RAT) can be used to generate diversity, too [146, 192].
In addition to diversity, advances in single technologies can improve reliability as well. An example is channel coding where improved channel codes enhance reliability without harming latency.
In the following different methods to improve reliability will be presented with many of them exploiting diversity in one way or another.
Packet Duplication:
If a packet is duplicated and each packet is sent over an independent link this is called PD [192, 191]. Thus, the reliability of this packet is improved. PD is standardized by 3GPP [15, 6].
In case the UE is only in the range of one BS, the duplicated packets can only be sent to the same BS via different frequencies. This is called Carrier Aggregation (CA). If the UE is within the coverage of two or more BSs, different frequencies can be used as well. Additionally spatial diversity can be exploited, if the BSs are not collocated at the same spot. The case involving two BSs is called Dual Connectivity (DC).
The usage of PD reduces the Signal-to-Noise-Ratio (SNR) requirement in comparison to LTE without PD in the dimension of $4\,\mathrm{dB}$ depending on the packet size and latency requirement [192]. In some scenarios, the resource usage of PD is higher than the resource usage without PD. A reduced resource usage by PD can occur based on the higher diversity and the thereby resulting ability of sending packets with a higher MCS. Thus, there is the need to dynamically decide, if PD is useful [192]. To optimize the resource usage Gebert et al. [92] propose to sent packets alternating over two different links instead of duplicating them and illustrate that this is advantageous if the application using the link can tolerate some lost packets.
Multi radio access technologies:
To improve reliability single UEs can use different RATs at the same time, because different RATs generally introduce diversity. This diversity emerges from different carrier frequencies, different BSs belonging to the different RATs and different times when packets are sent. The usage of different RATs at the same time is called Multi-RAT.
The used RATs can be 3GPP or non-3GPP RATs. An example for Multi-RAT with a non-3GPP RAT is the usage of WiFi for load offloading as it is standardized from Release 15 upwards [8]. URLLC traffic however, can not be offloaded to a WiFi-network, because no latency can be guaranteed in this case. Anyway, eMBB traffic can be offloaded and this frees resources for URLLC.
Multi-RAT within 3GPP-RATs can happen in case of packet duplication with dual connectivity, if the involved BSs are LTE and 5G.
In LTE and 5G there is a standardized direct communication link from one UE to another

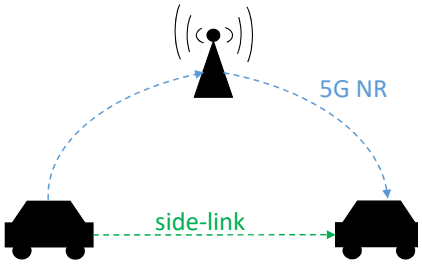

Figure 6: Side-Link and 5G New Radio

for vehicle-to-everything (V2X) communication [167]. This direct communication link is called side-link and uses the PC5 air-interface [146] and thus is an additional 3GPP-RAT. With side-link, Multi-RAT with two 3GPP-technologies is possible and hence of high interest for URLLC. The possible usage is shown in Fig. 6.
Side-link has four different modes. Modes 1 and 2 are not suitable for URLLC, because they are designed for long battery lives at the cost of high latency. Hence, only the modes 3 and 4 are of interest for URLLC applications [167]. While mode 3 needs cellular coverage, mode 4 does not. Additionally, mode 4 can be configured in a way that every packet is sent twice to improve reliability [167]. Side-link uses own resources and semi-persistent scheduling is enabled in mode 3 and 4 [10].
Side-link alone does not enable URLLC generally and is highly depended on parameters like data-traffic occurrence, number of UEs and mobility [167]. But the usage of side-link in addition to the LTE-RAN can improve reliability. Hereby, the improvements compared to LTE only are in the magnitude of 10% enhanced packet arrival rates [146]. The simulation in [146] illustrates this for the use case of cars in a city with a density of $500 - 1000\, UEs/km^2$, packets with $212\,\mathrm{byte}$ that are sent with a frequency of $10\,\mathrm{Hz}$ and a communication range of $200 - 300m$. The maximum speed of the UEs in the simulation is $50\,\mathrm{km/h}$ [146]. Although this is not an industry scenario, it examines a case where the combination of infrastructure based and P2P communication provides advantages.
Another way to improve reliability is cooperation. Side-link messages can be repeated by UEs that are neither the source nor the destination node. This repetition can extremely improve reliability. In static scenarios improvements of the PER in the magnitude of two dimensions per repeating UE are possible [172]. For details on the usage of cooperation refer to [172, 125].
Multiple-Input Multiple-Output:
To further exploit diversity it is possible to use large numbers of antennas at the BS and several ones at the UE [50]. The usage of multiple antennas at receiver and sender is called MIMO or in cases of larger numbers of antennas Massive Multiple Input Multiple Output (MMIMO) [50, 94].
Already an antenna-configuration with a diversity order of 16 (which includes the antenna configurations $1 \times 16, 2 \times 8, 4 \times 4, 8 \times 2, 16 \times 1$) improves the SNR for a $100\,\mathrm{bit}$ packet that needs a reliability of 10^{-9} by approximately $75\,\mathrm{db}$ [122].

Generally, MMIMO can be used at any frequency as long as there is enough space for the antennas. For example at $2\,\mathrm{GHz}$ an antenna array with 400 dual-polarized antennas is sized $1.5m \times 1.5m$ [50] and thus only fits into a BS.
In a field test by Huawei with several static UEs it was shown, that there are significant improvements due to MIMO. In a multi-user scenario compared to a single user scenario the total throughput is 10 times higher. Thereby an antenna configuration of 64×2 (BSxUE) is used [77]. Diversity via MIMO is standardized. Hereby, up to 256 antennas at the BS and 32 at the UE are proposed [6, 7, 12]. For high-reliability networks MIMO with a 4×4 antenna configuration and with second order macroscopic diversity is proposed for practical implementations [218, 185]. The second order macroscopic describes that each UE is always able to connect to two different BS at the same time.
Channel State Information Process:
Link quality in wireless networks describes the disturbances a radio signal experiences during propagation. In a wireless network the propagation environment changes dynamically and thus the quality of the wireless link as well [139].
The Channel State Information (CSI) process in cellular networks is used to measure the quality of the wireless channel between UE and BS [15]. The UE measures the link quality and indicates it to the BS by the use of the Channel Quality Indicator (CQI) [184, 183]. The link quality can be measured periodically, semi-persistent or event triggered depending on the use case [15, 9]. During periods with communication the CSI process constantly determines the channel quality and thus introduces overhead. Thereby, 5G enables shorter cycle time for the channel measurements in its CSI process [218].
Cellular networks use dynamic MCSs that have to be chosen accordingly to the link quality. Therefore predetermined MCS exist [184, 183]. The BS uses the CQI to determine which MCS can be used so the UE still can successfully receive messages.
Block Error Rate (BLER), spectral efficiency and latency correlate [184, 122]. The choice of MCS aims for a certain BLER. In LTE this BLER is 10%, because this enables a high spectral efficiency but introduces the drawback of a higher latency on the air interface [184]. For 5G MCS aiming for BLER of $90\,\%$ as well as for $99.999\,\%$ are available [9, 145], with the latter one being part of Release 16. As well, for certain scenarios it is advantageous to use a fixed MCS that is enabled in 5G [145, 117]. CQI and BLER are related directly. For 5G it is necessary to adjust the BLER target, so TTI-length, load conditions and the service type are taken into account [183].
URLLC especially introduces another problem with the CQI. Due to the sporadic nature of URLLC traffic and the short messages, more mismatches between the real channel conditions and CQI appear. The usage of a low-pass filter for CQI is proposed in [184] and works well as long as UEs are not moving with high speed. Further, during one URLLC transmission the channel can be viewed as static, because the TTI is shorter than the coherence time of the channel. This especially accounts for shorter TTIs [218, 241].
Channel coding:
Channel coding is used in modern wireless communication systems to add redundant information and to correct errors that arise due to imperfect channels [244, 219]. This

redundant information is added by the usage of channel codes. This enables to correct errors without resending a message and to check if messages are received correctly.
The choice of channel codes is of high complexity as there are several parameters that influence this decision [244, 41, 219]. The most important parameters are:

- error-correction performance
- hardware efficiency
- flexibility
- decoding latency
- energy efficiency
- implementation complexity

Additionally the performance of each channel code depends on block-length, coding rate and channel conditions and thus an optimal channel code does not exist [219, 41].
So, the most significant reasons for the choice of channel coding are depicted.
Only channel codes that are able to approach the Shannon-limit [111], which is the theoretic limit of information that can be sent via an imperfect channel, are relevant for URLLC.
For 5G Low-Density Parity-Check (LDPC) codes and polar codes are intended by standardization [15, 14, 3]. While polar codes achieve low-complexity decoding and encoding [41, 219], LDPC codes have the ability of parallel decoding [244]. Both provide a good error-correction performance to improve reliability [219] and have lower decoding latencies than turbo codes [219, 244], that are used in LTE [76, 38]. In field test with several static UEs it was shown that polar codes outperfom turbo codes by means of throughput by approximately 10% [235, 77].
For further information refer to [244] for a complete overview and to [41, 219] for a focus on LDPC, polar and turbo coding. Note that the results are not completely congruent as research in this field is ongoing.
In summary, the most important factor for a latency reduction is a shortened TTI and for reliability it is diversity, preferably in the dimension space. Anyway, the overall performance is highly dependent on precise channel quality measurements [218]. This is accompanied by the fact that real world implementations providing empirical data are needed for complete system evaluations due to implementation loss [186].

2.3.5 6G - short outlook

Currently, the first early research regarding 6G as successor of 5G is published e.g. in [95, 220, 186, 198, 34] outlining ideas for research directions and changes from 5G toward 6G. As in cellular systems every ten years a new "G" emerges but only every 20 years a new value market emerges [186], 6G generally aims for similar use cases as 5G but needs to enhance them. Examples here are holographic teleportation, extended reality [220] or experience sharing [95]. These use cases as well as completely fulfilling the 5G vision leads to new demands towards 6G that are beyond just higher data rate, higher reliability and lower latency. Thereby, Fitzek et al. [86] claim that a new "G" as equivalent for a new generation of cellular networks is only a valid term, if the technological advance supports a change in generation. As well they propose that the

thinking in generations may get obsolete until 6G and will be replaced by a continuous evolution.
A trend that started with the evolution from LTE to 5G is the trend towards a microservice based architecture for the core network. From LTE to 5G, the transition toward a service-based architecture took place, and with 6G, this continues towards the microservice-based architecture [220]. However, this does not apply for the RAN that has to take its journey towards a service based architecture. Thereby, the RAN has to overcome the challenges of a physical layer that evolves faster than the user plane, several different physical layers that need to co-exist in 6G and to enable hardware like implementation for the physical layer [220]. Due to the different physical layers in 6G the core needs to be access agnostic or at least allow for a tight integration of different communication technologies [95, 220]. This is of high importance as it can be expected that not one single communication technology will suit all use cases [186] although a first step toward that integration is taken with the non-3GPP access function in 5G that enables to use other communication technologies within 5G [8].
Furthermore, the previously mentioned use cases illustrate that the number of cases needing deterministic networks grows and research therefore is conducted [198]. Thus, 6G is seen as an opportunity to overcome the best effort Internet Protocol (IP) architecture and replace it with an deterministic one. Also, this protocol needs to support a network of networks due to the expectation that a single network will not support the requirements of coverage and performance [220].
The thereby emerging trend may be called a mandate driven architecture. The mandate is the collection of all services that are needed to support a certain QoS requirement that the network is supposed to provide [220].

2.3.6 Visible Light Communication

Visible Light Communication (VLC) enables highly reliable communication in a small area and dense communication due to spectrum re-use in small areas. It is conceptually older then WLAN [148]. Generally, VLC can be integrated into current networks by either employing it as layer two equivalent Local Area Network (LAN) or by integrating it into 5G networks [148]. Additionally, VLC LANs can be used as stand-alone networks or as pure ad-hoc networks [178].
The propagation of light brings the drawback for deployment of mainly LOS. At the same time this provides the advantage of the inherent security of not penetrating any walls [178]. AS VLC is highly reliable in LOS conditions it can serve as an extension of wireless networks to enhance their URLLC features or enable a more dense network [148, 178].
The physical layer in VLC systems mostly uses Light Emitting Diodes (LEDs) to transmit and receive with photo-diodes or with imaging sensors and thus, is able to re-use existing infrastructure [178]. In differentiation to other wireless communication in VLC the modulation can not use phase or amplitude and hence uses for example intensity modulation or direct detection modulation techniques with four variants [178]:

- On-off keying

- Pulse modulation (PWM)
- OFDMA
- Color Shift Modulation (CSK)

There is a wide variety of standardization activities ongoing and some standards are already finished [113, 166]. Thereby, the validation for scenarios is often open [166] and no clear leading standard is established yet.

2.4 Statistical analysis of rare events

Although rare event analysis is a well investigated field of research [196, 231, 209, 51, 126, 43, 120] empirical data from wireless networks has some specialties while the definition of URLLC leads to the need of employing rare event analysis methods. Those specialties are an autocorrelated behavior of the empirical data and having rare events therein.

Often the significance of statistical data is determined by confidence intervals, as there are different simple methods to calculate those and can be intuitively understood [174]. Those methods construct confidence intervals typically based on the standard normal distribution together with the assumption of identically and independent distributed variables. Challenges like the precision of confidence intervals are discussed comprehensively in [174].

In the context of wireless networks in industrial contexts the challenge arises that the distribution of latency values is so far unknown. Thus, those values cannot be assumed to be normally distributed and most analysis methods approximate this distribution. This leads to the need to discuss methods that are designed for rare event analysis with unknown distributions in the data: analysis methods for rare events in network simulation are mostly based on Markov-Chains Monte-Carlo methods [150, 196, 151, 152, 233, 231].

A general overview of Monte-Carlo based methods is provided by Rubion et al [196]. The methods therein are categorized into purely Monte-Carlo, splitting and importance sampling. Thereby, the basic idea of Monte-Carlo is to solve problems by statistical approximation where problems can merely be solved analytically. Due to the large amounts of data this method needs, it can only be applied to rare events with some drawbacks [89, 236, 150]. This leads to the usage of importance sampling or splitting in such cases.

- *Importance Sampling* employs the basic idea to change the probability of a rare event within a simulation so the event occurs more often. Changing the probabilities in this manner is called "to perform a change of measure" [233, 89, 120] and is the key challenge of this method.
- *Splitting* in simulations is based on the idea of simulating segments more often in which the rare event occurs. This is done by saving simulation states from where on the rare event occurs more often and re-running the simulation from that state several times [196]. Splitting was first proposed by Kahn et al. [126] and rediscovered by [231, 43].

RESTART is an optimized sub-variant of splitting and was first proposed in [231] and is regularly used [101, 233, 151, 152, 232] and often combined with the Limited Relative Error (LRE) algorithm. In that case it is typically named LRE/RESTART. The LRE algorithm is described and further developed in [101, 208] while it was first proposed in [209]. The results of data analysis with this algorithm are the probability of the rare event, the correlation of the analyzed data and the relative error. The analysis is based on deriving a two sided Markov-chain from the original data and counting which states and state changes appear [209, 208]. It is highly relevant in the context of wireless URLLC that the LRE algorithm takes correlation into account. For the LRE algorithm Mueller et al. [171] discuss the usage of confidence intervals based on approximating the standard normal distribution. Although proof is provided that the central limit theorem applies, it is not stated how much data is needed for that approximation [171]. Anyway, this discussion was not included in following usage of the LRE algorithm [150, 151, 152, 233].
A theorem that provides a measure of the quality of the approximation towards the standard normal distribution is the Berry-Esseen theorem. It was first proposed in [47]:

$$|F_n(x) - \Phi_{(0,1)(x)}| \leq \frac{C \cdot \rho}{\sigma^3 \sqrt{n}} \tag{20}$$

With $F_n(x)$ being the normalized empirical CDF, $\Phi_{(0,1)(x)}$ the standard normal CDF, C the Berry-Esseen constant, ρ the third and σ the second moment.
All the discussed methods, although being used in the context of network simulation [150], have the challenge of being designed purely for simulations. However, there is a need to work with empirical data [186]. Furthermore, there is the constraint that the latency value from wireless networks or networks in general are autocorrelated [157, 156].
With the challenges of empirical data, that is limited in its amount, re-sampling methods are obviously helpful in this context. An overview on those methods is provided in [143] and especially relevant here is Moving Block Bootstrapping (MBB). Re-sampling methods generally are based on the idea to draw samples from the original data set to recreate the inference between estimated value and real value [143]. MBB was proposed in [142, 149] and has the significant advantage of being able to deal with dependent data. The difference to other re-sampling methods is based on drawing large blocks instead of single values from the original data set.
This overview illustrates that there are different statistical analysis methods available that are designed to analyze similar problems. None of them has the ability of working with autocorrelated empirical data and the rare events therein. Thus, there is a need to discuss new approaches on how to analyze measurement data from wireless URLLC networks.

3 Modeling Factory Environments

The modeling of factory environments has several facets. From those facets this section discusses firstly channel modeling and propagation, secondly the mobility of AGVs on the factory floor and thirdly encounters of mobile nodes in ad-hoc networks on the factory floor. So, this section focuses on lower layer parameters and parameters of intra-logistic processes in contrast to the following section that focuses on the higher layer parameters latency and reliability.

3.1 Propagation and channel modeling

Factory environments, as already discussed in Section 2, have their own specialties and are fairly scenario specific [207]. Thus, there is a need for further insights on the propagation conditions and how to model them. To enable this, measurements were performed on the factory floor of SEW-EURODRIVEs show-case production facility in Graben-Neudorf where electric drives and gears are mounted. The production was running during all measurements.
The measurements are split into three different scenarios within the production environment. The measurements took place in three different areas:

- AGV station
- AGV drive lane along a Production Cell (PC)
- inside a PC

Thereby, the AGV station represents an area that is used to exchange pallets between AGVs, different AGV fleets and other transportation systems. So, this area is open with lots of mobility including the pallets that are exchanged there. The AGVs employed in this area drive under the pallets that are placed on pallet stands to pick them up or set them down. Thus, in this area LOS and NLOS propagation conditions are available and the NLOS measurements result from placing antennas under pallet stands with a pallet on top. On those pallets gear and drive parts are stored consisting of conductive materials. The AGV station is shown in Fig. 7 including one AGV carrying a pallet and one of the antennas of the AGV is marked red.
The other two scenarios are illustrated in the scheme in Fig. 8. The triangle named *Tx* is the send-antenna mounted at $\approx 2.4\,\mathrm{m}$ height. The two black bold lines show the paths along which the antennas were moved to gain measurement from different distances. This means that the receiving antennas were placed at different positions on these black lines. In the scheme the production area is part of a PC where gears are assembled and are mounted to electric drives. AGVs that drive on the AGV drive path along which was measured are identical to the one in Fig. 7. Inside the production area collaborative AGVs operate to support the workers.
The modeling of propagation environments is based on the measurements of over 6000 Power-Delay-Profiles (PDPs) at approximately 100 locations with different antenna spacing. The measurements are split evenly along the three scenarios described previously. From that measurement data firstly path loss models are parameterized and secondly the Saleh-Valenzuela (SV) model is parameterized and an optimization for that model

is proposed.

For all propagation measurements the same measurement set-up was used [159, 158] and the measurement data is published at [100]. The measurement set up was described for the first time in [159].

The measurement set up consists of one Signal Generation (SG) and two Vector Network Analyzers (VNAs). The exact measurement hardware are a Keysight SG N5171B EXG X-Series RF and the VNAs are a Keysight P9371A and a Keyisght P9375A. They are used to perform measurements similar to so called S21 measurements. In a two port measurement system an S21 measurement describes the signal received at port 1 relative to the signal sent from port 2. The difference here is that there are four receiving ports of two VNAs. One of those ports is used as the reference and the other three are used to record PDPs. The signal source here is a SG instead of one port of the VNAs. This includes the difference that the reference signal is transmitted over the air. Thereby, the reference input port of the VNAs is connected to an antenna with $1\,\mathrm{m}$ distance to the antenna of the SG to receive the reference signal. For this purpose, a low loss coax-cable is used. The three remaining antennas are used to record three PDPs per measurement. Thereby, different distances between the three measurement antennas and between the sending antenna and the receiving ones are realized. The set up is depicted in Fig. 9.

Thereby, all antennas are omnidirectional antennas with $2\,\mathrm{dBi}$ antenna gain (Huber & Suhner Sencity Omni-S Thimble). The measurement bandwidth is $100\,\mathrm{MHz}$ with a time resolution of $1\,\mathrm{ns}$. The measurement frequencies are $2.15, 2.65, 3.85$ and $5.1\,\mathrm{GHz}$ and each PDP has a length of $1.5\,\mu\mathrm{s}$. The send power is set to $19\,\mathrm{dBm}$ and the send antenna is placed at $2.4\,\mathrm{m}$ height. The receiving antennas are at $20\,\mathrm{cm}$ height in accordance to the AGV use case depicted in Fig. 7. The spacing of the antennas was between $0.06\,\mathrm{m}$ and $1.5\,\mathrm{m}$. Per distance and antenna spacing ten PDPs were recorded.

From that data path loss models, delay spread, coherence bandwidth, the number of MPCs including their distribution and a completely parameterized SV model, that statistically describes PDPs, are derived in the following subsections.

Figure 7: AGV station with AGV

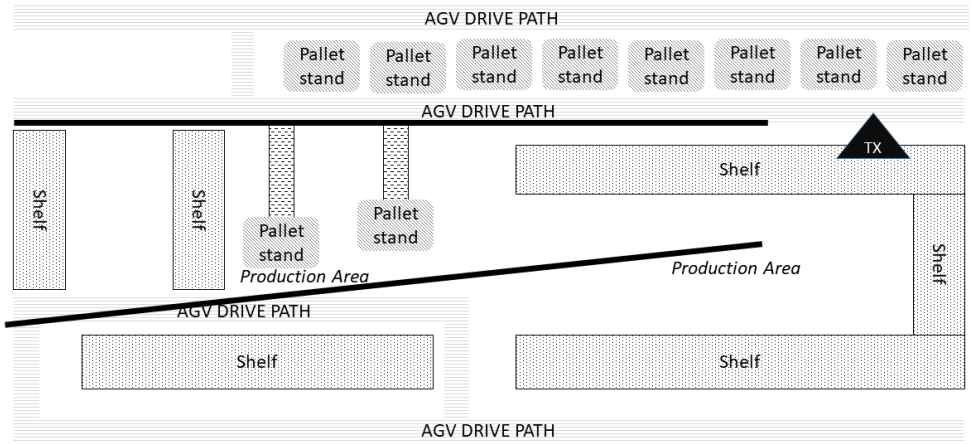

Figure 8: Measurement scenarios AGV drive lane an PC

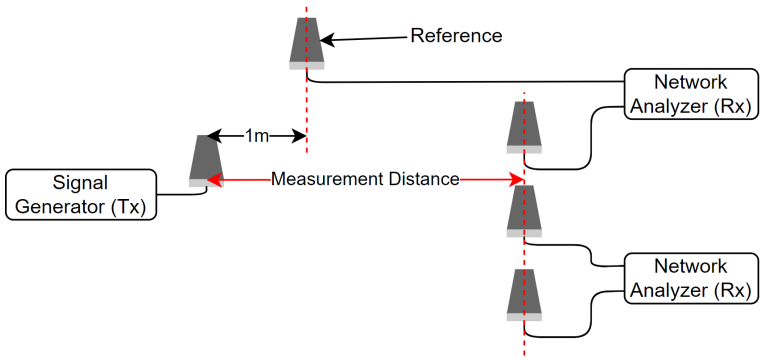

Figure 9: S21 measurement set up

3.1.1 Path loss

Based on the measurement data that was described previously three path loss models are parameterized. Three models were chosen because there is a wide variety of models that are regularly used and thus for reuse purposes it is advantageous to work with several models. The three models used here are:

- Alpha Beta Gamma (model) (ABG) model
- Close-in (CI) model
- log-distance model

The one-slope model is not used here, although [70, 71] provide the parameters for this model, but they provide the parameters for several other models as well and the difference to the CI model is rather small. The fitting for the ABG model is done by the least-square error method using the closed form equations provided by Sun et al. [217].

Table 4: Path-loss values ABG-model [159]

Source	PLE (α)	β	γ	σ
LOS (AGV lane)	1.12	28.63	2.98	3.20
NLOS (inside PC)	1.12	31.40	2.76	1.92
Schmieder et.al [207] LOS	2.27	27.29	1.94	1.62
Schmieder et.al [207] NLOS	3.02	28.35	1.78	1.61
TR 38.901 LOS [5]	2.15	31.84	1.90	4.30
TR 38.901 NLOS [5]	3.57	18.60	2.00	7.20
Jaeckel et.al [118] LOS	1.83	36.30	1.95	1.63
Jaeckel et.al [118] NLOS	2.41	29.10	2.54	3.58

With those equations Sun et al. extremely enhanced the ease of use of this model.
The parameters for the ABG model are shown in Tab. 4 including our measurements as well as the ones from previous work. Thereby, the smaller path loss exponent α is an obvious deviation from previous work. By looking at Fig. 10 this seem to be due to the shorter measurement distances. Those shorter distances are anyway realistic in industrial set ups as a macroscopic second order diversity is envisioned in dense deployments [218].
Tab. 4 summarizes the path loss values for the ABG model. The largest deviation is in the NLOS case between our measurement and Jaeckel et al. [118] as well as the 3GPP model [5]. In these models the NLOS case has a higher σ than the LOS case. This is completely contrary to our measurement results and may be due to the lesser mobility our NLOS scenario experiences compared to the LOS scenario. The NLOS case inside the PC is isolated from the high mobility areas like the AGV drive lane by the shelves that are shown in Fig. 8.

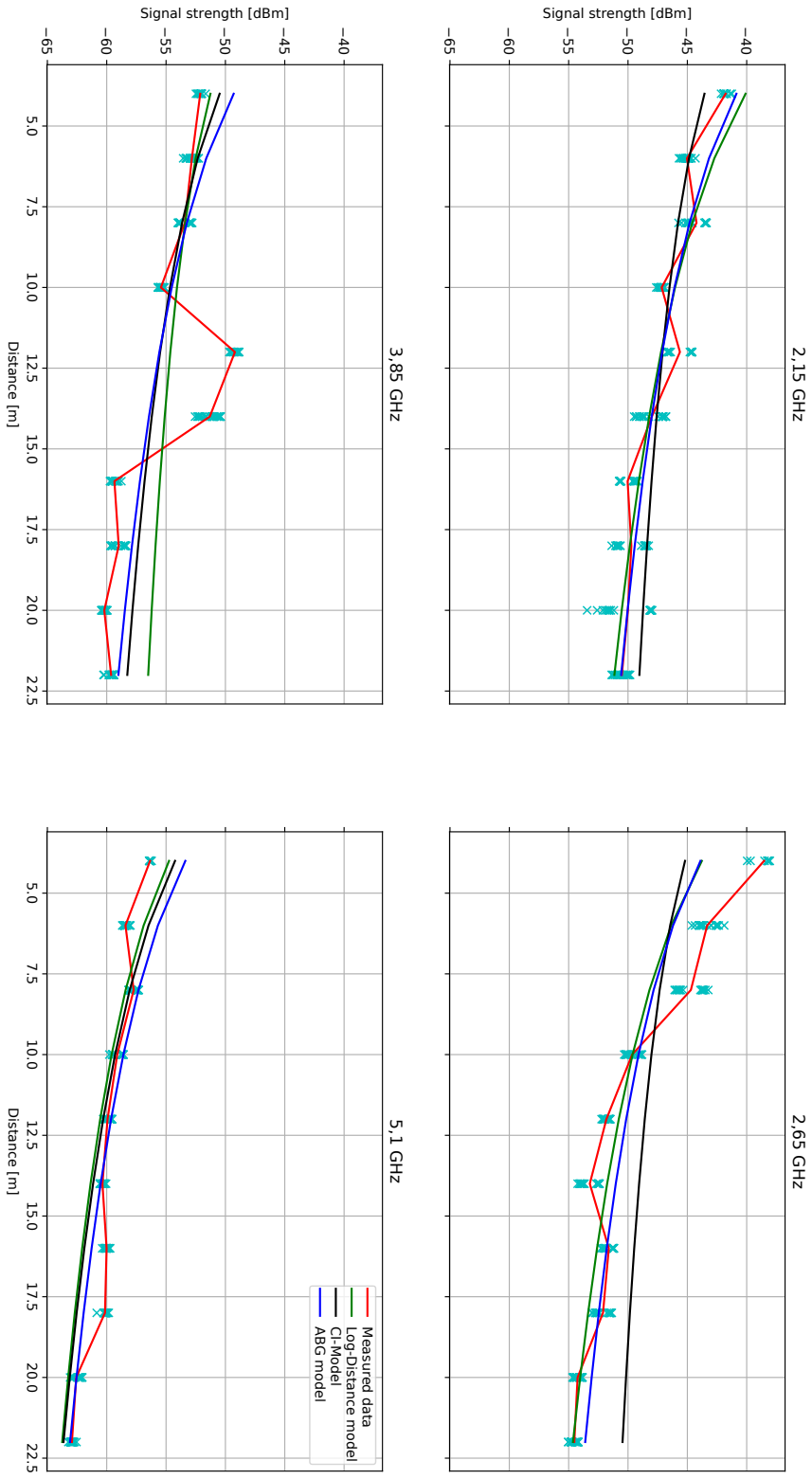

Figure 10: Path loss models in AGV lane, all frequencies [159]

In our case the main difference between LOS and NLOS is the initial path loss that is significantly higher in the NLOS case. This accounts for all path loss models. The parameter in the ABG model showing this relation is β that is $3\,\mathrm{dB}$ larger for NLOS propagation.

Table 5: Path loss values CI and log-distance model for AGV-lane (LOS) and inside PC (NLOS) [159]

Model	Frequency	α		σ	
		LOS	NLOS	LOS	NLOS
CI-model	$2.1 - 5.2\,\mathrm{GHz}$	1.23	1.44	3.22	2.30
Log-distance	$2.15\,\mathrm{GHz}$	2.39	3.08	5.95	5.74
Log-distance	$2.65\,\mathrm{GHz}$	1.54	1.35	4.02	4.45
Log-distance	$3.85\,\mathrm{GHz}$	1.70	1.54	3.65	3.93
Log-distance	$5.1\,\mathrm{GHz}$	1.83	2.56	4.21	5.86

The relatively small path loss exponent that occurs in the ABG model is also evident in the CI and log-distance model as shown in Tab. 5. The only outlier is the path loss in the log-distance model at $2.15\,\mathrm{GHz}$. Although not included in the table the values for both models with the antennas placed under the pallet stands are fairly similar to the NLOS propagation in Tab. 5.
All those values are in contrast to Chrysikos et al. [70, 71] due to far larger path loss exponents in their measurement. Generally, all this supports the statement of highly specific scenarios as stated by Schmieder et al. [207].

3.1.2 PDPs and the Saleh-Valenzuela model

This subsection discusses all parameters that are based on PDPs instead of only signal strength. Thus, the number of MPCs per Average Power Delay Profile (APDP), the delay spread and the resulting coherence bandwidth are included as well as parameterizing the SV model. This is done to provide further details regarding channel parameters in industrial environments.
Number of MPCs per APDP: when evaluating MPCs in PDPs the process of finding the peaks needs to be automated. There are two methods available in research literature: visually [127, 29] or one algorithmic based solution for peak searches that is challenging to implement [238]. As an algorithmic solution was needed here due to the vast number of PDPs a new, simpler method was developed: The idea is to use a search for local maxima in numerical data and evaluate the needed prominence. The evaluation for the prominence was done visually (prominence equals vertical distance). In implementation we used the function *find_peaks()* from *scipy.signal* with the prominence set to three and the lower bound for the peaks set to $5\,\mathrm{dB}$ above the highest value in the last $0.5\,\mu\mathrm{s}$ of the PDP [159].
Two example APDPs are shown in Fig. 11 including the results of the peak search with each peak marked by a yellow cross. Thereby, each peak represents a cluster in accordance to Eq. 19 which describes PDPs. Such a cluster is equivalent to a MPC. Generally,

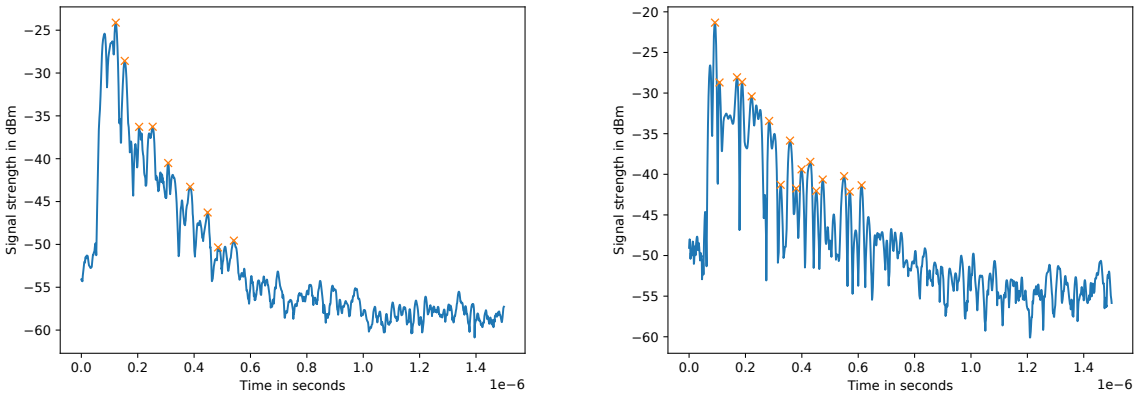

(a) LOS APDP at $5.5\,\mathrm{m}$ distance in the AGV station

(b) NLOS APDP at $6.9\,\mathrm{m}$ distance, antenna under a pallet stand

Figure 11: Example PDPs at $3.85\,\mathrm{GHz}$ with marked MPCs

the APDPs in our measurements are relatively long. Schmieder et al. [207] measured an APDP that reaches the noise floor after $550\,\mathrm{ns}$. This is in contrast to our measurements as therein the APDPs reach the noise floor after up to $750\,\mathrm{ns}$. Additionally, compared to [207] the MPCs in our measurements are far more distinct. This means that each MPC can be easily identified visually. In our measurements between two and 22 MPCs can be found.

The number of MPCs per APDP can be modeled using the gamma distribution [159]. By using the maximum likelihood method for fitting the parameters are determined to the following values: $\alpha = 18.9$, $\beta = 1.22$ in LOS and $\alpha = 14.3$ and $\beta = 0.83$ in NLOS conditions. The fitting with the empirical distribution and the fitted gamma distribution is shown in Fig. 12.

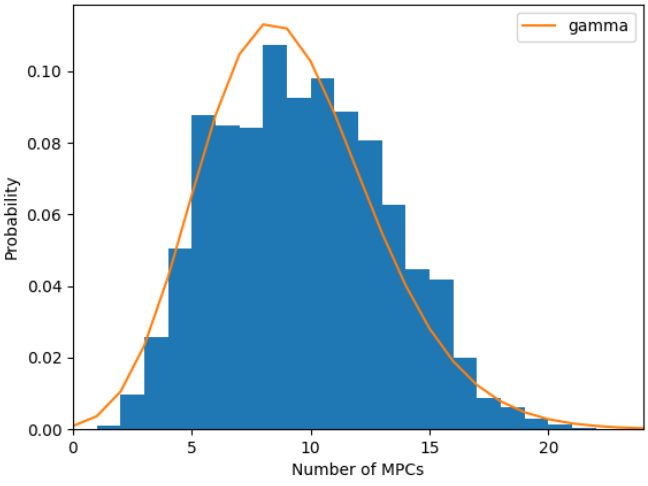

Figure 12: Fitting the Gamma distribution to the number of MPCs [159]

Further, we evaluated the reflective behavior of floor and roof. Therefore, we used a directional antenna facing the roof. In this set up clear MPCs can be identified with a delay that suit the propagation time between floor

Table 6: Delay spreads over all measurements and coherence bandwidths. PS describes the values from measurements from underneath of pallet stands

Scenario	2.15 GHZ			2.65 GHZ		
	LOS	NLOS	PS	LOS	NLOS	PS
Delay Spread [ns]	72,7	58,3	76,6	78,2	72,1	85,0
Coherence bandwidth [MHz]	2.2	2.7	2.1	2.0	2.2	1.9
Scenario	3.85 GHZ			5.1 GHZ		
	LOS	NLOS	PS	LOS	NLOS	PS
Delay Spread [ns]	62,2	56,0	83,2	47,2	42,8	43,5
Coherence bandwidth [MHz]	2.6	2.8	1.9	3.4	3.7	3.7

and roof. So, floor and roof show to be clear reflectors.
The *delay spreads* of all scenarios are shown in Tab. 6 together with the respective coherence bandwidths. As already examined the APDPs from the measurements are long and thus the delay spreads are large compared to previous works [118, 207, 5]. The only exception is from Jaeckel et al. [118] at $5.4\,\mathrm{GHz}$ where they found a delay spread of $80\,\mathrm{ns}$. This further illustrates that factories are rich scattering environments and current models do not fully cover the variances on the factory floor.
The *coherence bandwidth* as a measure of similarity in behavior can be calculated based on the delay spread. The delay spreads in our measurements are large. Thus, the coherence bandwidth is small, as shown in Tab. 6. From the viewpoint of exploiting diversity the smaller coherence bandwidth is highly relevant, because frequencies with an independent behavior are than closely collocated. In case of e.g. packet duplication the frequency selection needs to mind this. This is especially interesting as many works on packet duplication assume independent channels [192, 191, 92].

The *Saleh-Valenzuela (SV) model* as a detailed channel model was parameterized based on those measurements as well.
The inter cluster decay in the SV model can be modeled by an exponential or a linear behavior on the logarithmic scale. Which of those two variants provides better results is open since Ai et. al [29] found that the exponential decay function fits better for modeling their PDPs. To further elaborate that statement we use both decay functions defined by:

$$P_{exp}(T_l)[dB] = c \cdot e^{-\frac{T_l}{d}} + e \tag{21}$$

$$P_{lin}(T_l)[dB] = a \cdot T_l + b \tag{22}$$

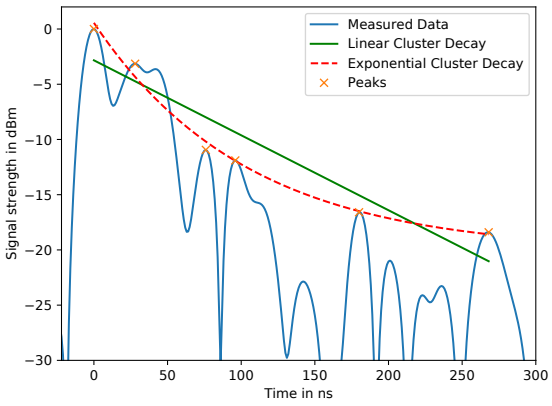

Figure 13: Example of fitting linear and exponential decay [159]

Table 7: σ of linear and exponential decay

Scenario	σ_{exp}	σ_{lin}	No. exponential fit better	No. linear fit better	σ_{fits}
AGV Lane	2.03	2.86	2022	125	0.046
PC	2.02	2.80	1330	131	0.034
AGV station	2.29	3.20	2913	127	0.029

Table 8: Correlation for number of MPCs and Γ [159]

Scenario	$\rho_{pearson}$	$\alpha_{Pearson}$	ρ_{rank}	$\alpha_{spearman}$
AGV Lane	0.011	0.60	0.42	< 0.001
PC	0.38	≈ 0	0.50	< 0.001
AGV station	0.027	0.14	0.28	< 0.005

as done in [29] and discuss their fitting quality. As a measure of goodness of fit the Root Mean Squared Error (RMSE) is used and per scenario (AGV lane, AGV station or inside PC) the median of all RMSEs is used. The RMSE is named σ in the following. The results are illustrated in Tab. 7 showing the clear advantages of the exponential fit. The exponential fit most of the time fits better.
Additionally, Tab. 7 contains the information in how many cases the linear or exponential decay fits better. In addition, the cases where the linear decay fits better the difference of the fitting was examined by $\sigma_{fits} = |\sigma_{exp} - \sigma_{lin}|$. Thereby, the results in Tab. 7 show that in those cases the difference of the two fitted curves is negligible.
Fig. 13 illustrates the difference between the linear and exponential fitting zoomed into one exemplary PDP. Overall, the RMSE is $29\,\%$ smaller when fitting with the exponential decay instead of the linear decay function.
Further, we evaluate the hypothesis that the number of MPCs and the inter cluster decay are correlated. For the evaluation of this the Pearson correlation coefficient $\rho_{Pearson}$ and the Spearman rank coefficient ρ_{Rank} are used. The Pearson correlation coefficient needs normally distributed variables while the Spearman rank coefficient does not need this. So, both coefficients were calculated as well as the error probabilities α for rejecting the hypothesis $\rho = 0$. The results are shown in Tab. 8 and illustrate clearly that there is a positive correlation of the number of MPCs and the inter cluster decay Γ.
Comparing our work to Ai et al. [29] we have up to ten times longer PDPs and this is reflected by a difference of factor three in the linear decay factor. For the exponential decay the factors c and e are similar from our measurements and Ai et al. [29]. Only the parameter d is larger by approximately eight. This has to be due to the longer PDPs. Interestingly, a similar behavior is seen in desktop LOS environment with mmWave [210] that shows results close to [29].
Close to our results is the outdoor NLOS measurement from Molisch et al. [168] but their other results are far from ours for the inter cluster decay. Also, the inter cluster decay in an apartment can be similar to our factory environment [67]. On body networks have

Table 9: σ of linear and exponential decay

Scenario	No. exponential better	No. linear better	σ_{fits}
AGV Lane	4894	14790	$9.60 \cdot 10^{-4}$
PC	3138	9536	$2.27 \cdot 10^{-3}$
AGV station	8863	26901	$2.20 \cdot 10^{-3}$

significantly smaller inter cluster decays [48].

For the intra cluster decay the evaluation whether a exponential or a linear decay fits our data better is performed as well. Thereby, the difference between linear and exponential decay was found to be small. The cases where the linear decay performs better and the number of cases where this is the case is illustrated in Tab. 9.

Although, in more cases the linear decay fits better the median of all RMSEs is $2.5\,\%$ lower for the exponential decay. Thus, the exponential decay should be favored to the overall lower RMSE for the fitting and the sake of smplicity of using the same kind of decay function.

When comparing intra cluster decays it is relevant that some work uses only the first cluster for the intra cluster decay evaluation [127]. Generally, the intra cluster decays our measurement have are similar to Adegoke et al. [26]. As well, results from a living room are similar [206]. Between [48, 67] and our measurements is a significant difference. Within our measurements we find no time dependence for the intra cluster decay as well as [168].

The cluster arrival rate is based on the assumption of single reflections as discussed in the related work section 3.1 [165], but this assumption does not hold true as already examined. Thus, for evaluating if a Poisson process [165] is suitable for modeling several distributions were fitted to our measurements. This fitting is illustrated in Fig. 14. The fitting errors of the different distributions illustrate that the Poisson process for the inter cluster arrivals is a reasonable choice. The fitting errors are shown in Tab. 10. The differences between Weibull, Gamma and the Exponential distribution are insignificant and Rayleigh, Rice and the Normal distribution have a larger fitting error than the first three. Thus, the original assumption on single reflection may not hold true, but modeling the cluster arrival with a Poisson Process is anyway suitable. All dis-

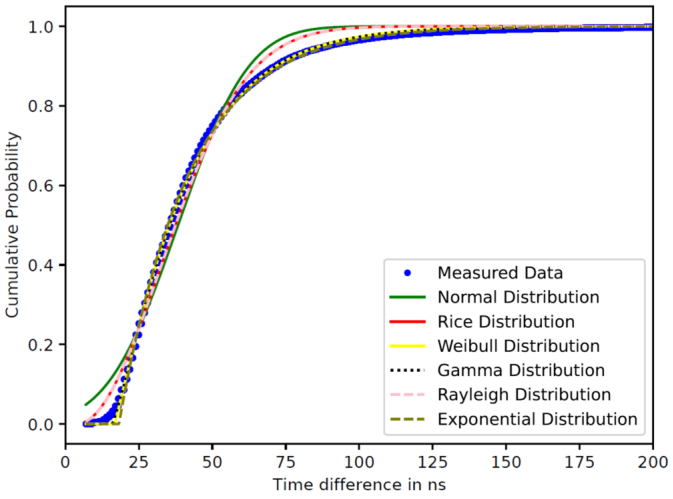

Figure 14: Fitting of the CDF of cluster arrivals

Table 10: RMSE of CDFs, AGV station

Distribution	Normal	Rice	Weibull	Gamma	Rayleigh	Exponential
σ	0.022	0.016	0.005	0.004	0.016	0.006

Table 11: Industrial SV Model Parameters

Scenario / Source	Γ in ns	a_γ	γ_0 in ns	$\frac{1}{\Lambda}$ in ns
AGV station	101.28	0.0064	6.28	23.93
AGV lane	90.75	0.0083	6.92	26.45
Production Area	80.86	0.0057	7.97	28.67
Assembly Room LOS [29]	-	0.36	-0.51	4.51
Mechanical Room LOS [29]	-	0.09	1.79	14.14
Incinerator Hall LOS [127]	12.62	0.80	3.52	15.83
Incinerator Hall NLOS [127]	29.78	1.19	4.13	13.10
Factory Hall B NLOS [127]	28.87	0.54	4.98	16.00
Factory Hall B NLOS [127]	24.01	0.69	2.53	12.53
Incinerator Hall LOS [128]	11.42	0.21	-	14.11
Incinerator Hall NLOS [128]	21.45	0.44	-	11.23
Machine WS LOS [26]	15.27 - 17.37	0.07 - 5.23	1.73 - 5.20	25.00
Machine WS NLOS [26]	19.74 - 29.12	4.34 - 5.13	6.65 - 106.3	33.33
Industrial [168]	13.47	0.93	0.65	14.10

cussed parameters from our measurements and other work are summarized in Tab. 11. Lastly, the relation of path loss and PDPs is examined. The idea is to change PDPs to power distance profiles and evaluate if they than match a typical path loss model. The idea is based on the assumption that the propagation of a MPC takes place in the same environment as the complete signal in a path loss scenario. The conversion of the PDPs can be performed using the speed of light and smoothing the curve. For the comparison the log-normal path loss model is used. When comparing the path loss parameters, that are derived from a PDP that way, they are similar to the path loss parameters obtained for the same model in [159] by the typical received power measurements at different distances. The measurements used in both cases originate from the same environment and scenario. So, this approach enables measuring path loss models from one location or defining the inter cluster decay based on received power measurements.
In conclusion, this section provides a complete parameterization and comparison to previous work of the SV model and illustrates the differences in industrial scenarios.

3.2 AGV movement descriptions

The mobility patterns and network encounter of AGVs on the factory floor need to be described to enable proper simulation and design of communication systems to connect these AGVs. Thus, this section discusses both those aspects. Firstly, the movement of AGVs is modeled statistically [199] and secondly Nodal Encounter Patterns (NEPs) from the factory floor [200] are examined.

3.2.1 AGV movement model

This section describes and analyzes the movement of AGVs on the factory floor. Therefore, the movement of 30 AGVs from an electronics production adhering to the industry 4.0 paradigm is examined. The movement was recorded over $48\,\mathrm{h}$. The AGVs use SLAM for localization and navigation with a precision of $\pm 5\,\mathrm{cm}$ and the locations of the AGVs are recorded.

The recorded movement patterns are compared to the typical mobility models RWPM [49] and the Manhattan model [162]. Furthermore, an improved node speed selection algorithm is developed. Lastly, a metric for describing the propagation conditions based on the mobility model is proposed.

Generally, properties of mobility models for MANETs are mobility metrics, connectivity metrics and protocol performance metrics [40, 224]. We focus on the mobility metrics here, as introduced by [40]:

- **Spatial dependence** describes the similarity between collocated nodes' movements
- **Temporal dependence** describes the relation of the same nodes' speeds at two points in time and is thus similar to autocorrelation
- **Relative speed** is the speed difference between two nodes
- **Geographical restrictions** describes the restrictions on movements of the nodes

Focusing on the mobility metrics circumvents the assumptions and parameterizations that are needed for the connectivity and protocol performance metrics.

The distance probability density function is described by:

$$P(a \leq \Delta < b) = \int_a^b PDF_\Delta(x)dx \tag{23}$$

with $\Delta = ||P_1 - P_2||$ as the distance between two nodes. The same equation applies for the speed PDF.

For the *approach speed PDF* it is important to note that we use the derivative of the node distance that includes the information if two nodes approach each other or move apart [199]. This is in contrast to Hsu et al. [114] who only use the absolute value.

The comparison of the empirical data to RWPM and the Manhattan model is done by operational validation. This means, that the model outputs are compared to the real world data.

Based on the recordings of the AGVs movement the parameters for the RWPM and Manhattan model were chosen. For RWPM the floor size was set to $170\,\mathrm{m} \times 170\,\mathrm{m}$ and for the Manhattan model to $150\,\mathrm{m} \times 150\,\mathrm{m}$ with a grid distance of $30\,\mathrm{m}$. The difference

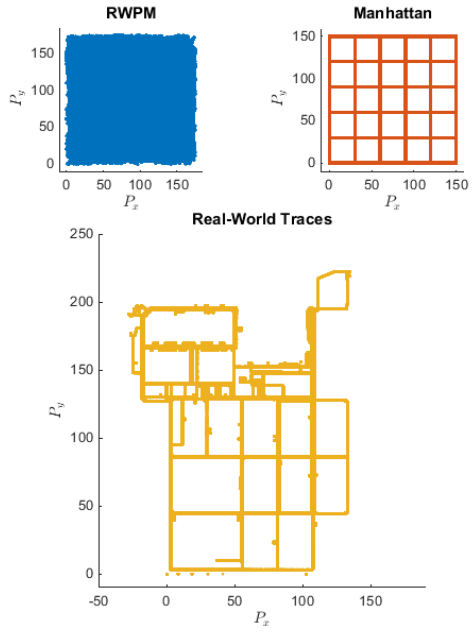

(a) Tracks of RWPM, Manhattan model and real world [199]

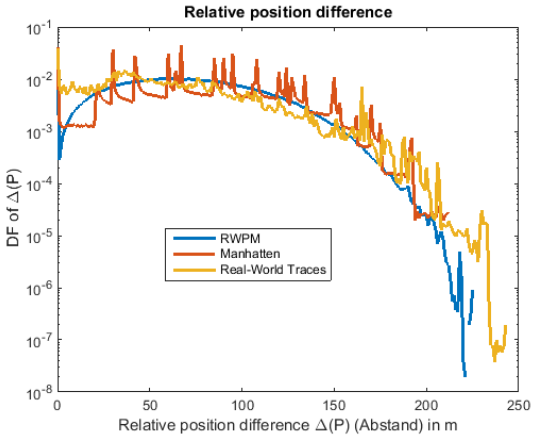

(b) Density of relative node positions [199]

Figure 15: Node density and movement patterns

results from AGV drive path normally not being directly at the edge of a factory. In both models the node speed is $v_r = 2\,\frac{\mathrm{m}}{\mathrm{s}}$. In the RWPM the node speed is chosen between 0 and v_r equally distributed in accordance to [49, 131, 80]. In the Manhattan model v_r is constant. This leads to the paths illustrated in Fig. 15a with an evident similarity between the real world paths and the Manhattan model. Thereby, the real world is an eroded Manhattan grid. In an eroded Manhattan grid some of the intersections and respective connections are missing but the general appearance is similar to a Manhattan grid.

Fig. 15b shows the PDFs of the nodes distances by means of the euclidean norm. Along the two models and the real world data a peak at $70\,\mathrm{m}$ appears. This is about one third of the maximum node distance. As well, the general behavior of the graphs is similar. Two characteristics thereby are noteworthy: the relative distances are smoother for RWPM and this is supposed to be due to the free movement of the clients. In the real world data and the Manhattan model the client movement is restricted by the tracks and thus certain distances have a higher probability of appearance. The second difference appears at distances $< 20\,\mathrm{m}$. For those shorter distances the probabilities in the real world data are significantly higher. This is due to AGVs in the factory aggregating in specific areas while they are parking, charging or generally not in use [199].

The approach speed of AGVs is a measure for the dynamics of a MANET deployed

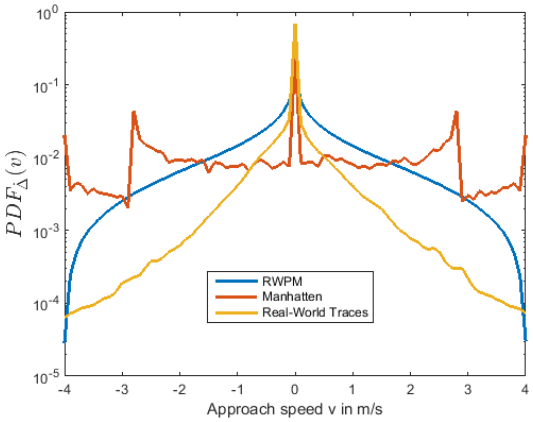

(a) Approach speeds from real-world and models [199]

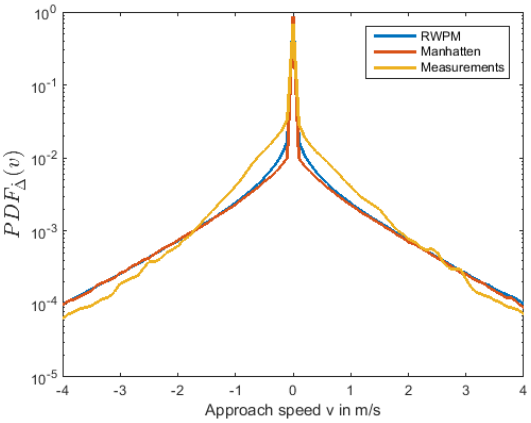

(b) Approach speed from real world and models with new speed selection algorithm [199]

Figure 16: Approach speeds

among the AGVs as higher approach speeds of the AGVs illustrate a more rapid change in the topology and shorter encounters between the AGVs. The comparison between the approach speed PDFs is illustrated in Fig. 16a and shows a significant deviation between the two models and the empirical data. Thus, it is evident that drawing speeds from an equal distributions or setting a constant speed are not sufficient to model real world behavior. To overcome this gap a new algorithm for selecting node speeds is proposed.
The new algorithm is based on:

$$V = \begin{cases} 0, & \text{with probability } P = \phi \\ \Gamma(\alpha, \beta), & \text{otherwise} \end{cases} \tag{24}$$

with V the AGV speed and $\Gamma(\alpha, \beta)$ as the Gamma distribution with its parameters. For the available data the Gamma distribution was fitted to $\alpha = 1.17$ and $\beta = \frac{v_r}{3}$ and $\phi = 0.88$. When applying this algorithm to the RWPM and Manhattan model the approach speed change to the PDFs shown in Fig. 16b. This illustrates the improvements of our new speed selection algorithm.
Based on the restriction of the tracks in the real world data we develop a simple algorithm for determining if the communication between two AGVs takes place along a driving path or intersects a production area. The algorithm aims to enable light-weight simulations based on the mobility model proposed here. Communicating along a drive path can be interpreted as communicating in LOS conditions and all other cases can be accounted as NLOS. The algorithm we propose here has its advantages in its simplicity and not needing further information and is called *simplified matrix propagation scheme* [199].

For matrix production environments it is assumed that drive paths are either parallel to the x- or y-axis and have a width of t. So, by defining a subset of node positions P that have an offset in horizontal or vertical direction of less than t from node position P_n for those LOS propagation is assumed. In the following the $t = 0.1\,\mathrm{m}$ is used.
This is properly described by

$$\oplus(P, P_n, t) = (P_i \in P|\ |P_{ix} - P_{nx}| \leq t \cup |P_{iy} - P_{ny}| \leq t) \tag{25}$$

and results in a subset of all node positions $\oplus(P, P_n, t) \subset P$. Based on this the average number of nodes within LOS propagation are calculated by:

$$N_{LoS}^{\oplus} = \frac{1}{|P|_c - 1} \sum_{P_i}^{P} |\oplus(P, P_i, t)|_c \tag{26}$$

with $N_{LoS}^{\oplus}$ being the percentile of the nodes experiencing LOS conditions. Based on all those assumptions two different errors can occur and are shown in Fig. 17.
Those errors are false positives and false negatives. With a false positive stating LOS conditions although only NLOS propagation being present and false negatives stating NLOS conditions although LOS propagation is available.

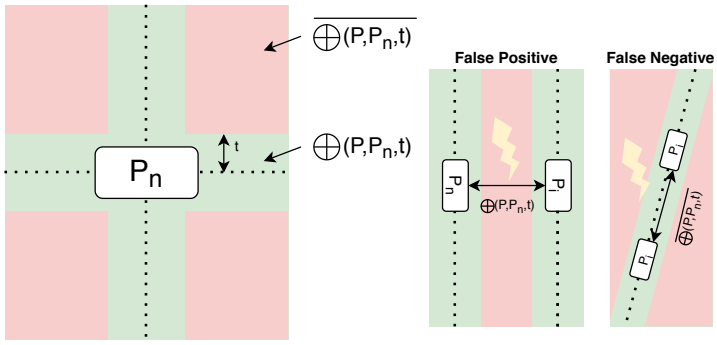

Figure 17: Errors in the *simplified matrix propagation scheme* [199]

When examining the possible false positive in the simplified matrix propagation scheme in the Manhattan model they have no statistical significance. This was evaluated by simulating 30 AGVs for $7 \cdot 10^4$s and comparing the results of ray casting and the simplified matrix propagation scheme. Thereby, the false positives have no statistical significance. Further, false negatives can obviously not occur in the Manhattan model, therefore paths that are neither parallel to the y-axis nor the x-axis are needed.
The quantity of LOS connections based on the simplified matrix propagation scheme can be compared to the real world data, the RWPM and the Manhattan model. The results illustrate that even with the adjusted speed selection algorithm neither RWPM nor Manhattan models this properly. In the Manhattan model the quantity of LOS connections is overestimated due to the perfect grid structure and in RWPM obviously only few LOS connections can be found.
To summarize this subsection: we compared measurement data from AGV movements and based on this developed a new algorithm for selecting AGV speeds in simulations. Additionally, we proposed the simplified matrix propagation scheme.

3.2.2 AGV nodal encounter pattern

In this section Nodal Encounter Patterns (NEPs) from the the factory floor from SEW-EURODRIVE show-case factory are presented where electric drives and gears are mounted. Thus, the factory floor differs from the one of the previous section (electronics production). The AGVs that are used in this section fulfill a multitude of intra-logistics tasks and connect the complete factory from a logistics point of view.

Therefore, this section contains a method for recording NEPs, recorded NEPs and an analysis of the recorded data. The recorded data and the insight gained from it enable simulations of MANETs for industrial environments without the need to simulate the environment. Further, the differences between NEPs and the typically used network traces are examined [200].

The method for recording NEPs is called trace protocol. It enables the direct recording of NEPs. The contrast between network traces and NEPs is the typical assumption that two nodes encounter each other while they are connected to the same Access Point (AP) [200, 114].

The two metrics for comparing direct recording of NEPs and using network traces are:

- Average number of encounters per node noted as $N_{\varnothing}^{XX}$
- Average duration of encounters noted as $D_{\varnothing}^{XX}$

The notation changes depending on the method of extracting the information to $N_{\varnothing}^{NT}$ for network traces or to $N_{\varnothing}^{TP}$ the trace protocol that is proposed here. The notation for the duration changes respectively.

By assuming equally distributed nodes and APs both methods can be compared without any need for simulations. In the following based on those assumptions the outcomes of using the trace protocol and for using network traces are compared. This is done to provide an understanding on the differences.

When comparing the average number of encounters per node $N_{\varnothing}^{XX}$ both metrics provide similar results if the examined area is completely covered by non-overlapping APs. For details on the calculation refer to [200]. Thus, when using network traces there is a dependence between the encounters and the coverage of the APs. This illustrates that there is a significant difference in the two methods. These results were also further evaluated by simulations based on the RWPM with the same outcome.

When comparing the average duration of encounters $D_{\varnothing}^{XX}$ this metric is mainly dependent on the mobility of the nodes and the coverage area of the nodes or the APs. So, the duration of encounters can be calculated by the average time two nodes are within the coverage of the same AP. For this metric the evaluation provides further challenges. Thus, comprehensive simulations were performed illustrating that for network traces there is a high dependency of the average encounter duration on the number of APs. This is an obvious difference to real ad hoc networks.

The tracing protocol is based on beacons that are sent in the time interval $\frac{1}{dt}$ and each node records each received beacon. Each node is identical in its function and the network load and the granularity of the recorded data can be adjusted by adjusting dt. A constraint for the choice of dt is that it should be faster than the coherence time of the

Table 12: Measurement parameters NEPs

Parameter	Unit	Office	Static	Mobile	Description
dt	s	0.2	0.2	0.2	Time resolution
T	s	> 11800	> 8800	> 10400	Duration measurement
N		6	7	8	Number of nodes
Mobility	Type	None	Group	AGV	Type of mobility
Environment	Type	Office	Industry	Industry	Environment description

communication channel. Every time a node sends a beacon it increments its counter. If a beacon is received the respective node records a tuple with the information and thereby implements a Lamport clock [144]:

- Receiver address
- Counter of node itself
- Transmitter address
- Counter of transmitting node

These tuples are directional, so if a node has a record of received information from another node it must be checked if that other node received beacons as well. By knowing dt the counter can be converted to time. The nodes can be time synchronized by the two time stamps in each tuple.
To evaluate the effects of the industrial environment measurements in three different setting were performed:

- Office environment with static nodes
- Static industrial environment with no relative movement between the nodes
- Mobile industry environment (nodes mounted to AGVs)

The test parameters are summarized in Tab. 12. The choice of parameters was restricted by measuring in a production environment and all tests were performed with IEEE 802.11n communication interfaces at $20\,\mathrm{dBm}$ send power and the implementation employed the click modular router [138]. The results and the source code are published at [97].
The measurement data is evaluated from four different points of view:

- Connectedness of the network (comparison along the three scenarios)
- Directionality of single links
- Route life-time
- Multi-hop routes

Network connectedness is defined as the number of neighboring nodes with which communication is possible [164]. In a network of n nodes $n - 1$ connections are possible. The connectedness describes with how many of those nodes a node can communicate [200]. In the follwing the connectedness is expressed in percent. Fig. 18 compares the connectedness of the scenarios office, static industry and mobile industry.
Thereby, the figure illustrates that the network connectedness decreases along the three scenarios. Noteworthily, the connectedness in the static industry scenario is already

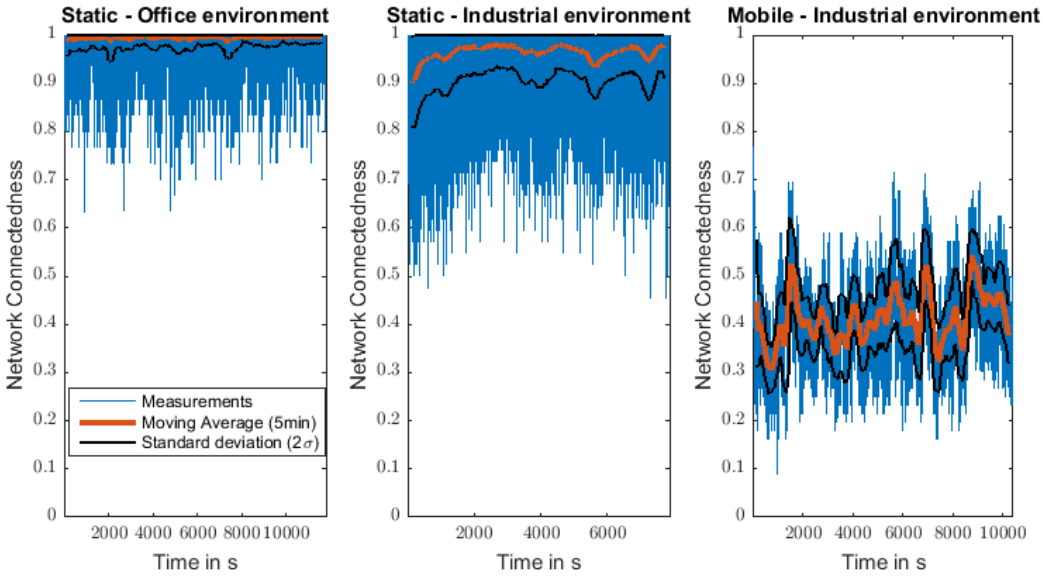

Figure 18: Network connectedness of office, static and mobile industry scenario

worse than in the as well static office scenario. This is supposed to be due to interference in that harsher environment. Also, the variations in the connectedness point towards spatial correlations [200].

A bidirectional link for this measurements is defined by two nodes recording encounters of each other with a maximum time difference of dt [200]. If only one node has a record of seeing the other node the link is defined as unidirectional. Unidirectional nodes exist due to channel variations with dt or interference with other communication networks.

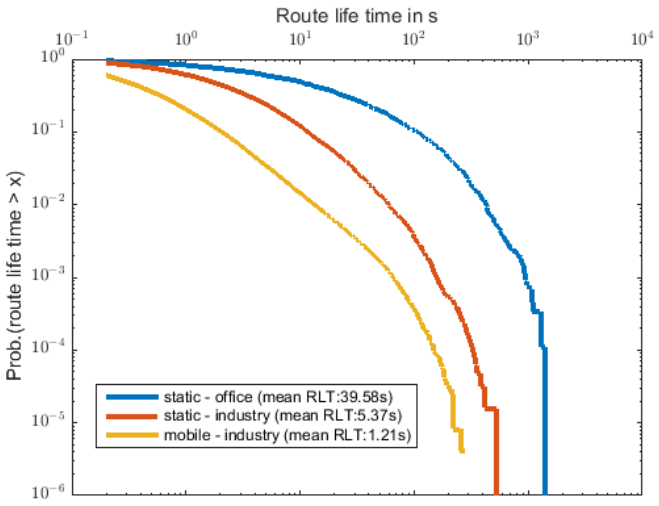

Figure 20: Complementary Cumulative Distribution Function (CCDF) of the route life times

Fig. 19 shows the percentage of unidirectional links in the three scenarios. This is of high relevance as typical routing protocols like Dynamic Source Routing (DSR) [123] or Ad hoc On-Demand Distance Vector Routing (AODV) [181] assume bidirectional communication links. The industrial environment challenges this assumption by having $\approx 33\,\%$ on average of unidirectional links. Of course, ad hoc routing protocols

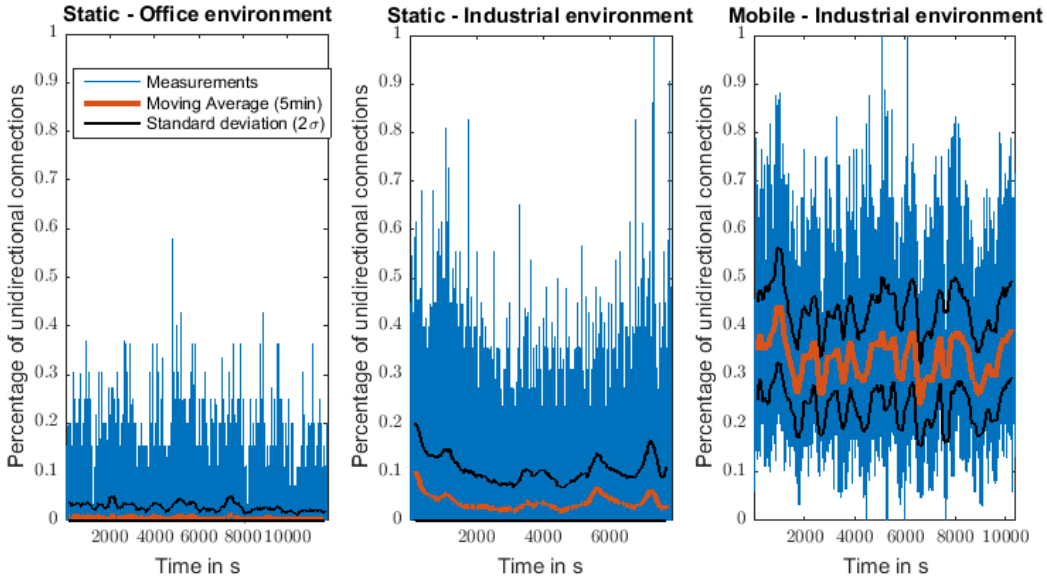

Figure 19: Unidirectional links in office, static and mobile industry scenario

can compensate this behavior but at the cost of higher overhead [37].

The route life time is a key parameter in MANET. The smaller the route life times the higher the protocol overhead gets due to route failures [200]. The probabilities of route life times are shown in Fig. 20. The result is inline with the previous ones: The mobile industrial network has the shortest route life spans and thus is the most challenging for designing routing protocols. As already discussed earlier the route life span is mainly dependent on the node speed. Hence, the results of the measurements support the results from reasoning about equally distributed nodes using RWPM. But also the difference between the static scenarios is major. The mean route life time in the offices environment drops from $40\,\mathrm{s}$ to $5\,\mathrm{s}$ in the static industrial scenario.

However, the mean route life span of the mobile industrial scenario cannot be explained by the mobility solely. Assuming $20\,\mathrm{m}$ communication range in combination with a node speed of $1\,\mathrm{m/s}$ and all nodes moving the route life span should be significantly larger at about $10\,\mathrm{s}$. This is due to AGV mainly meeting when driving in opposite directions.

In ad hoc networks not only single connections but also multi-connections are employed. Thus, it is relevant to have a look at the improvements of the connectedness if multi-routes are employed. Fig. 21 shows the connectedness improvements and route life spans in multi-hop cases. The figure only contains the mobile industry scenario.

The first additional hop introduces by far the best improvements in terms of connectedness and route life span. This, as well as the whole Fig. 21 is based on employing redundant multi-hop connections. Any further additional link decreases in its improvement.

In summary, this section illustrated that for NEPs direct recording is significantly more precise than using network traces and NEPs from three scenarios were recorded and

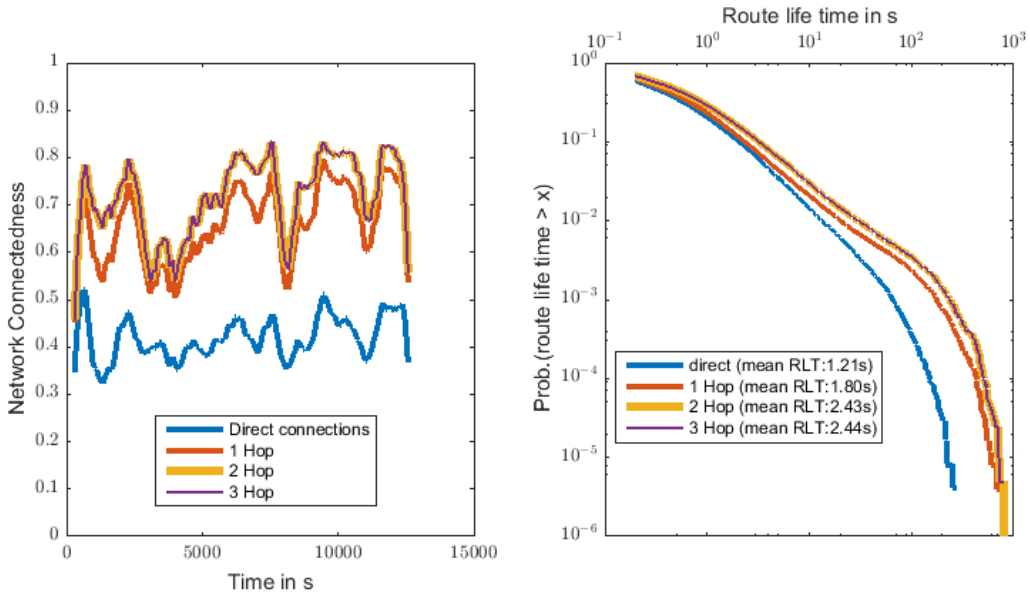

Figure 21: Unidirectional links in office, static and mobile industry scenario

presented. Thereby, NEPs can be used in simulations instead of simulating the lower layers of a network. Additionally, if they are recorded in a suitable environment no further validation is needed compared to a simulation.
The challenges industrial MANETs experience due to unidirectional links, lower connectedness and shorter route life spans were illustrated.

3.3 Conclusion on Modeling factory environments

The section on modeling factory environments provides two perspectives: First, the physical layer measurements presented in this section further support the statement that factory environments behave highly scenario specific as stated by Schmieder et al. [207]. This was done by analyzing measurements for path loss, multi-path components and parameterizing the SV model. By examining the SV model we showed that an exponential decay function for the inter and intra cluster decay is advantageous and support the statement of Ai et al. [29] who stated that for the inter cluster decay.
The second perspective is on the mobility of AGVs and the network encounters they have on the factory floor. The key outcomes when analyzing the mobility on the factory floor were that the movement pattern is an eroded Manhattan grid and that we proposed a new speed selection algorithm that fits the real world measurements better than typically used models. Further, NEPs were recorded by a new recording method. The source code of the recording protocol and for the analysis are published. The results of the NEP analysis showed that there are significant differences to the behavior of network traces and that the industrial environment is highly volatile by means of network encounters.

4 Empirical Performance Analysis of WLAN and cellular

Currently, in factory automation a wide set of communication technologies is used [154]. In this section, the most relevant technologies in this sector that are WLAN, pLTE and 5G are examined based on measurements from industrial scenarios. Those measurements focus on latency and reliability. This section is separated from the previous one because here higher layer communication parameters are evaluated instead of physical layer parameters and the behavior of intra-logistic processes.

Although IEEE 802.11 n WLAN is standardized since 2009 it is still the most used solution on the factory floor [154, 84, 119, 153]. Thus, latency measurements from an IEEE 802.11 b/g/n network with WPA2-PSK security composed of several access points are provided as performance base line. Those measurements are compared to pLTE and to 5G performance data.

We focus on the latency measurements from application perspective including mobility in industrial facilities. This is in contrast to Rischke et.al [195] who focus on isolating single latency components in a 5G network by performing high precision measurements without mobility.

The measurements of WLAN and pLTE were performed on the same factory floor. The factory encloses the final assembly line of an automotive production covering $16\,000\,\mathrm{m}^2$ and contains a lot of conductive material. The pLTE network uses 36 small cell antennas and six of those antennas are combined to form a single cell and two antennas form a 4x4 MIMO transmission point. The network employs $40\,\mathrm{MHz}$ of bandwidth in FDD evenly split between uplink and downlink. The network operates in LTE Band 7. The antennas are mounted $\approx 8\,\mathrm{m}$ above ground and the network is an Ericsson LTE network with a fully virtualized core. For the measurements two different UEs were used. Both are typical industry grad clients. The Siemens Scalance M876-4 that is a Category 3 Release 9 device and the PhoenixContact TC-Router 4G that is a Category 4 Release 9 device. Both devices have a maximum uplink of $50\,\mathrm{Mbps}$ and the Siemens device has a maximum downlink of $100\,\mathrm{Mbps}$ and the PhoenixContact device has $150\,\mathrm{Mbps}$. Both devices are connected to two antennas with $2\,\mathrm{dBi}$ antenna gain.

For the WLAN measurements as client the Siemens Scalance W734-1 was used.

The measurement architecture is illustrated in Fig. 22. The clients (WLAN as well as LTE) connect to a test-PC via Ethernet. This PC has an E3950 Processor, $8\,\mathrm{GB}$ RAM, runs a debian server and is a Pokini-F2. In the architecture Fig. 22 three paths are illustrated that a packet may take. Those are

1. Via the WLAN-Client towards Application-Server 1
2. Via the Siemens LTE-Client towards Application-Server 1
3. Via the PhoenixContact Client towards Application-Server 2

Obviously, there exist further paths. The difference of the application servers is their placement, as in a virtualized Evolved Packet Core (EPC) or a 5G core processing power for third party applications can be directly placed inside the core network. The key advantage of the placement of Application Server 2 is that it avoids the usage of an additional network. In this particular case this is the internal factory network.

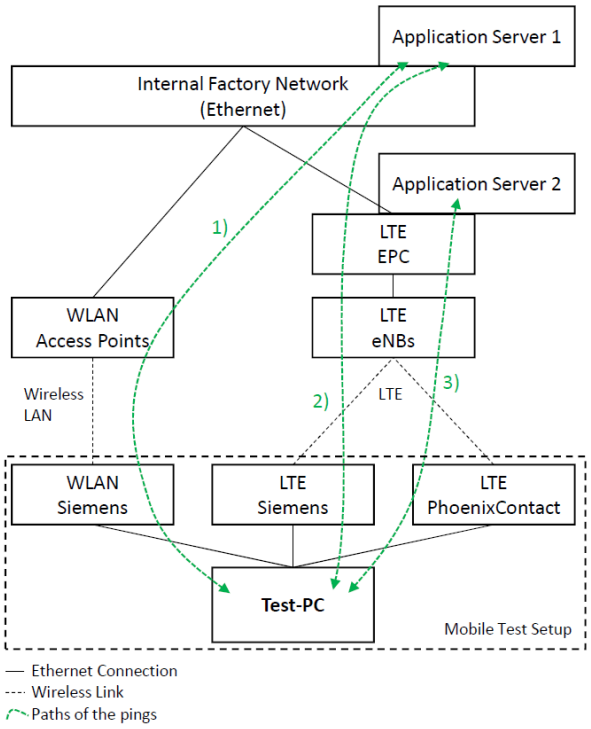

Figure 22: Network architecture [157]

The measurements are ping-based and thus RTTs are measured. The UE / client is moving randomly on the factory floor at walking speed on paths that an AGV may use. During all tests the production is running. So, the WLAN experienced a low load additional to the measurements, because the present AGVs use that WLAN as well. The pLTE network is only used by the test equipment. Thus, those measurements enable an evaluation of latency and reliability of pLTE and WLAN under production conditions [157]. Those conditions are characterized by the physical environment of a factory floor.

The 5G measurements were performed in a different environment but with the same measurement architecture. The measurement data was acquired in an AGV testing facility with similar conditions as a factory floor [156]. The network is a 5G Stand-Alone (SA) NPN Proof-of-Concept (PoC) from Ericsson. It implements Release 15, uses a short TTI with $0.5\,\mathrm{ms}$, is TDD and operates at $3.7\,\mathrm{GHz}$ with $100\,\mathrm{MHz}$ bandwidth. The TDD scheme provides the same amount of uplink and downlink resources. The UE used in this test is the prototype of the Siemens Scalance MUM856-1. To mimic PD we worked with two connections with separate sockets on application layer. This approach was chosen because neither the UE nor the network support PD.

An overview on the measurements is provided in Tab. 13 and by the CDFs in Fig. 23. Tab. 13 shows the exact measurement results and parameters. The pLTE measurement in the Fig. 23 are with $40\,\mathrm{byte}$ payload and $50\,\mathrm{ms}$ cycle time. The same accounts for

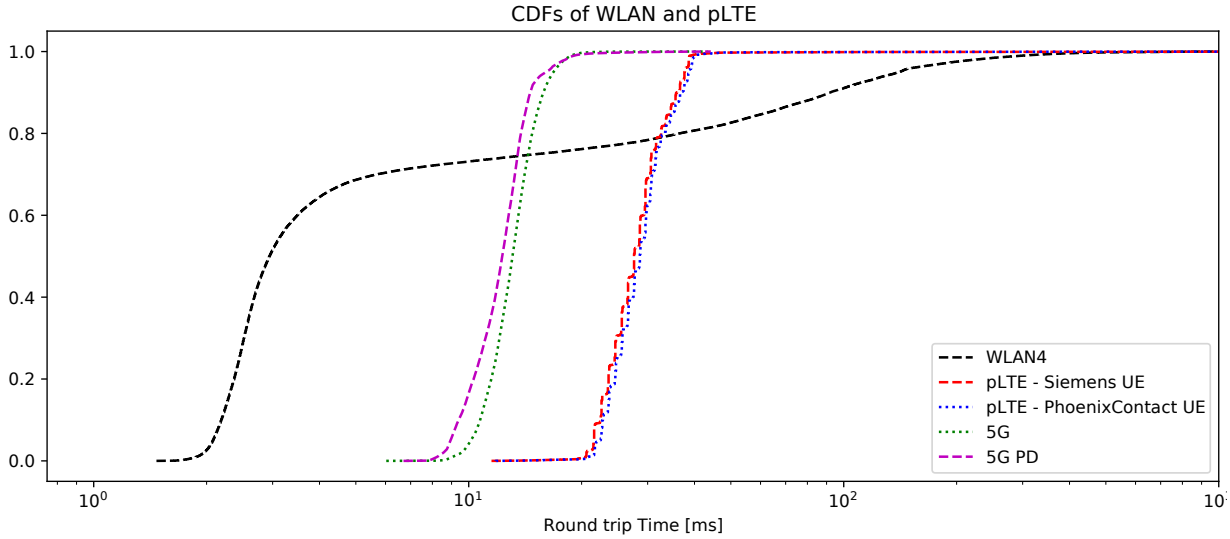

Figure 23: CDFs of pLTE, WiFi4 and 5G with and without PD. Data from [157, 156]

Table 13: Test overview and results of pLTE and WLAN [157]

Client	Cycle	Payload	RTT 99%	PER
Scalance M876-4 (LTE)	50 ms	40 byte	40.4 ms	$1.1 \cdot 10^5$
TC-Router 4G (LTE)	50 ms	40 byte	38.9 ms	$1.1 \cdot 10^5$
Scalance W734-1 (WLAN)	50 ms	40 byte	259 ms	$2.2 \cdot 10^5$
Scalance M876-4 (LTE)	10 ms	250 byte	44.2 ms	$1.01 \cdot 10^6$
Scalance W734-1 (WLAN)	10 ms	250 byte	301 ms	$8.1 \cdot 10^5$
Scalance M876-4 (LTE)	5 ms	1000 byte	35.9 ms	$1.01 \cdot 10^6$
Scalance MUM856-1 (5G Prototype)	5 ms	32 byte	17.1 ms	10^6
Scalance MUM856-1 (5G Prototype, PD)	5 ms	32 byte	15.9 ms	10^6

WLAN. The 5G measurements are with the same payload but 5 ms cycle time. The shorter cycle time in 5G closer matches use cases that are envisioned for 5G.
The general aspects are illustrated by the CDFs: WLAN has the fastest RTTs for the first $\approx 70\,\%$, but its performance for the remaining packets declines extremely. So, the CDF of the WLAN measurements illustrates clearly its key properties: The majority of packets is delivered fast but the technology is unreliable and has a long tail in the latency distribution.
Both cellular technologies have steep curves that illustrate a small variance in the latency. As the transition from LTE to 5G on the air interface was evolutionary and the air interface has the largest influence on latency [195] the majority of the latency reduction must be due to changes on the air interface. The key difference is the duration of the TTI with the short TTI in 5G having only half the length of the 1 ms in LTE. The result is an approximate bisection of the latency. So, 5G has half the latency compared to pLTE.

Additionally, the curve of the 5G latency rises steeper.
A closer look at the behavior of WLAN facilitates the previous statements. A section of 1500 measurements from the WLAN is shown in Fig. 24. Thereby, the figure illustrates that there are always some packets with longer latencies in contrast to the majority of fast packets. When examining the same kind of network under optimal conditions with roaming (changing APs) the result is that besides collisions and queuing each scan for alternative APs and change of the AP add up on the latency. The optimal conditions were assured by using coax-cables and adjustable attenuation at the antenna ports of the two clients and the two APs.
The behavior was tested with five different industry grade clients. All those clients have the same behavior of longer latencies when changing the AP or scanning for an alternative AP. The latency of those packets are at 150 to $350\,\mathrm{ms}$ depending on the device and number of channels being scanned. Additionally, the measurement results are in line with the evaluations by [153]. Also in optimal conditions the effects of additional load are similar among different clients with already $10\,\mathrm{Mbps}$ degrading the network performance significantly. Combining this knowledge with the values from Tab. 13 illustrates that WLAN is not sufficient to support most of the recent use cases that are presented in Sec. 2 or in e.g. [1, 19] like cooperative AGVs or many edge computing use cases.

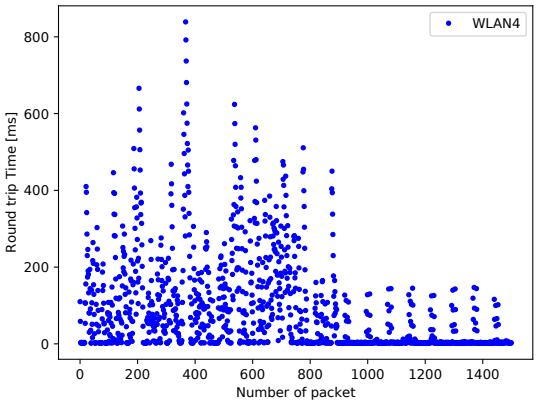

Figure 24: RTTs of WLAN4 of 1500 packets

In the pLTE network handovers do not correlate with long latencies. During the measurements in the pLTE network the handovers between different cells were recorded and did not match the latency peaks.
When evaluating the 5G measurement data for $40\,\mathrm{ms}$ RTT that the pLTE network achieves with a reliability of approximately $99\,\%$ or a PER of 0.01, the 5G network has a PER of $4.2 \cdot 10^{-5}$ or a reliability of $99.996\,\%$. This illustrates the advantages of the 5G network. When using PD on application layer the PER even drops to $9.1 \cdot 10^{-8}$. Those values already arise with PoC hardware. This also shows that the 5G network experiences by far less latency peaks. Although only two CDFs are shown, the results presented here were further verified by measurements with different payloads and cycle times. The payloads range from $40\,\mathrm{byte}$ to $1000\,\mathrm{byte}$ and cycle times between $1\,\mathrm{ms}$ to $50\,\mathrm{ms}$. Only cycle times $\leq 2.5\,\mathrm{ms}$ lead to slightly higher latencies.

4.1 Statistical analysis

In this section and its subsections a new method for analyzing rare events in measurements from wireless URLLC networks is proposed. That method is based on the LRE algorithm but overcomes the drawback of relying on approximating the standard normal distribution. So, a method is developed that is applicable for auto-correlated, empirical data and does not approximate the standard normal distribution. Further, we apply this method to the 5G measurements from Chapter 4 and its results are used to evaluate the performance of a black channel protocol using 5G.

4.1.1 Method description

As discussed in Section 2.4 there is a need for an analysis method for empirical data of wireless networks. This is due to the two specialties of the data:

1. real world measurement with rare events
2. correlation [203]
3. unknown distribution

Those properties show that the typical assumption of independent identical distributed variables cannot be used. In addition, all methods designed for simulations are not applicable without adjustments. Thus, a new method is developed here by combining the Limited Relative Error (LRE) algorithm with Moving Block Bootstrapping (MBB). We call this method *bootstrapping LRE*. The LRE algorithm is able to deal with correlated data and MBB can be used to overcome the problem of the unknown distribution. The unknown distribution is a challenge because the most used assumption of approximating the standard normal distribution is insufficient. That approximating the standard normal distribution does not work is illustrated later by usage of the Berry-Esseen theorem.

The *bootstrapping LRE* is used here to construct confidence intervals around the real value. Beside that, an empirical probability distribution is constructed, the relative error determined and the correlation of the data is determined. Due to better consistency the LRE algorithm is described in this section instead of the related work. Thereby, the description of the algorithm, the enhancements and usage are closely collocated. The motivation why to use the LRE algorithm is given in the related work section. A short explanation of MBB is also provided. The following explanation on the LRE algorithm, MBB and the *bootstrapping LRE* algorithm was first proposed in [156].

The LRE algorithm is designed to analyze chronological sequences $x_1, x_2, ..., x_n$ with n values. Inherent to the algorithm design are the assumptions that the sequence is:

- autocorrelated
- its underlying stochastic process is stationary
- its distribution is unknown

In our case the chronological sequence consists of latency values and that data adheres to the assumptions. The LRE algorithm provides three outcomes:

- rare event probability and confidence intervals around it
- correlation of the data
- relative error

The relative error can be reduced by adding more data and the key characteristics are the rare event probability and the confidence intervals around it.
To perform the LRE algorithm a two-sided Markov chain is derived from the sequence $X = (x_1, x_2, ..., x_n)$ with n elements. The states of the Markov chain are $S_0(x)$ and $S_1(x)$ with the latter one being the rare event. For evaluating whether the rare event occurred the function

$$L(x) = \begin{cases} 0 \text{ if } x \in X | x \leq l \\ 1 \text{ if } x \in X | x > l \end{cases} \tag{27}$$

is defined. Thereby, l is the latency limit a packet may experience before being accounted as lost. As the LRE algorithm is based on analyzing the number of state changes and the number of occurrences of each state those are counted by:

- $v = \sum_{i=1}^{n} L(x_i)$ the number of occurrences of $S_1(x)$
- $r = n - \sum_{i=1}^{n} L(x_i)$ the number of occurrences of $S_0(x)$
- $c = 0.5(\sum_{i=1}^{n-1} |L(x_i) - L(x_{i+1})| + \sum_{i=1}^{n-1} L(x_i) - L(x_{i+1}))$ number of state changes from $S_1(x) \rightarrow S_0(x)$
- $a = 0.5(\sum_{i=1}^{n-1} |L(x_i) - L(x_{i+1})| - \sum_{i=1}^{n-1} L(x_i) - L(x_{i+1}))$ number of state changes from $S_0(x) \rightarrow S_1(x)$

Thereby, the algorithm needs a minimum number of appearances of each state and state change to be applicable. Those are:

- $n \geq 10^3$
- $r, v \geq 10^2$
- $c, a \geq 10$
- $v - c \geq 10$

These values are constraints. If the constraints are fulfilled the complementary distribution function equaling the rare event probability can be calculated by

$$\tilde{G} = \frac{v}{n} \tag{28}$$

the local correlation coefficient $\tilde{\rho}$ by:

$$\tilde{\rho} = 1 - \frac{\frac{c}{v}}{1 - \frac{v}{n}} \tag{29}$$

the correlation factor by:

$$\tilde{cf} = \frac{1 + \tilde{\rho}}{1 - \tilde{\rho}} \tag{30}$$

and the relative error by:

$$d_G(x) = d = \sqrt{\frac{1 - \tilde{G}}{v} \tilde{cf}} \tag{31}$$

The relative error decreases with growing n. This equals adding more data and is evident as in case of a stationary process $\tilde{G}$ and $\tilde{cf}$ are approximately constant.

Originally, the LRE algorithm is used to determine the run-length of simulations by evaluating the relative error [231, 209, 101, 151]. Mostly, the limit $d_{max} = 0.05$ for the relative error is used [171] and thus the simulation is run until $d \leq d_{max}$.
We propose the first change and improvement: In use cases employing wireless URLLC networks worst case latency and reliability are defined and no tolerable error. Thus, we propose to employ the upper confidence interval as an additional measure. Confidence intervals can be constructed by:

$$\sigma_G{}^2 = Var(\bar{X}) = \frac{\widetilde{cf} \cdot v(1 - \frac{v}{n})}{n^2} \tag{32}$$

with

$$[\bar{X} - z_{1-\frac{\alpha}{2}}\sigma_G < \mu < \bar{X} - z_{\frac{\alpha}{2}}\sigma_G] \tag{33}$$

if the standard normal distribution is approximated. Thereby, they have the additional advantage to shrink with a different rate and parameter than the relative error. As stated in Section 2.4 the Berry-Esseen Theorem with

$$|F_n(x) - \Phi_{(0,1)(x)}| \leq \frac{C_{BE} \cdot \rho}{\sigma^3\sqrt{n}} \tag{34}$$

is used to evaluate the quality of that approximation. For the sake of completeness the pseudo code of the LRE algorithm is shown. The pseudo code consists of the two parts:

1. Counting the events and state changes
2. Calculating equations 28, 29, 30, 31, 33

This pseudo-code does not include the loop of running the algorithm, evaluating d_G and rerunning the algorithm. The loop is normally run until $d_G \leq d_{max}$. The pseudo code is identic to [156].

```
limit = l
for data <= l do
    data = 0
for data > l do
    data = 1
a, c, r, v  = 0
for i from 2 to end data do
    if (data[i - 1] == 0)
        if data[i] == 0 do
            r = r +1
        else
            a = a + 1
        else
            if data[i] == 1
                v = v +1
            else
```

```
                c = c + 1
calculate correlation and
correlation factor
calculate RE and confidence intervals
```

When evaluating the Berry-Esseen C_{BE} constant for the 5G measurements from Section 4 $C = 14.6$. This illustrates that the approximation is far from being applicable as the Berry-Esseen constant is in the dimension of $C_{BE} = 0.47$ [246]. Thus, MBB is used to construct an empirical distribution to overcome the problem of approximating the standard normal distribution. Thereby, MBB works by drawing blocks from the original data to recreate the inference between the real value and measurement. The principle is illustrated in Fig. 25.

To construct an empirical distribution of the original data $l = n^{\frac{3}{4}}$ blocks are drawn that have a length of $n_l \approx \sqrt[4]{n}$. This is in accordance to the recommendations from [105]. Afterwards, the empirical distribution is constructed by calculating G_l, σ_l, d_l for each resampled block. The empirical distribution T_n is than normalized by:

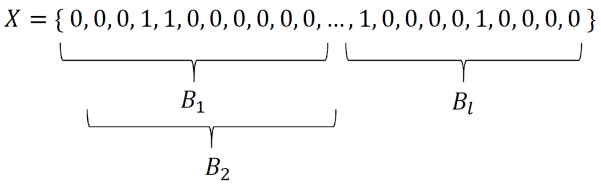

Figure 25: Drawing blocks from a sequence

$$T_l = \frac{\bar{G}_l - E(G_l)}{E(\sigma_l)} \tag{35}$$

From those l single values the distribution T_n is constructed and the quantiles are drawn from there. As this distribution is not necessarily symmetrical the quantiles $t_{0.025}$ and $t_{0.975}$ must both be evaluated for a $95\,\%$ confidence interval. Then the confidence interval can be calculated by

$$[\tilde{G} - t_{\frac{\alpha}{2}} \cdot \sigma_G; \tilde{G} - t_{1-\frac{\alpha}{2}} \cdot \sigma_G] \tag{36}$$

with α the confidence level. As this approach does not approximate the standard normal distribution, the Berry-Esseen theorem cannot be used to evaluate the quality of the confidence intervals based on the empirical distribution.

Generally, when evaluating measurement data towards a fit for use cases the upper confidence interval level should be used to provide a suitable worst case evaluation [156].

The overall bootstrapping LRE algorithm has a complexity of $\mathcal{O}(n^{\frac{7}{4}})$.

4.1.2 Application of bootstrapping LRE

In this Section the *bootstrapping LRE* algorithm is applied to two 5G measurements. The results thereof are used to evaluate the performance of black channel protocols using 5G.

Bootstrapping LRE applied to measurements

Two sets of measurements are analyzed here. Those are the two 5G measurements previously described in Section 4 representing a measurement with PD on application layer

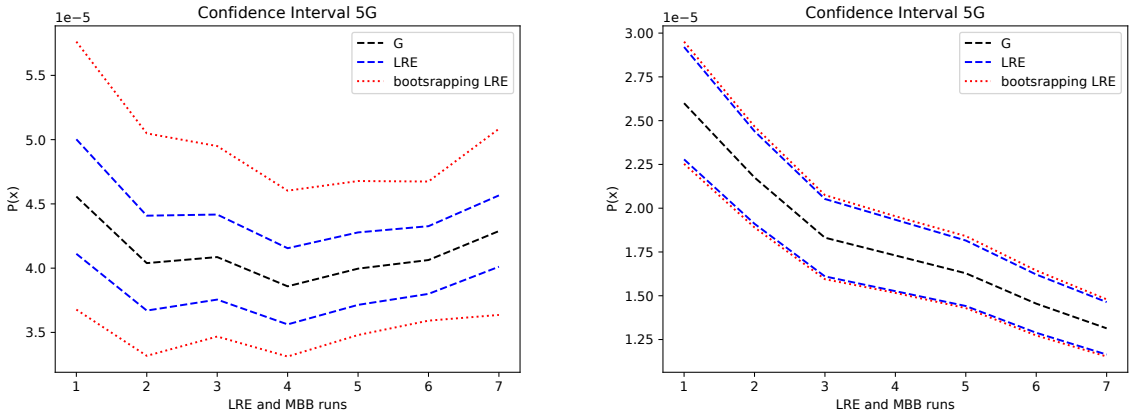

(a) Confidence intervals without PD

(b) Confidence intervals with PD

Figure 26: Comparison of confidence intervals

and one standard measurement. In both cases $n \approx 4 \cdot 10^7$ packets with a cycle time of $5\,\mathrm{ms}$ and a payload of $40\,\mathrm{byte}$ were sent. The PD measurement is evaluated for a RTT of $25\,\mathrm{ms}$ and has a PER of $1.3 \cdot 10^{-5}$ and the standard measurement is evaluated for a RTT of $40\,\mathrm{ms}$ having a PER of $4.2 \cdot 10^{-5}$. The key data of both measurements are illustrated in

Table 14: Without PD RTT $40\,\mathrm{ms}$

n \ n+1	$S_0(x)$	$S_1(x)$	$\sum$
$S_0(x)$	$3.6 \cdot 10^7$	1152	$3.6 \cdot 10^7$
$S_1(x)$	1152	396	1548
$\sum$	$3.6 \cdot 10^7$	1548	$3.6 \cdot 10^7$

Table 15: With PD RTT $25\,\mathrm{ms}$

n \ n+1	$S_0(x)$	$S_1(x)$	$\sum$
$S_0(x)$	$4.4 \cdot 10^7$	394	$4.4 \cdot 10^7$
$S_1(x)$	394	191	585
$\sum$	$4.4 \cdot 10^7$	585	$4.4 \cdot 10^7$

Tab. 15 and Tab. 14. Thereby, both tables contain the number for all state changes and the sums of the appearances of each state in the last line and column.
Fig. 26 shows the different confidence intervals. Firstly, the set of intervals constructed by approximating the standard normal distribution and the classic LRE algorithm is shown. Secondly, the other set constructed by the bootstrapping LRE algorithm that employs an empirical distribution for this task is illustrated in Fig. 26. To have a view on the stationarity of the process the data is split into 7 evenly large sets and the data is successively added to the analysis. The confidence intervals are constructed for a confidence level of $95\,\%$. In the figures the red dotted lines are the confidence intervals constructed by bootstrapping LRE and the blue dashed lines show the confidence intervals based on approximating the standard normal distribution. Especially in the case without PD there is a significant difference in the intervals. This aligns with the Berry-Esseen-Constant of $C = 14.6$ that is found in this case. This is far from a proper approximation [246] and illustrates that the approximation towards the standard nor-

mal distribution cannot be precise. This shows why it should be refrained from using the approximation although [171] proofed that the central limit theorem applies. Thus, either an empirical distribution should be used or at least the quality of the approximation evaluated.
The correlation of consecutive packets in 5G in the measurements in all examined cases is $1.7 \leq cf \leq 2.4$. Those values can be transformed to a normalized ρ to describe correlation. Normalizing ρ to $-1 \leq \rho \leq 1$ our values correlations are $0.26 \leq \rho \leq 0.42$. As approximating the standard normal distribution assumes independent variables this is also an explanation why the approximation is not precise.
The difference in the confidence intervals when using PD is smaller. We suppose this to be due to PD cutting the long tails of the distribution. Optimistic confidence intervals are inappropriate for URLLC networks as by their definition there is a high need for accuracy and fulfilling requirements.
The quality of the confidence intervals that is needed is defined by the use case. Thereby, the upper limit of the confidence interval is of interest [156]. The relative error declines from $6.8\,\%$ to $3.4\,\%$ when adding the data and thus the typical stopping criterion as used by e.g. [151, 208] is fulfilled.
The key parameter to discuss whether this method is useful is the number of measurements that is needed to perform an analysis. The number of measurements is bounded by $v, r \geq 10^2$ stating that each event has to occur at least 100 times. So, if an event (equally PER) is considered that has a appearance rate of 10^{-5}, 10^7 measurements are needed. Additionally, the drift of the confidence intervals should be examined to keep track of the stationarity of the process. Further, assuming a measurement cycle of $1\,\mathrm{ms}$ would result in a measurement duration of $\approx 8.33\,\mathrm{h}$. Thereby, adding MBB to the whole process has no influence on those requirements.
As the method works with adding further data it can be used for continuous evaluation of networks.

Black channel via 5G

As discussed previously, one of the KPIs of black channels is its cycle time and the reliability by means of avoiding false positives. False positives are safety stops that only happen due to communication errors. The number of false positive safety stops that happen when using a 5G network can be evaluated based on the results from the bootstrapping LRE algorithm.
The analysis is based on the Markov chains that are derived from using the bootstrapping LRE algorithm. Thereby, the Markov chains have the advantage to include the correlated behavior. The Markov matrix for a two sided Markov chain describing the measurements without PD is:

$$\begin{Bmatrix} 0.99996808 & 0.0000319 \\ 0.7442 & 0.2558 \end{Bmatrix} \tag{37}$$

with P_{00} describing the probability of transitioning from S_0 to S_0, P_{01} the probability of transitioning from S_0 to S_1 and so forth. S_0 is the state of the latency being faster than the latency bound. This Markov matrix has the time basis of the original measurements and

thus assumes a cycle time of $5\,\mathrm{ms}$ and does not consider the confidence intervals [156]. Both should be taken into account for the following evaluation.
As a first example we assume a timeout of $80\,\mathrm{ms}$ with a cycle time of $40\,\mathrm{ms}$ of a black channel using the 5G network without PD. So, one lost packet is tolerated. The probability to be in $S_0(x)$ tends towards $1 - 4.3 \cdot 10^{-5} = 0.999957$ for a long duration. This probability is called P_{S0}. Obviously, the probability to be in $S_1(x)$ is $4.3 \cdot 10^{-5}$. A false positive safety stop occurs when $S_1(x)$ is reached and after $40\,\mathrm{ms}$ the Markov chain is still or again in $S_1(x)$. The probability for this event is called P_{S11}. So, the probability of a false positive can be calculated by:

$$\begin{aligned} P_{ConLoss} &= P_{S1}(x) \cdot P_{S11}(x) \\ P_{ConLoss} &= 4.816 \cdot 10^{-9} \end{aligned} \tag{38}$$

with $P_{S11} = 1.12 \cdot 10^{-4}$. So, without accounting for the confidence intervals an uninterrupted operation of a black channel via 5G is possible for about $90\,\mathrm{days}$ with a $40\,\mathrm{ms}$ cycle and one lost message being tolerated. If the upper bounds of the confidence intervals are used, the results for P_{S11} differ significantly, as well as the duration of an uninterrupted operation. $P_{ConLoss} = 6.32 \cdot 10^{-9}$ with the confidence interval constructed by using the empirical distribution and this leads to an expectation of only $73\,\mathrm{days}$ of uninterrupted operation. For the confidence interval that approximates the standard normal distribution $P_{ConLoss} = 5.3 \cdot 10^{-9}$ resulting in the far longer expectation of $86\,\mathrm{days}$ of uninterrupted operations. This difference properly illustrates the problems introduced by optimistic confidence intervals. The KPI of uninterrupted operations of the black channel changes dramatically [156].
Some different outcomes emerge by an example using the PD measurement data and evaluating the black channel performance for a cycle of $25\,\mathrm{ms}$ and one lost message being tolerated. The respective Markov matrix is:

$$\begin{Bmatrix} 0.99999097 & 0.00000903 \\ 0.6735 & 0.3265 \end{Bmatrix} \tag{39}$$

Thereby, $P_{S1}(x) = 1.3 \cdot 10^{-5}$ and $P_{S11}(x) = 0.011$ leading to $P_{ConLoss} = 1.43 \cdot 10^{-7}$. The difference to the previous example is due to the different time basis and a change in the dominant term that has the highest influence on $P_{ConLoss}$. The probability to remain in S_1 is significantly higher due to the change of the time basis. This relation, that the probability to remain in S_1 increases can be interpreted as an effect of the coherence time on the application layer. So, an uninterrupted operation can only be expected for $2\,\mathrm{days}$. Using the confidence intervals this duration shrinks to $1.8\,\mathrm{days}$, but with both confidence intervals providing similar value.
Conclusively, this shows that 5G is a suitable technology to enable stable black channels in industrial environments. Especially, the achievable cycle times and duration of uninterrupted operation are far beyond other works [182, 104] who both use WLAN with different protocol stacks.

5 Performance Improvements

This section describes optimizations for wireless communication on the factory floor that are designed to improve network performance. All the solutions proposed here focus on scenarios on the factory floor and are illustrated in four subsections. Three of the solutions include MANETs used by AGVs, two deal with safety relevant communication, one includes orchestration aspects of different networks and one optimizes the usage of cellular networks on the factory floor. Thereby, parts of the mobility modeling are reused for the adaptive mobility control of AGVs in subsection 5.2, subsection 5.3 expands the black channel evaluation from section 4.1 by improving the black channel algorithm and subsection 5.4 is a consequence of the WLAN performance evaluations in section 4.

The general focus along the following subsections is reducing bandwidth usage and improving reliability and coverage. Reducing bandwidth usage is crucial because bandwidth is a scarce resource [154] and reliability and coverage are key requirements in industrial use cases [1, 204, 19].

5.1 Real-time alarm dissemination

For many industrial applications it is necessary to transmit information in real time and simultaneously keep track of the connectedness although wireless networks are used. Fire alarms are an example and need to be received within $500\,\mathrm{ms}$ by AGVs [203]. This reaction time is due to the need to evacuate escape routes. So, we propose the Real-Time Alarm Dissemination (RTAD) system here. This system is a network protocol that deals with the challenge of not being able to guarantee a transmission and the need to detect connection losses. So, either a packet is transmitted with hard real-time or the client is informed that a transmission was not possible. This system is designed to work in MANETs.

The concept of the RTAD system is depicted in Fig. 27. This includes a wired and a wireless network that are connected by WLAN Access Points (APs), different wireless mobile clients and fire alarm and process controller. Typically, in production environments critical areas like escape routes are present that have to be evacuated in case of fire alarms. Such an area is colored red in Fig. 27.

Table 16: Connection-aware robot operation

Connectivity State	non critical area	critical area
Connected	normal operation	cautious operation
Disconnected	cautious operation	stop operation, reconnect

Thereby, the figure not only contains the components but also shows the process of alarm dissemination: first, the alarm is transmitted from a sensor to the fire alarm controller. Second, the alarm controller informs clients like operators and the RTAD system. Third, the RTAD system forwards the alarms to all APs. The APs broadcast the alarm. Fourth, the alarm is disseminated by network flooding with each client forwarding the message

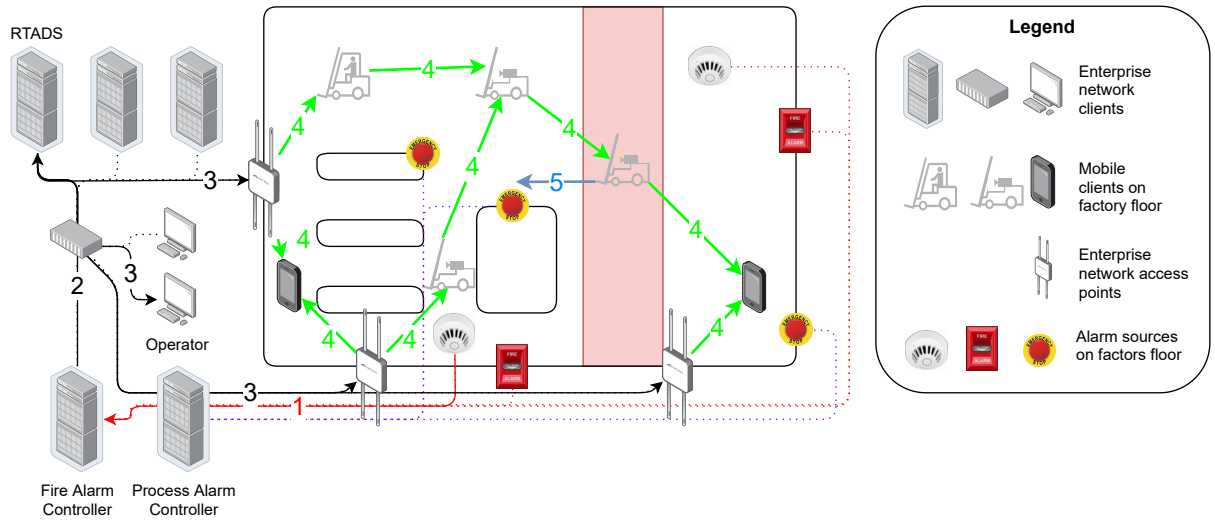

Figure 27: Concept of the RTAD system

once. Thereby, each client sends the alarm only once. Fifth, the clients perform their reactions.

Thereby, the combination of the clients knowledge about its locations and the knowledge about alarm and connection state from the RTAD enables a new reactive behavior. The behavior of mobile robots is depicted in Tab. 16 [203] and the RTAD systems enables the knowledge in the table. So, when using the RTAD system a node is always aware of its connection state. This is necessary as this protocol is designed to perform well in dynamic industrial environments where a wireless real time connection cannot be guaranteed. Thus, the classification of connected / not connected is needed because safety relevant communication has to know if it is able to receive alarms and if an alarm is present.

To do so, the RTAD system uses Flooding-based Network Monitoring (FBNM) [202]. Within this system the messages intended to monitor connection states can be replaced by alarm messages. The system works by flooding the network, as the name suggests starting at the APs. Underlying is the assumption that messages following each other have similar delays and probabilities to get lost. In RTAD slots are defined and within each slot a message must be received or the node is defined as disconnected. Thus, within each slot a message has to be sent and a slot must be shorter or equal to the detection time of an error.

The overall process with two robots establishing and losing connection is illustrated in Fig. 28. Thereby, the robot states indicate an available connection by color based on received messages. If a message is received within a time slot the robot is connected (color green) and if no message is received it is marked as disconnected (color red). Thereby, the clocks of the clients and the alarm source do not need to be synchronized.

If the frequency of sending messages is set higher than the slot duration requires it, short term connection losses can be compensated by receiving a test message per slot

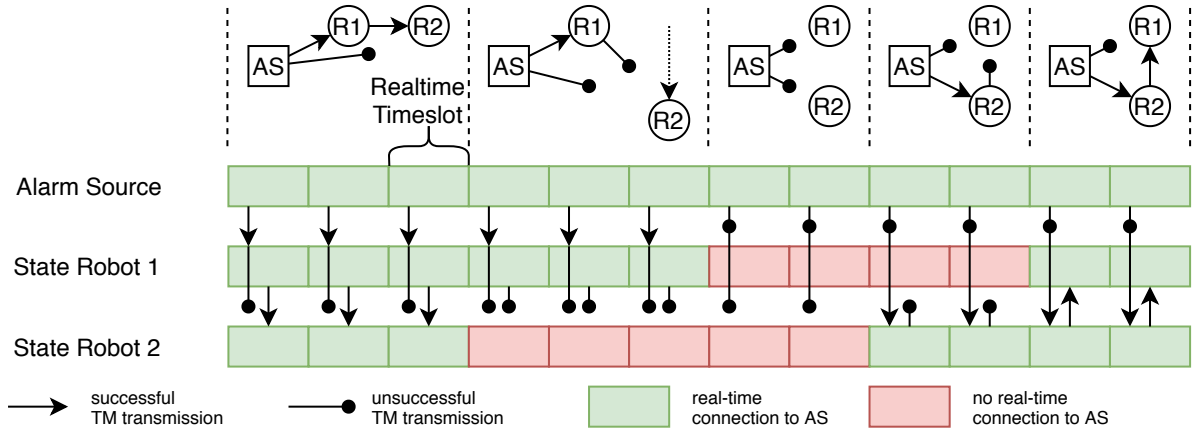

Figure 28: Process of the RTAD system and two robots using it

although one message is lost. This reduces the number of disconnections on the cost of more network traffic.

A KPI of MANETs is the complexity. The complexity is used to compare solutions for MANETs. Thereby, the complexity is based on the number of clients and the change of number of messages and the size of those messages. So, let n be the number of nodes in the network. As each node in the RTAD system forwards the alarm once the complexity for the number of messages is $\mathcal{O}(n)$. These messages only contain the information if an alarm is present if no alarm is present the message size is constant. Thus, the message size complexity is $\mathcal{O}(1)$ [203]. So, this opens the questions which system as well can provide a complexity of $\mathcal{O}(1)$ by means of message size and $\mathcal{O}(n)$ for the number of messages as the RTAD system does.

By means of complexity our solution outperforms APR, Liao01, Liao02, Lin-Liu, OP-MP, QMPR and TBD [44] (abbreviations in the reference). By means of complexity the algorithms Forward Algorithm (FA), ad-hoc QoS on demand routing (AQOR) and Chen-Heinzelman protocol (CHEN) [44] provide equal performance. Thereby, the two approaches FA and CHEN [64] have the same disadvantage. Both are not designed for high mobility scenarios and thus are not comparable to our solution and not suitable for the use case of AGVs. AQOR has two other specialties. The nodes are state-full as it discovers routes and AQOR is designed for bi-directional communication [240].

So, the RTAD system is unique with its properties of being designed for high mobility scenarios, having optimal complexity, being stateless and focusing on one way communication.

Furthermore, the RTAD system was implemented and tested in an active production facility. The implementation is based on a single board computer employing an IEEE 802.11 b/g/n network in ad-hoc mode. The clients are mounted to active intra-logistics AGVs. The $2.4\,\mathrm{GHz}$ band is used. Some of the nodes used additional Low Range Communication (LRC) (VLC) that has a higher reliability, lower throughput and similar la-

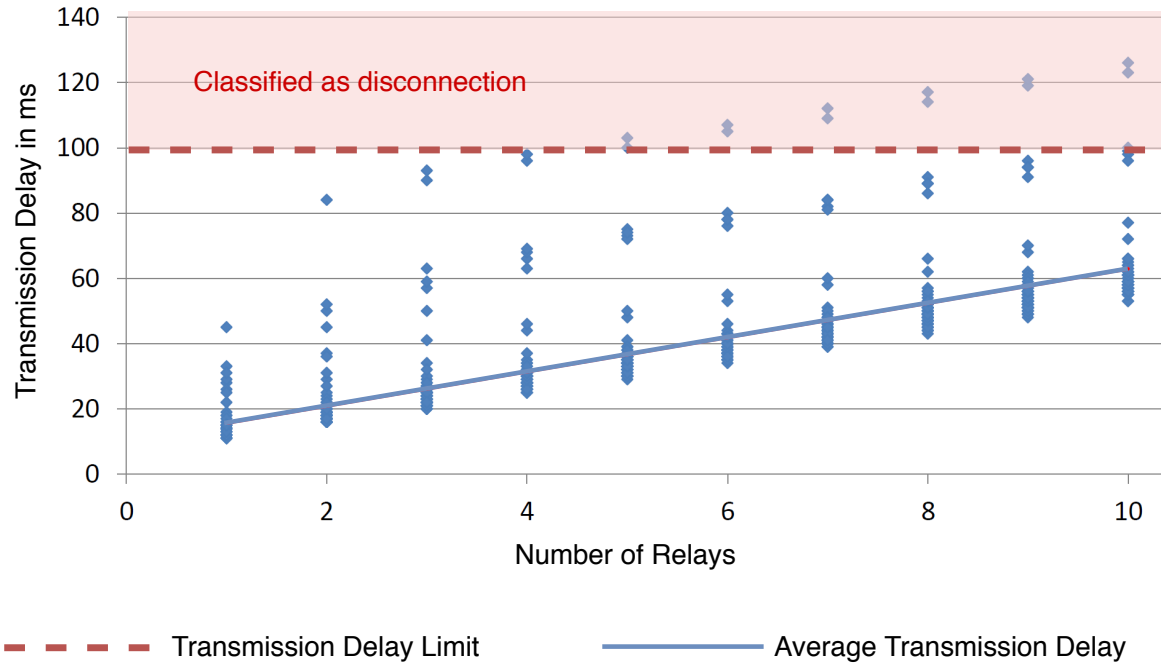

Figure 29: Delay per hop in FBNM or the RTAD system [203]

tency as WLAN and the nodes were able to switch between both communication technologies. As it was needed to measure one way latencies the nodes were time synchronized by Network Time Protocol (NTP). The quality of the synchronization was $\pm 2\,\mathrm{ms}$. During the tests a time limit of $100\,\mathrm{ms}$ was set to experience a disconnection and stop forwarding messages that are older than that limit.
Within that test $99.2\,\%$ of all message were received within the $100\,\mathrm{ms}$ limit after ten hops. The overall performance is depicted in Fig. 29 showing the latencies and a linear regression of the latencies. The figure clearly illustrates that there is a linear relation between the number of hops and latency. Thus, the slot length of the RTAD system should be chosen in accordance to the number of hops that is expected. Based on the data of Fig. 29 with linear regression Eq. 40 was derived:

$$\Delta t = 5.24n + 10.5 \tag{40}$$

with Δt being the expected latency and n as the number of hops. The figure also shows that up to four hops are tolerable for a sufficient performance.
As well, the RTAD approach is robust against the commonly known problem of congesting the network by flooding because only one node can initiate the flooding and each further node only forwards the information once. The additional traffic introduced by the RTAD system with a frequency from $1\,\mathrm{Hz}$ to $10\,\mathrm{Hz}$ is between $180\,\mathrm{Byte/s}$ and $1.8\,\mathrm{kB/s}$. So, in conclusion the RTAD is a viable solution to overcome the typical problem of disseminating critical real-time information independent from infrastructure. The system

is based on a flooding scheme and as real-time cannot be guaranteed the clients are aware of their connection status.

5.2 Optimizing wireless network coverage using MANETs with AGV mobility control

This section proposes an AGV mobility control method to improve the connectedness of AGV fleets on the factory floor. As mobile systems need connectivity on the factory floor to function properly, an improvement of the number of AGVs being properly connected to the wireless network improves the system performance of the AGV fleet [200].

This mobility control method here expands previous work by adaptively placing AGVs on the factory floor [119] while adhering to the restrictions that are found in factory environments. Therefore, the following research questions need to be examined:

Can a MANET be used to improve the connectivity of an AGV fleet and does this improve the transport performance of the fleet. So, inherently to this the correlation of connectivity and transport performance must be examined. Further, we evaluate whether AGV mobility can be controlled in a manner that improves connectivity. Thereby, learning the coverage of the deployed network, choosing the position of AGVs that are part of the MANET and the choice of AGVs to participate in the MANET are discussed. Lastly, we elaborate on how to answer the previous questions generically. This means that we overcome the dependence on a single or a few factory floors in our examinations.

This chapter is based on a simulation. The rest of this section is structured by describing the use case the simulation is based on and the simulation parameters. Afterwards, the algorithm for choice of AGV and position of that AGV to participate in the MANET is described and than the simulation outcomes are illustrated. The use case the simulation is based on AGVs performing transportation tasks in industrial environments. The communication and control of the AGVs is based on the VDA5050 [228] interface. The VDA5050 standard employs a central fleet control and cyclic communication between each AGV and the controller. The AGVs send status messages and the controller sends control messages towards the AGVs.

The performance of the fleet is measured in tasks per hour per AGV $T/h/AGV$. The connectedness of the fleet is the percentage of AGVs connected to the controller. The basic simulation parameters are the AGV movement, the signal attenuation and the network infrastructure. Out of the parameters, the AGV movement in the simulation is based on the findings from [200, 199] and thus is partly based on section 3.2 that uses [199]. So, the AGVs drive on predefined paths and task points are positioned along those paths. AGVs only move while having an active order. Furthermore, the signal attenuation is modeled using the multi-wall model that includes shadowing and attenuation. This model proved to be applicable for indoor and industrial scenarios in [65, 62, 59]. The network infrastructure as a part of the simulation set up consists of a wired network and APs that constitute the wireless network together with the wireless clients. The APs are placed in dependence of the simulation scenario.

The AGVs that are used for relaying cannot be positioned freely. Placing an AGV to work as a relay is only possible at a parking point. Parking points are present where two closely collocated task positions can be found. So, the AGV can park at a position where it does not block the execution of the task of another AGV.

Table 17: Table of subsequently used parameters

Parameter	Value	Unit	Description
A	$7000 < A < 150000$	m^2	Factory floor size
r_S	$0.33 < r_S < 3$		Ratio of x and y length of the factory
D_g	$7 < D_g < 20$	m	Distance of paths in navigation graph
P_{nd}	$10 < P_{nd} < 30$	$\%$	Irregularity percentage of navigation graph
P_{TP}	100	$\%$	Number of task points added
d_{TP}	2	m	Distance of task points to original graph
d_{TPmin}	5	m	Minimal edge length to add task points
d_{minP}	5	m	Max. distance of task to be parking point
P_{AGV}	50	$\%$	Number of AGVs in relation to task points
n_o	$10 < n_o < 100$		Number of obstacles
S_o	$1 < S_o < 10$	m	Size of obstacles
P_{AP}	75	$\%$	Number of APs as ratio to number of AGVs

Two factory scenarios are simulated. A static one and a dynamic one. In the static case the factory floor and the signal attenuating objects are static for the simulation time and the coverage provided by the APs is non-complete. In the second, dynamic scenario, the simulation starts with complete coverage provided by the APs. After some time into the simulation the environment changes, so some APs cease operation and some signal attenuating objects are moved. This results in incomplete coverage by the APs.
To overcome the problem of being scenario specific we employ so called procedural simulation. This means that the simulation generates over 300 factory floors for each scenario. Based on this general insights can be gained. The same challenges are faced by [35] and they employ procedural generation as well. So, the overall process of the simulation is to firstly generate factory floors and afterwards evaluate the performance of different network solutions on those factory floors.
The process of generating the factory environments is depicted by the following pseudo-code:

```
Generate factory floor space
Generate AGV navigation graph
   Generate basic manhattan graph
   Erode regular grid
   Place task points
   Define parking points
Place AGVs
Place obstacles
Place access points
```

The whole process is based on a random seed. This seed is used for any randomized decision. This enables to recreate each simulation by using the same seed. The actions

performed in the pseudo code are described in more detail in the following: for generating the factory floor the floor size A is chosen as well as the ratio of the length of its sides. The ratio is $r_s = \frac{L_x}{L_y}$. Size and ratio are chosen randomly.

Generating the navigation graph consists of four sub set ups. Firstly, generating a Manhattan grid with the distance D_g between the paths of the grid. Factories typically have a non perfect Manhattan grid. Thus, a percentage P_{nd} of the nodes in the Manhattan grid is deleted and task points are placed along some of the edges. The ratio is described by the percentage P_{TP}. Closely collocated task points are defined to be parking points as well. This is based on the assumption that the task can be fulfilled from both closely collocated positions.

Figure 30: Legend to factory examples [204]

AGVs are placed on P_{AGV} % of the task and parking points. Signal attenuating objects are then place without intersecting with the navigation graph. The size and the position of the objects is random. Lastly, the APs are placed. The placement of the APs is dependent on the scenario. In the static scenario only $N_{AP} = P_{AP} \cdot N_{AGV}$ are placed, so the coverage is non-complete. For the dynamic scenario the APs are placed in a Manhattan grid guaranteeing complete coverage. The complete set of the parameter can be found in Tab. 17.

All parameters are chosen from experience from actual factories and if available from their descriptions in [199] and the application examined therein. The navigation graph is based on the experiences from the application in [199] that is as well described in Sec. 3.2. Furthermore, the behavior of the simulation was validated against the findings from [200] that is used in Sec. 3.2.2.

The generated factories are added to a custom simulation tool that is presented in [200] and is able to simulate wireless communication according to IEEE 802.11 b/g/n. The overall simulation tool is published at [99].

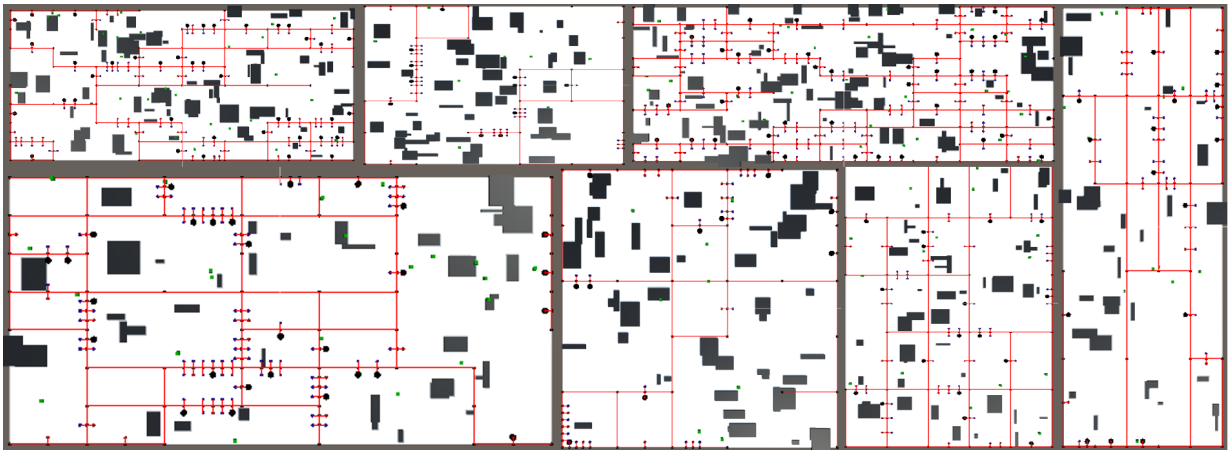

Figure 31: Seven examples of procedurally generated factories [204]. Legend see Fig. 30

With the factory models that are now available, a first general examination on the question whether a MANET improves the connectivity of the AGVs is performed. With the same simulation it is examined if an improved connectivity leads to an improved transport performance. As the communication is based on the VDA5050 standard, the AGVs notify the fleet controller of their status periodically. The periodicity in the simulation is $3\,\mathrm{s}$ and an AGV is accounted disconnected if two consecutive status message are missing at the fleet controller. The connectedness of AGVs is evaluated from the perspective of the controller.
Results based on $\approx 10\,000\,\mathrm{h}$ of simulation in ≈ 380 factories provide two insights:

- the ad-hoc network improves the connectedness
- A higher connectedness improves the transport performance

Because ad-hoc networks proofed to enhance the performance of an AGV fleet, the basis to discuss the adaptive positioning of AGVs is set.
To further enhance the performance of the network the approach is to use the mobility of AGVs to improve the network coverage and thereby, also improve the AGV fleet performance. This approach is called adaptive networking. The adaptive network positions AGVs actively to function as relaying nodes. For this approach three steps are needed [204]:

1. Learning network coverage
2. Selecting relay positions
3. Selecting relaying AGVs

Learning the network coverage is mandatory to know when relay nodes are needed. The three steps are described in detail in the following:
Learning the network coverage can be performed by each AGV on its own or cooperatively. Those two solutions are compared now. Network coverage is not an absolute value but a probability. Thus, for each task position a probability to have network coverage is determined. Each time the position P is visited the counter N_P is incremented. If there is network coverage at P the counter N_{CP} is as well incremented. So, the probability of having a connection at that task position is determined by:

$$P_P = \frac{N_{CP}}{N_P} \tag{41}$$

This approach to learning the network coverage has the drawback of being limited to the observing AGV and thus a long time is needed to know the coverage of a whole factory.
The cooperative approach to learn the network coverage is decentralized and based on exchanging the learned data. Exchanging the data is based on each AGV broadcasting the counters N_P and N_{CP} via the ad-hoc network of a random position P at a given time interval. These two approaches are compared in Fig. 32.
Thereby, the difference in the time needed to learn the coverage of both approaches is evident. So, subsequently the decentralized cooperative learning approach is used. At the beginning, if the coverage at a task position is not known, the AGV requests a relay

AGV regardless of the actual coverage. The threshold to request relaying AGVs is set to $85\,\%$ for P_P.
Selecting the relay positions is also performed decentralized. In the scheme for choosing the relay position the AGV that needs relaying determines the target position for the relay AGV. The positions for the relaying AGV are limited to the parking positions P_{park} because those are the only positions where an AGV may remain for a prolonged time. From all parking positions a sub-set that connects the task position P_{TP} and the next AP at its position P_{AP} is chosen. For determining relay positions d_{max} defines the maximum distance between two AGVs that need to communicate. This includes the assumption that at any other shorter distance AGVs can communicate. All positions where AGVs need to be placed to guarantee coverage at the task position are called route subsequently. This collection of positions is called route because the AGVs positioned there span the network needed for coverage. The algorithm for finding the relay positions is described now beginning with calculations needed for that algorithm and the complete pseudo code subsequently. To determine the route the distances from all points $P_p \in P_{park}$ to the direct path are calculated by:

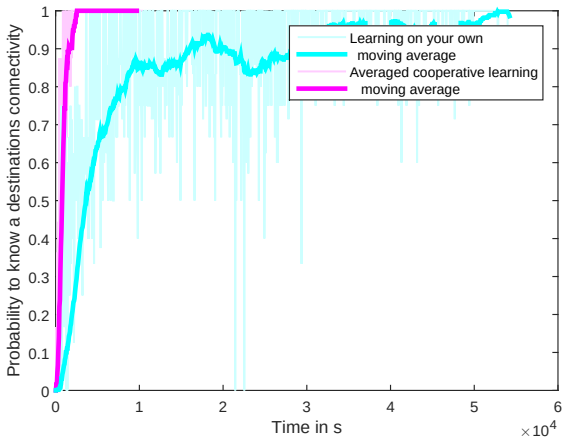

Figure 32: Comparison of learning coverage [204]

$$D_p = (|P_p - P_{AP}| + |P_p - P_{TD}|) - |P_{AP} - P_{TD}| \tag{42}$$

with $|p_1 - p_2|$ being the euclidean distance. Then all distances are sorted in ascending order [199]. The minimal length by means of relay AGVs can be determined by:

$$n_{min} = \left\lceil \frac{|P_{AP} - P_{TD}|}{d_{max}} \right\rceil \tag{43}$$

To be able to add extra AGVs for safety to the route the parameter s is defined and the length of the route then is $n_{min} + s$. The route search process starts with $s = 0$ and with the position with the smallest D_p. Four operations can be performed on a route:

- Sort: The positions of the route are sorted by their distance to P_{AP}
- Check: The distance of all positions of the route are checked to be smaller then d_{max}
- Expand: One position is added to the route, so $s + 1$
- Optimize: If a position p_i can be found with $|p_{i-1} - p_{i+1}| < d_{max}$ that position is removed

Using these operations the route finding algorithm is defined by the pseudo-code:

```
if(Check route):
   Optimize route
   Return route
else:
   if(n_min + s < |P_park|):
      Expand route
   else:
      Optimize route
      Check route?
      if(Check route):
         Return route
      else:
         No route found
```

Although it is possible that no route is found by this algorithm this case did not appear in $> 10^5$ cases on different factory floors. The probability of not finding a route remains an open question here and can be further examined in real industrial scenarios or a simulation focusing on that question.
Fig. 33 shows exemplary results of the algorithm in a simulated factory. After knowing the relay positions it is possible to select the AGVs that need to be placed at that positions. Selecting these AGVs is based on a decentralized auctioning scheme. The steps of that scheme are described in the following:

- The requesting AGV broadcasts the positions where relay AGVs are needed
- AGVs receiving that broadcast answer by broadcasting their state
- The requesting AGV chooses the relay AGVs
- The relay AGVs drive to their parking positions

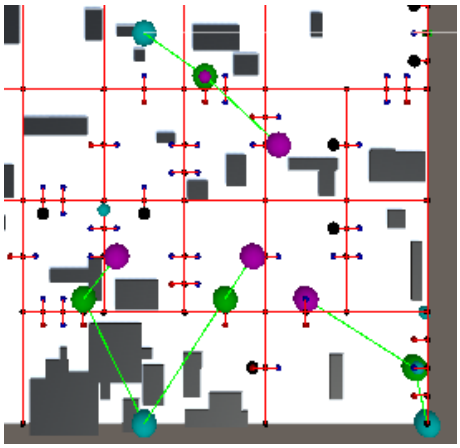

Figure 33: Relay routes in a simulated factory [204]

Depending on the exact scenario the choice on the relaying AGVs can be based on different parameter sets. AGVs that already have a task cannot be chosen. Other parameters can be the battery state, the availability of certain communication technologies on the AGV or its current position. The availability of communication technologies is based on the assumption that future AGVs will employ several communication technologies.
The coverage optimization is tested in the two previously described scenarios. The static scenario with non-complete network coverage and the dynamic scenario that starts with complete network coverage but experiences environment changes and failing APs after half the simulation time.
We expect the following outcome: the adaptive network outperforms the ad-hoc net-

work that outperforms the staic scenario. In the dynamic scenario the three networks (non ad-hoc, ad-hoc and adaptive) should perform identically for the first half and afterwards the performance should drift apart. The best performance should be provided by the adaptive network.
The joint behavior of the parameters fleet performance and connectedness over time are illustrated in Fig. 34. The figure shows the close relation of network connectedness and AGV fleet performance. This is especially highlighted by the second half of the figure for the ad-hoc network.
The adaptive network solution comes at a cost. AGVs that are used for relaying cannot fulfill transport tasks. Typical AGV fleets are oversized and thus no over utilization of AGVs for relaying occurred [204, 199]. Using the AGVs instead of additional network installation has the advantage of being robust against changes.
To evaluate the static scenario 360 different factories were generated. Within those factories the three network types non-ad-hoc, ad-hoc and adaptive are simulated. Fig. 35 shows the PDFs of the simulation results.

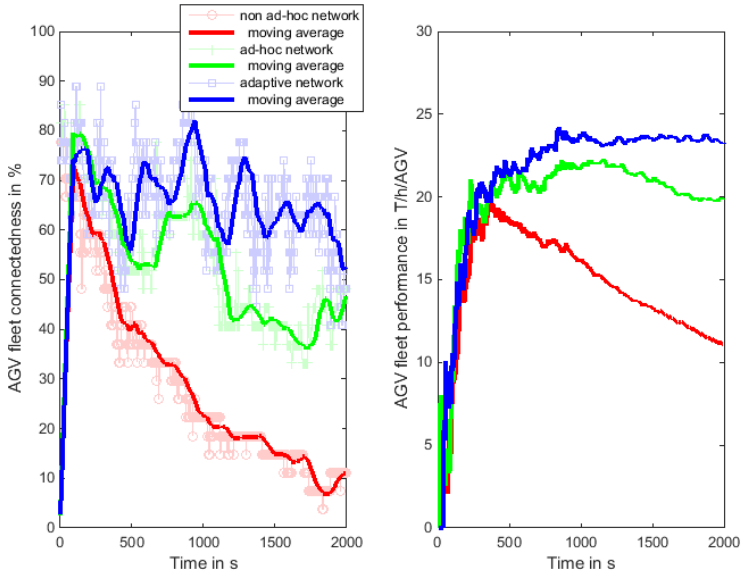

Figure 34: Connectedness and Performance over time for the three network types [204]

All three network types reach all connectedness values between $0\,\%$ and $100\,\%$. Thereby, for the highest values of the connectedness the adaptive network has the highest probabilities while the non-ad-hoc network has the highest probabilities for the lowest connectedness. So, these results are in line with the expectations and illustrate the advantages of the adaptive network by means of connected nodes.
For an AGV fleet the transport performance is the more important parameter. The difference in the transport performance is not as clear as in the connectedness. The mean value of the transport performance of the non ad-hoc network is $16.89\,\mathrm{T/h/AGV}$. The ad-hoc network has a mean value of $17.35\,\mathrm{T/h/AGV}$ and the adaptive network is at $18.69\,\mathrm{T/h/AGV}$. The distributions of all mean values of the ad-hoc and non ad-hoc network were constructed by Moving Block Bootstrapping (MBB) to evaluate whether the small difference of the values is significant and the distributions only have a minimal overlap.

Conclusively, it can be said that the adaptive network improves AGV fleet performances in environments with incomplete coverage.

The dynamic scenario is designed to recreate modern, changing factories. Those factories are planned with coverage in mind, but due to changes and faults in the network areas, without coverage can emerge. Thus, the simulation starts with complete network coverage and after 1500 s some APs stop working and some signal attenuating objects are moved.

380 factories were simulated in the dynamic scenario. Each factory is simulated for 3000 s.

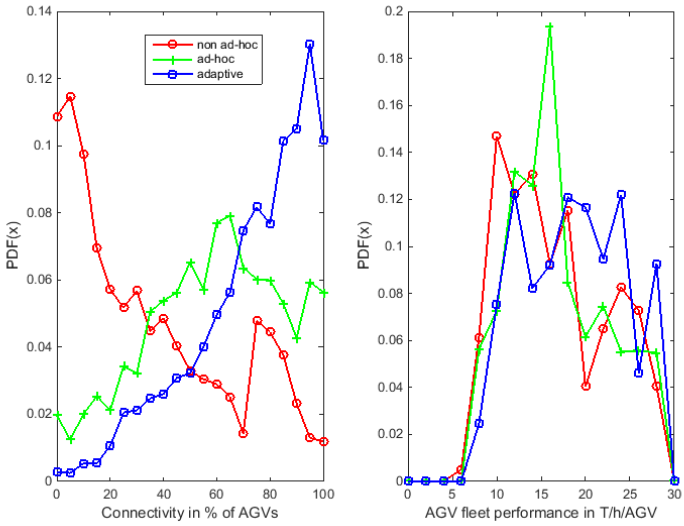

Figure 35: PDFs of connectedness and performance for the three network types [204]

In this scenario the focus is on the key parameter AGV fleet performance. In Fig. 37 the transport performance over time is shown. Thereby, the first plot shows the sliding median of all three network types over time. The next three plots show the median and the range of values for each network type.

The networks behave identically for the first 1500 s because the coverage is complete during that time. After the changes in the environment the performance differs significantly. The non ad-hoc network is affected most intensely by the changes and loss of coverage. In the time from 1500 s to about 1750 s the ad-hoc and the adaptive network perform still identically. This is the time period that the adaptive network needs to learn the network coverage. After the adaptive network has learned the coverage it outperforms the ad-hoc network solution.

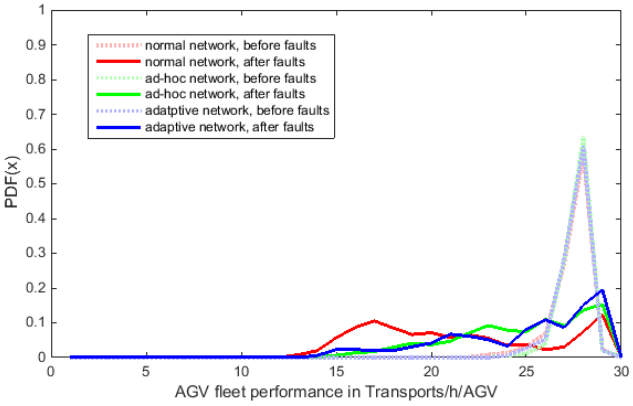

Figure 36: PDFs of AGV fleet performance [204]

For further comparison two PDFs of each network can be employed. Fig. 36 contains two kinds of PDFs. The PDFs of the transport performance for the time interval from

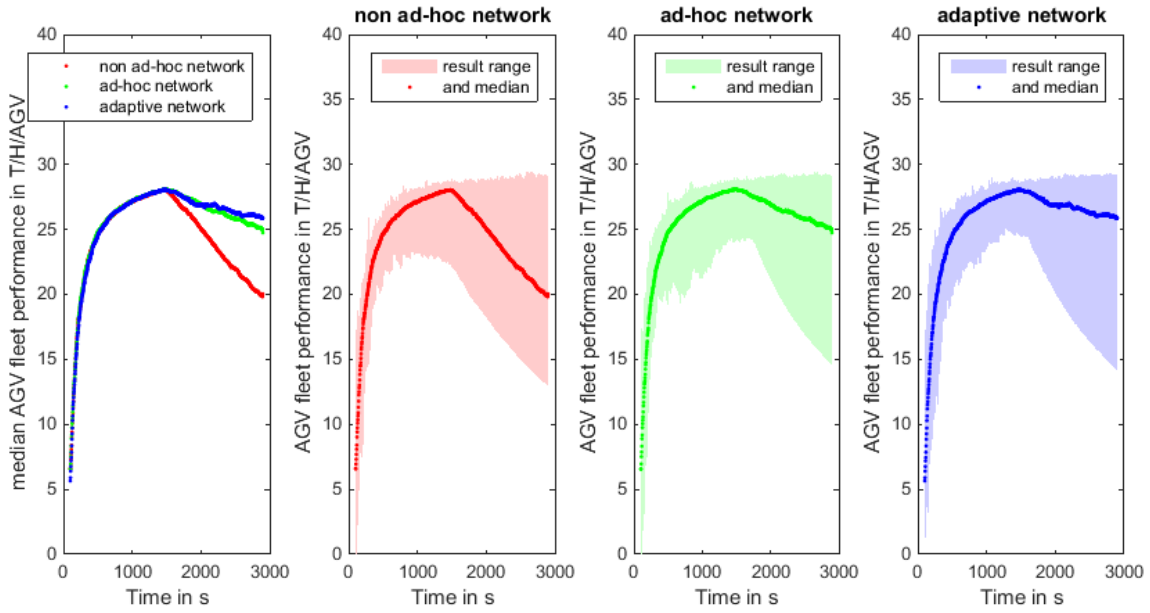

Figure 37: Change of performance over time [204]. Legend see Fig. 30

Table 18: Performance of networks in dynamic environment

Network type	Pre-Change performance in $T/h/AGV$	Post-change performance in $T/h/AGV$	Change
Non ad-hoc	27.67	20.52	$-25.8\,\%$
Ad-hoc	27.73	25.41	$-8.6\,\%$
Adaptive	27.68	25.93	$-6.3\,\%$

$1000\,\mathrm{s}$ to $1500\,\mathrm{s}$ in the light colored dashed lines and the PDFs for the time interval from $2500\,\mathrm{s}$ to $3000\,\mathrm{s}$. The PDFs confirm that during the first time period the networks behave identical. Secondly, the difference after the changes in the environment and the learning period of the adaptive network is illustrated. The overall performance of the networks as illustrated by the PDFs provides the same impression as the performance over time. Tab. 18 contains the median values. The table shows the clear differences between the networking approach with significant differences between the networks. The primary expectation is met by the values of the table by the adaptive network outperforming the ad-hoc network that outperforms the non ad-hoc network.
So, in this section we showed that the usage of MANETs improves the connectivity of AGV fleets. If an adaptive networking approach is chosen the performance is further improved. Thereby, adaptive networking is robust against changes in its environment. The connectivity of an AGV fleet is directly related and thus the adaptive networking approach proofed to improve AGV fleet performance.

5.3 Black channel optimization by employing channel state information

On the factory floor there is an increasing need for reliable wireless communication, more specific for safe communication. Typically, the black channel paradigm is used in such cases [82]. At the same time 5G gains more interest from the industrial community and thus the combination of black channels over 5G is discussed [156]. Black channel protocols use cyclic messages to keep track of the connection state. Those messages are exchanged on the application layer and will further be called *keep-alive messages*, as their only intend is to observe if the communication channel is still available.

The core idea of this section is to eliminate those keep-alive messages on the application layer by employing the information from the Channel State Information (CSI) process of the 5G network [155]. The CSI process is part of the 5G Control Plane (CP) and provides information on the quality of a channel in a cellular network. The information from the CSI process is always present to the UE and the network itself [17]. So, this information must be made available to the application, in this case a black channel. The bandwidth usage can be reduced by eliminating the keep-alive messages on the application layer.

As not only black channel protocols use keep-alive messages but as well other critical communication of non-safe applications the approach presented here is equally applicable for those cases. Both are similar in the fact that the connection between a mobile device using a wireless network and a server must be monitored. The rest of this section is structured by providing a more detailed problem statement, describing the solution in detail and evaluating the bandwidth reduction.

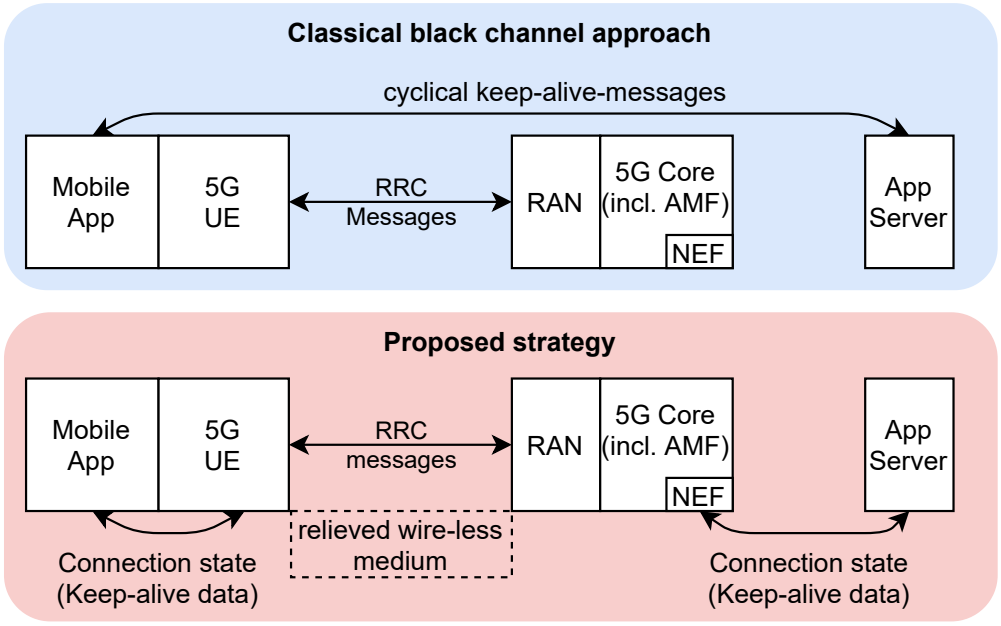

Figure 38: Comparison of the classical and the new communication architecture [155]

Fig. 38 depicts the communication architecture of a standard black channel in the top blue part of the figure and the newly proposed solution is in the bottom red half. The key difference between both approaches is the path the keep alive messages travel. In the first case they travel the whole way between App Server and Mobile App. In the second case no keep alive messages are sent via the wireless medium.

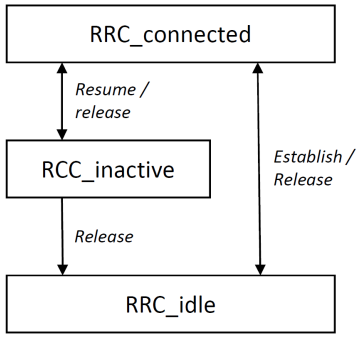

Figure 39: RRC states and state changes in 5G [17]

Cellular networks are divided into CP and User Plane (UP) whereas the UP is responsible for transmitting user data and enforcing the policies therefore. The CP is responsible for the network managing functions like authentication, mobility management, resource allocation and so on. So, the CP sets up the resources of the UP that are needed for communication.
Further, part of the CP is the RRC state. An UE in a 5G network can have three different RRC states, as there are connected, inactive and idle [17]. Gathering channel quality information is located in the CP within the CSI process [17]. This process takes place without regards to the UP communication. Thus, the CQI is always present.
State changes in the RRC are only possible with signaling on the CP. For dropping out of the RRC connected state a timer for inactivity is set. So, after a certain time of inactivity UEs drop out of RRC connected. In industrial scenarios the timer should be configured in a way so UEs are always RRC connected.
To enable our approach the 5G CP needs to be enhanced, as the proposed functionality is not intended originally. Only cyclic messages inside the core network and on the other wired networks remain. An overview is provided in Fig. 40. The figure shows the overall process of establishing our approach to eliminate the keep-alive messages on the air interface for the stationary and the mobile part of the application. In addition, it shows which parts of our approach are already part of the current standard and which are missing (gray background boxes in the figure are new steps).

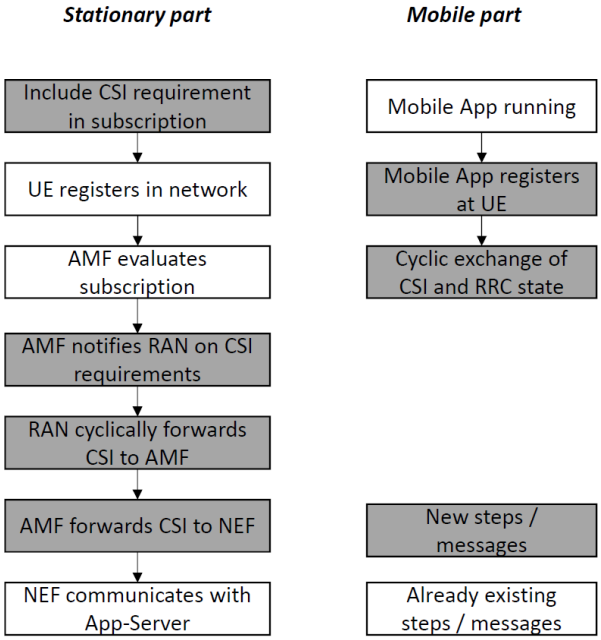

Figure 40: Process of establishing connection monitoring [155]

For the process of establishing the connection monitoring additional information is

needed. On the stationary side the core network needs to be informed which UEs need connection monitoring, so the forwarding mechanism to provide channel quality information to the NEF can be set up. The mechanism must be set up within the core and between core and application.
On the mobile side only the UEs and the mobile application need to communicate. In most industry applications the mobile application is running on a dedicated device. This is due to typical industry grade 5G UEs being dedicated devices without significant compute power. Thus, the UE and that device have to communicate. Thereby, all information are present in the UE anyway.
The CSI process takes place between UE and RAN and is of key importance to this approach. The CSI process exchanges different messages to determine the channel quality. The components of the 5G core that are involved are the RAN, AMF and the NEF [8]. Thereby, the NEF provides the Application Programming Interface (API) for the application server to interact with. So, our approach extends the state of the art by the following steps: the information the NEF provides based on the CSI process and the RRC state which is known to the RAN and forwards via the AMF towards the NEF. This enables to always provide connection quality information to the application server and if necessary to even filter them in the 5G network.
Within this three processes need a more detailed view:

- Registration of the UE
- Generating the cyclic messages
- CSI process itself

In our approach all devices send cyclic keep-alive messages regardless whether they employ safe or non-safe communication. Anyway, the process of registering an UE to the network and the RAN respectively needs to be extended. Although the CSI process takes place between every UE and the RAN the CSI information is not forwarded further. As this information is of interest to applications outside the network we propose that during the registration process of the UE the AMF extracts the subscription information from the UDM [8] and notifies the RAN on the necessity of forwarding connection state information. This enables the AMF and RAN to have knowledge on the UEs that need connection monitoring. This information needs to be included in the device subscription. Then, the RAN has to forward the connection information to the AMF. So, the RAN shares the connection information with the core network. As illustrated in the related work section and shown in Fig. 4 the RAN is only connected to the AMF in the CP of the core network [8]. This whole process is particularly easy in NPNs. In NPNs the owner of the network and the UE is the same entity making it easy to gain the knowledge on the UEs and their usage.
The generation of the cyclic messages in the core network takes place once the UE is registered. To do so, the RAN stores the connection information as a part of device context. So, the RAN creates N2 notifications (shown in Fig. 4) to inform the AMF on the connection state. Thereby, N2 notifications also include device identification.
Finally, we discuss the configuration and usage of the CSI process. The CSI process is part of the CP of the RAN and uses dedicated channels on the air interface. Thereby, the

carrier frequencies of UP and CP are closely collocated within the coherence bandwidth. We focus on the trigger states of the CSI process and the information that is transferred. The process can be event-triggered, semi-persistent or periodic [15, 9]. For avoiding the keep-alive messages a periodic report from the CSI process is needed. Two different reference signals for channel quality measurements can be used from network side in 5G. Those are the Synchronization Signal Block (SSB) and the CSI-Reference Signal (RS) and both can be configured to be periodically. The SSB has the smaller overhead while enabling sufficient channel measurements and thus is the choice for the reference signal. The periodicity is mostly configured on a frame base so in tens of ms but can configured in a granularity down to slots. Already a configuration of the periodicity in the dimension of frames is significantly faster compared to current works on black channels with cycle time of $150 - 250\,\mathrm{ms}$ [30, 194, 182, 104].
Within the whole CSI process the Channel Quality Indicator (CQI) is the key information that is needed. Based on the CQI the Modulation and Coding Scheme (MCS) is chosen defining how much information fits into the resources on the air interface. Together with the knowledge on how many resources are available the network can determine whether communication requirements can be fulfilled. Combined with the RRC state the NEF can provide all necessary information to the application.
At the mobile application the processes are simpler because today's industry grad UEs provide the information on channel quality already. Additionally, it must be clear which latency for providing this information they have and of which cycle times for providing that information they are capable of. The cycle time and the latency depend on the application using the black channel.
The gains of our approach by means of traffic reduction can be evaluated analytically. This is based on the cyclic messages that are avoided on the air interface. The cycle time of those messages is denoted as T. In addition, the size of the messages must be evaluated. As a reference the message size of the black channel protocol *SafetyNet p* is used. In that protocol each message has a header of $11\,\mathrm{byte}$ [60] in addition to the message content. The header consists of a process ID, length, session ID, consecutive number and a Cyclic Redundancy Check (CRC). Thus, the overall overhead of the cyclic messages introduced can be calculated by:

$$O = \frac{(11 + D) \cdot 2}{T} \tag{44}$$

with D being the size of the information contained in byte and O the overhead in $\mathrm{byte/s}$. The overhead introduced by the *safetyNet p* protocol is relatively low as it is not reliant on underlying protocol layers but only on Ethernet [60]. This is in contrast to other protocols that can be based on TCP, UDP or MQTT [104].
As an example we assume $T = 0.2\,\mathrm{s}$ and $D = 8\,\mathrm{byte}$ as this suits any one parameter closed-loop control. This leads to $190\,\mathrm{byte/s} = 1.52\,\mathrm{kbps}$ per black channel instance for keep-alive messages. Thereby, one device can have numerous black channel instances [30]. Several black channel instances can be available in case of an AGV where

the former example represents the safety stop and the next instance is the non-safe status updates. The frequency of such status updates is typically slower with $T = 0.5\,\mathrm{s}$ but contains more data [1]. This is due to the different information that describe an AGV status. So, $D = 50\,\mathrm{byte}$ can be assumed reasonably. The AGV example has an additional specialty: The example does not employ symmetric communication and for such cases Eq. 44 needs to be extended to:

$$O = \frac{(2 \cdot 11 + D_{\text{up}} + D_{\text{down}})}{T} \tag{45}$$

with D_{up} being the uplink data and D_{down} being the downlink data from the UE perspective. For calculating a complete scenario 800 devices are assumed on a $10\,000\,\mathrm{m}^2$ [154]. Further each device may have three black channel instances. As some keep-alive messages contain new information $25\,\%$ are assumed to be needed anyway. This is in line with [199] where only $12\,\%$ of all AGVs are moving and thus need to send status updates while all remaining communication are keep-alive messages. Setting the average message to $D = 11\,\mathrm{byte}$ and the protocol header still to $11\,\mathrm{byte}$ with $0.1\,\mathrm{s/msg}$ leads to an overall data rate of $1.65\,\frac{\mathrm{Mbyte}}{\mathrm{s}} = 13.2\,\mathrm{Mbps}$. This can be seen in the following equation:

$$0.75 \cdot (11 + 35)\frac{byte}{msg} \cdot \frac{1}{0.1\frac{s}{msg}} \cdot 2400 = 1.65\frac{Mbyte}{s} \tag{46}$$

Although the overall data rate is not that high a large number of small messages is avoided that could congest a network anyway.
Besides the pure elimination of keep-alive messages this approach offers another advantage: Significantly faster cycle times for monitoring the channel are possible. As already stated the CSI process can be configured down to slot size and thus in a granularity of $0.125\,\mathrm{ms}$. So, the frequency of the connection monitoring can be enhanced significantly compared to current solutions [182, 104]. Furthermore, the data rate reduction gets larger on a linear scale if the communication system is capable of faster cycle times for keep-alive messages.

5.4 Orchestrating redundant links by SDN - Using VLC and WLAN

This section discusses a communication solution that uses Software-Defined Networking (SDN) to orchestrate Visible Light Communication (VLC) and WLAN. Both communication technologies are assumed to be used by the same AGV at the same time [160]. Thereby, a clustering approach and global knowledge about the AGV tasks is employed by the SDN controller to enlarge route life spans. The combination of these two technologies has the advantage that they are orthogonal. Using communication clusters is an approach long known [42] and an overview on algorithms and strategies for clustering may be found in [243].
A suitable use case are AGVs cooperatively transporting goods. This means that at least two AGVs together carry one object and thus have to precisely keep their formation. Based on this formation communication clusters are formed using VLC for intra cluster

communication. The transport tasks are managed by an AGV fleet controller. Thus, the AGVs need to communicate their state and the controller the task. This use case is presented in the related work section 2.1.2. As the topic of control algorithms is out of scope of this section, details on this may be found in [110, 176].
The use case example of cooperative AGVs illustrates clearly the need for two different kinds of communications:

1. global high throughput communication
2. short range low latency high reliability communication

For the first variant WLAN is used, as per quasi industry standard and the second kind of communication is realized by VLC. For short range communication the choice of spectrum is of high importance [63] and visible light has the advantage of providing lots of bandwidth without interference from other communicating devices and high spatial re-use [160]. SDN is used for the decision which packet is sent over which interface employing knowledge on the AGV task. The SDN controller gains that knowledge from the Manufacturing Execution System (MES). This knowledge enables the formation of clusters based on tasks using VLC, which minimizes handovers and hence reduces latency.
So, the contributions of this section are twofold. Firstly, providing a solution to orchestrate redundant links in a network of different physical layers. Secondly, different communication architectures because VLC is an ad-hoc network. Further, all solutions are implemented to overcome the lack of quantitative and qualitative data from implementations of Software-Defined Wireless Sensor Network (SDWSN) [137]. In addition, the latency reductions achieved by employing the two communication technologies is based on the combination of the two technologies and their orchestration instead of the more often discussed topics like faster re-transmissions, grant-free uplink or improved scheduling [63].

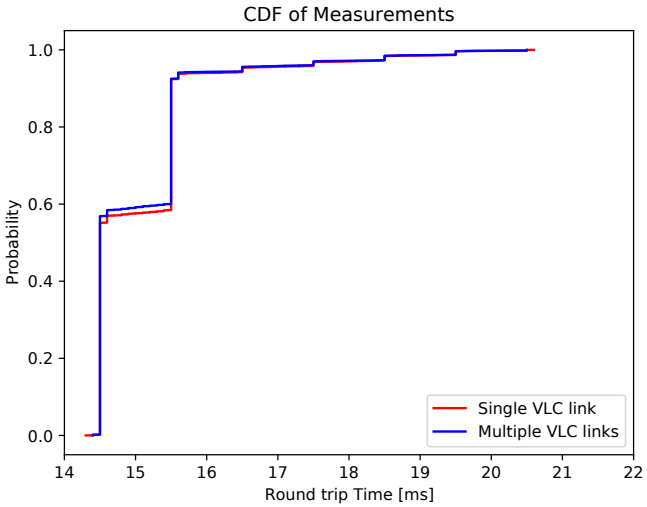

Figure 41: CDF of VLC with and without interference [160]

The VLC interfaces used here are a proprietary implementation by SEW-EURODRIVE GmbH & Co.KG with four LEDs for emitting signals and four independent receivers. The implementation is similar to other state of the art implementations [178] with a physical layer that focuses on robustness. A differential coding and an error correction scheme are used and enable the VLC modules to cope with dust, mud and other light sources. Each

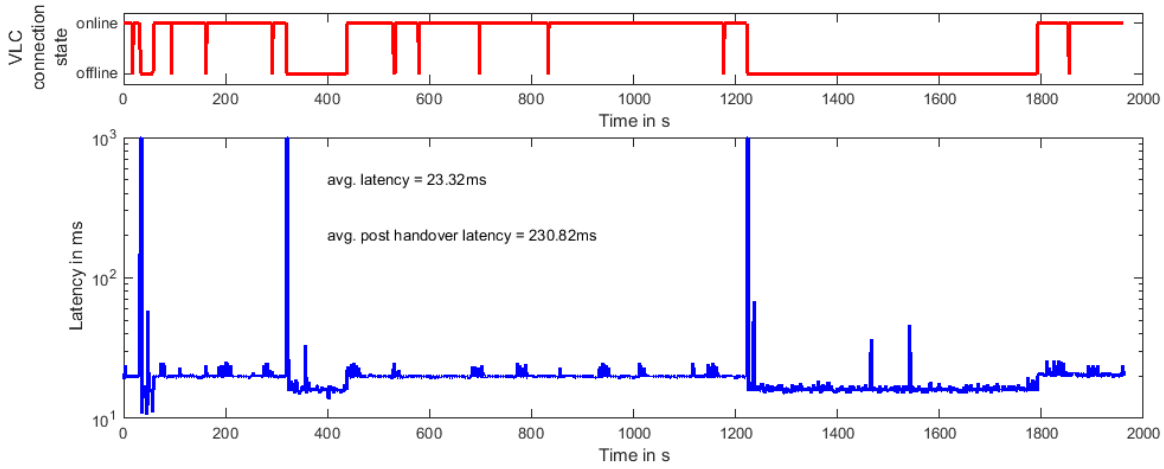

Figure 42: Handover behavior from VLC to WLAN [160]

module has an effective opening angle of $120\,^\circ$ and with each AGV having four modules $360\,^\circ$ of communication range are enabled. The maximum distance for communication is $\approx 5\,\mathrm{m}$.

Fig. 41 shows the CDF of the RTT of VLC connections with and without interference. For the interference measurement two closely collocated VLC links were used. The additional link in the multiple VLC links test performed maximum throughput to simulate high interference. The tests were performed using ping sending $4 \cdot 10^5$ with $32\,\mathrm{byte}$ payload at a $50\,\mathrm{ms}$ cycle. During the tests the VLC modules experienced slight relative movement to emulate real environments.

This test is of high importance to illustrate that communication clusters, that use VLC, perform as intended. And the two CDFs clearly illustrate this by their nearly identical behavior. $100\,\%$ of the packets arrive within a RTT of $21.5\,\mathrm{ms}$.

As VLC and WLAN are used the routing between those two orthogonal technologies must be examined. Handovers in this scenario happen in two dimensions: Within one technology, e.g. the change of the AP in WLAN, or changing which communication technology is used. The latter one is further examined in Fig. 42. The figure shows the RTT of packets sent while the used communication technology is changed due to blocking the VLC connection. Blocking the VLC connection is clearly visible by the latency peaks in the bottom part of Fig. 42. Thereby, it is obvious that each handover between VLC and WLAN introduces long latencies. The average RTT after a handover is $231\,\mathrm{ms}$ while during the remaining measurement the average RTT is $23.3\,\mathrm{ms}$.

This illustrates that two key question for the usage of VLC and WLAN in one client or AGV arise:

1. How to design routing rules?
2. How to distribute those rules?

The design of the routing rules aims for reducing the number of handovers due to the previously examined handover behavior. To achieve this by clustering, the clusters are

based on active tasks.
We assume that defining the clusters based on active transport tasks significantly enhances the route life spans of the VLC connections. By doing this the AGVs executing a cooperative task communicate using VLC along each other and use WLAN only to communicate with nodes outside their cluster. To test the assumption that clustering based on active tasks enlarges route life spans, measurements on the factory floor between intra-logistic AGVs are performed. The used communication technology was WLAN in ad-hoc mode because no VLC on AGVs for testing was available. The results are compared to the duration of transport tasks. During a transport task a VLC connection is not interrupted. The communication routes are assumed to be stable during a cooperative task as the VLC did not lose any packets in our tests.
In Fig. 43 the route life spans are shown by two PDFs. Both PDFs are defined by:

$$PDF(x) = P(x - \delta x < M < x + \delta x) \tag{47}$$

The definition of the PDF is necessary here because the measurement results are in different dimensions. Thus, for readability in the results δx for the two data sets is set to different values. For the measurements of route life spans with current AGVs $\delta x = 1\,\mathrm{s}$ and for the transportation task representing the route life span in clustering $\delta x = 30\,\mathrm{s}$. Those values are chosen to suit the respective route life spans. Further, those adjusted values for δx are necessary to provide a readable graph in Fig. 43 [160].
The mean value for the route life spans are $5.7\,\mathrm{s}$ and $183\,\mathrm{s}$. This is based on measurements of routes using WLAN on the factory floor and task duration respectively. This clearly illustrates that in industrial scenarios clustering based on tasks is advantageous. Further, VLC is a suitable technology for the intra-cluster communication as between cooperating AGVs VLC connections are not interrupted. This result is relevant to SDWSNs because mobility is a key challenge for those networks [137] and can be overcome with VLC clusters.

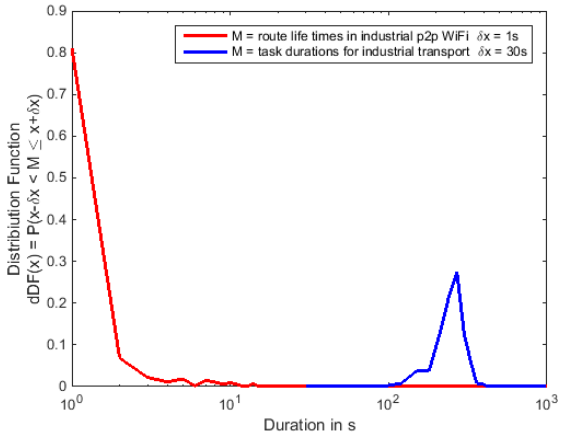

Figure 43: Comparison of route life spans [160]

The task based cluster comes with a drawback. The tasks and their participants are global knowledge on transportation tasks and AGV states. So, to enable task based clustering the entity defining the routing rules must have global knowledge. That knowledge includes the start and end times as well as the participants of a task.
The routing algorithm we propose minimizes the bandwidth usage in the WLAN while improving the KPIs latency and reliability of the communication inside the communication clusters. These clusters are identical to groups of AGVs performing cooperative

tasks. SDN is used here to employ global knowledge about the production process and based on this defines the routing rules. The pseudo code of the algorithm is [160]:

```
receive task (participants, start_time)
if time = start_time
    foreach participant in participants
        foreach partner in participants
            if partner != participant
                generate flowtable_entry to partner
    send flowtable_entry_list to participant
```

There are different strategies to define and distribute routing rules. Our approach is bound to be centralized due to the knowledge it is based on. Thus, the network has to consist of a central SDN controller and an SDN switch in each node. Each node employs a WLAN and a VLC interface.

We implemented the algorithm at a centralized SDN controller as a proof-of-concept. Thereby, the SDN controller gains its information from the AGV fleet management and translates it into routing rules. These are then distributed to the SDN switches in the clients. On the client side the Click modular router is used [138] as a so called Click Switch. The Click modular router was missing some elements and those were implemented so it was enabled to function as an SDN switch.

The overall architecture is shown in Fig. 44.

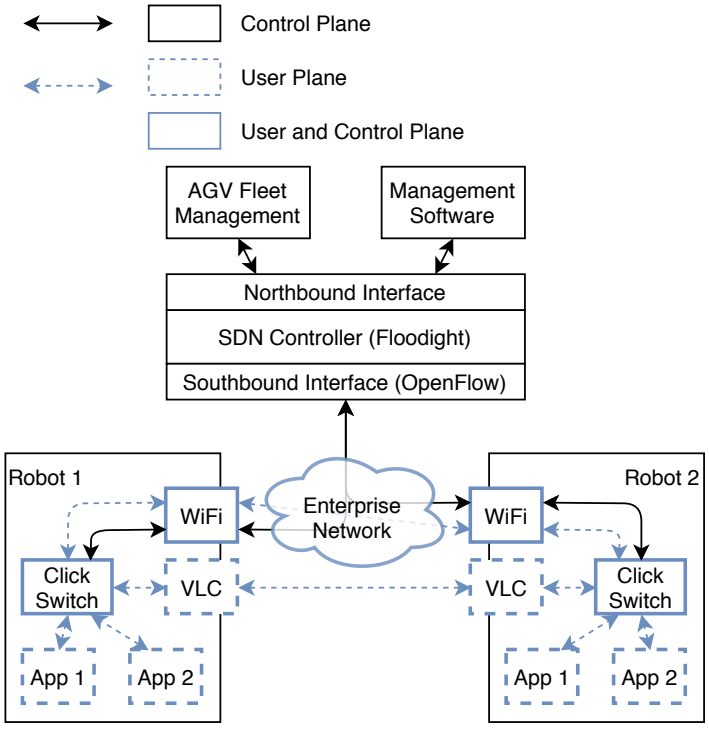

Figure 44: Architecture SDN clustering implementation [160]

The southbound interface of the controller uses OpenFlow version 1.4 and the controller software is Floodlight. The information from the AGV fleet management is communicated via the north bound interface.

When implementing this PoC some challenges arose. OpenFlow and Floodlight are based on standard switch behavior. This includes the instant forwarding of multi- and broadcast messages. In case of a redundant link formed by WLAN and VLC a network

loop is formed. To avoid this the software switches in the clients were configured such that no multicast and broadcast messages were transmitted via VLC. Additionally, the port types in OpenFlow do not support wireless links properly. At least the following information and actions are missing for a wireless port:

- data rate
- SNR
- Base stations available from client perspective
- Force client to perform handover

In this PoC implementation the missing port type could be worked around based on the high reliability of VLC. As this illustrates the need for further empirical evaluations, the source code of the Click-OpenFlow implementation is provided at [98].
In summary of this section, we showed by a PoC implementation that the combination of two orthogonal wireless communication technologies can be orchestrated to gain a significant performance improvement by means of latency and reliability. Thereby, for the short-range high-reliability technology clustering the communication is of high importance. The clustering can be performed by using SDN to exploit global knowledge about cooperative AGV tasks.

6 Conclusion

There is an evident need on future factory floors for wireless URLLC and the state of the art technology stack is challenged to deliver that kind of communication [154, 84, 245, 19]. To develop networks towards wireless URLLC on all protocol layers enhancements are discussed and this thesis contributes to this from physical layer evaluations to protocol optimizations. In addition, empirical performance evaluations are presented.
As this thesis provides insights along the whole networking protocol stack based on different methods the conclusion has three focuses in three subsections. Firstly, a comparison of the empirical performance evaluations and the use cases from related work is provided. Secondly, a discussion on the remaining aspects of the thesis including the mobility aspects of network nodes, physical layer measurements and performance improvements on different protocols. Lastly, an outlook towards open and newly emerged research questions as well as 6G in general is provided.

6.1 Use cases and empirical evaluations

Today on the factory floor different mobile applications are already in place. Those applications amongst others are AGVs, mobile control panels without safety functions and video functions or connected tools. Mostly, these applications use WLAN.
The shifting towards more challenging use cases needs the performance of the cellular technologies, combinations of orthogonal technologies and further enhancements.
When looking at pLTE there is a homogeneous picture along several use cases. Remember that pLTE is able to provide a RTT of $< 40\,\mathrm{ms}$ at a reliability of $99\,\%$. The latency of pLTE nearly fulfills the requirements of numerous use cases including cooperative driving, mobile control panels without safety functions, massive wireless sensor networks and some of the lesser demanding cases from the family of flexible modular assembly area [157]. In all cases the reliability of pLTE is a significant challenge. Hence, the need for further improvements to get closer to fulfilling the requirements is evident.
For the use cases that can employ short range communication the clustering approach based on SDN, VLC and WLAN may be a solution. Large scale evaluations are an open question here although it works on the small scale. As previously stated in our test with interference VLC showed a worst case RTT of $21.5\,\mathrm{ms}$. Furthermore, we explained why no connection losses during cooperative tasks between AGVs happen. So, cooperative use cases with a latency requirement of $\approx 10\,\mathrm{ms}$ are possible and this meets the cooperative driving use case described in related work without drawbacks.
The measurements from the 5G NPN provide a different perspective. For the same RTT as pLTE the reliability is about two dimensions better and thus 5G is significantly closer to fulfilling the aforementioned requirements. More interestingly is the case of Packet Duplication (PD) mimicked by two UEs or two sockets using one UE. Here a $25\,\mathrm{ms}$ RTT is realized with a reliability of $1 - 1.3 \cdot 10^{-5}$. Even taking into account the upper bound of the confidence interval this reliability remains at $1 - 1.48 \cdot 10^{-5}$. With that reliability value there is a cellular technology that nearly matches the requirements of all use cases in the dimension of $10\,\mathrm{ms}$ latency and a reliability of $1 - 10^{-5}$. This includes

mobile control panels without safety functions, cooperative driving for AGVs as well as several use cases from the use case family of flexible modular assembly area. All this is showing that the further evolving wireless communication technologies are on the path of fulfilling communication requirements for the factory of the future.
So, the empirical results and performance enhancements in this work depict that the path towards modern use cases with wireless URLLC is set.

6.2 Discussion

Modeling lower network layers is essential for simulation based evaluations from different perspectives. To support the data basis and modeling of the physical layer extensive measurements were performed. In addition, a model optimization is proposed [159, 158]. With the currently available data the physical layer on the factory floor seems to be extremely scenario specific [159, 158, 207] and thus any further data is relevant. By providing over 6000 PDPs and the analysis thereof, this work significantly contributes to the evaluation of propagation conditions in industrial environments. The research question on describing and classifying the scenarios in relation to their propagation environments remains open.
Of course, modeling the physical layer in detail is not always a suitable approach [200]. More light-weight approaches are preferable sometimes and one light-weight approach are Nodal Encounter Pattern (NEP). Network traces can be used to extract NEPs but this has some drawbacks. Hence, a method to record and analyze NEPs is provided as well as the raw data from the NEPs [200].
So, besides the raw data, we provide new insights in the behavior of mobile nodes on the factory floor. In cases where the NEPs are insufficient, a model for AGV mobility on the factory floor is presented as well [199]. As the same challenge of the scenario dependence as for the physical layer seems present on this layer an approach to overcome this in simulations is presented in Section 5.2 and in [204]. The simulation is available at [99].
Descriptions and modeling as well as performance improvements are provided. Ad-hoc network coverage optimization and alarm dissemination are discussed and illustrate the viability of ad-hoc networks on the factory floor.
The combination of ad hoc networks and infrastructure based networks can not only be used for coverage optimization but as well as for improving latency and reliability. Section 5.4 illustrates this by orchestrating the use of VLC and WLAN [160]. The PoC implementation illustrates the viability of the approach and contributes to overcome the lack of implementation in the field of SDWSNs [137].
For cellular networks a protocol improvement for black channels is developed that reduces the bandwidth usage on the air interface and at the same time enables channel monitoring at a higher frequencies [155]. Based on the usage of information from the Channel State Information (CSI) process monitoring frequencies down to the dimension of slots ($0.125\,\mathrm{ms}$) in 5G is possible. This is particularity useful for use cases that incooperate cooperation between robots and humans. Such an approach must be standardized

to find its way into applications on the factory floor. With the advances of cellular NPNs there is a reasonable chance to find this optimization in future applications.
So, overall this thesis provides several worthwhile contributions by providing raw data, modeling characteristics off or on the factory floor as well as improved algorithms under the umbrella of wireless URLLC for factory environments.

6.3 Outlook

With the trends of industry 4.0 and digitization continuing on the factory floor aiming toward the ever changing factory new research questions evolve. Additionally, 6G emerges on research road maps. Besides this, empirical evaluations remain open for wireless URLLC on the factory floor in general as well as for 5G on its path towards B5G and 6G.
5G and its performance evaluations still fall short on evaluating the range of configurations the standard enables, especially adjusting BLER, TTI, HARQ process the distribution of slots in the TDD scheme. The usage of 5G thereby experiences in Germany the challenge of being restricted to a TDD frequency for industrial usage [56].
On the track toward 6G two key topics for the factory of the future need attention: the network of networks and overcoming best-effort IP [220]. This contrasts 6G aiming for further improving latency, reliability and throughput. With the rising number of different network technologies employed on the factory floor [154, 160] the network of networks will be implemented.
Lesser obvious is the need to overcome best-effort IP. The air interface of any technology, on first sight, has to behave statistically because of the underlying medium. Anyway, in the rest of this network the statistical behavior should be minimized. Whether the trend of Time-Sensitive Networking (TSN) will just continue or complete new protocols and architecture will emerge, remains open. Industrial applications in general have a high need for deterministic behavior and thus, networks with a tendency to fulfill this need are favorable but open for research.
The contributions of this thesis also opened up new research question: Although we showed that the orchestration of orthogonal wireless technologies is advantageous, a large scale evaluation in terms of the number of technologies and nodes is open. The same accounts for further automating the processes involved. The physical layer descriptions, although providing much data, made clear that the need for further measurements is high. This is required to provide models along the differently behaving scenarios on the factory floor. In addition, developing a new algorithm for the statistical analysis opens up further research questions: The precision of the confidence intervals was optimized but the number of measurements needed is still in the same dimension, thus further optimizations might be possible.
Finally, based on the ongoing track in evolving flexibility on the factory floor and the track toward 6G, further research questions emerge. This thesis provides contributions along several challenges around wireless URLLC on the factory floor.

References

[1] 3GPP. *TR22.804 Study on Communication for Automation in Vertical Domains (Release 16)*. 3GPP, 2018.

[2] 3GPP. *TR22.886 Study on enhacement of 3GPP Support for 5G V2X Services (Release 15)*. 3GPP, 2017.

[3] 3GPP. *TR38.802 Study on New Radio Access Technology Physical Layer Aspects (Release 15)*. 3GPP, 2017.

[4] 3GPP. *TR38.804 Study on New Radio Access Technology; Radio Interface Protocol Aspects (Release 14)*. 3GPP, 2017.

[5] 3GPP. *TR38.901; Study on channel model for frequencies from 0.5 to 100 GHz (Release 16)*. 3GPP, 2019.

[6] 3GPP. *TR38.912 Study on New Radio (NR) Access Technology (Release 14)*. 3GPP, 2017.

[7] 3GPP. *TR38.913 Study on Scenarios and Requirements for Next Generation Access Technologies (Release 15)*. 3GPP, 2018.

[8] 3GPP. *TS 23.501 System Architecture for the 5G System (Release 15)*. 3GPP, 2020.

[9] 3GPP. *TS 38.214 Physical layer procedures for data (Release 16)*. 3GPP, 2020.

[10] 3GPP. *TS36.213 Evolved Universal Terrestrial Radio Access (E-UTRA); Physical Layer Procedures (Release 15)*. 3GPP, 2018.

[11] 3GPP. *TS36.321 Evolved Universal Terrestrial Radio Access (E-UTRA); Medium Access Control Protocol Specification (Release 15)*. 3GPP, 2018.

[12] 3GPP. *TS38.202 NR; Services provided by the physical layer (Release 15)*. 3GPP, 2018.

[13] 3GPP. *TS38.211 NR; Physical channels and modulation (Release 15)*. 3GPP, 2018.

[14] 3GPP. *TS38.212 NR; Multiplexing and channel coding (Release 15)*. 3GPP, 2018.

[15] 3GPP. *TS38.300 NR; NR and NG-RAN Overall Description Stage 2 (Release 15)*. 3GPP, 2018.

[16] 3GPP. *TS38.321 NR; Medium Access Control Protocol Specification (Release 15)*. 3GPP, 2018.

[17] 3GPP. *TS38.331 Radio Resource Control (RRC) protocol spcification (Release 16)*. 3GPP, 2021.

[18] 3GPP. *TS38.401 NR-RAN; Architecture description (Release 15)*. 3GPP, 2018.

[19] 5G ACIA. *5G for Connected Industries and Automation*. Tech. rep. ZVEI - German Electrical and Electronic Manufacturers, 2018.

[20] 5GPPP. *5G and the Factories of the Future*. Tech. rep. 5GPPP, 2015.

[21] Ameer Ahmed Abbasi and Mohamed Younis. "A survey on clustering algorithms for wireless sensor networks". In: *Computer communications* (2007).

[22] Ayoub Abdellaoui, Jamal Elmhamdi, and Halim Berradi. "Multipoint Relay Selection based on Stability of Spatial Relation in Mobile Ad hoc Networks". In: *International Journal of Communication Networks and Information Security* (2018).

[23] A. Abdi et al. "On the estimation of the K parameter for the Rice fading distribution". In: *IEEE Communications Letters* (2001).

[24] Abdulaziz Abdulghaffar et al. "Modeling and evaluation of software defined networking based 5G core network architecture". In: *IEEE Access* (2021).

[25] E. I. Adegoke, E. Kampert, and M. D. Higgins. "Empirical Indoor Path Loss Models at 3.5GHz for 5G Communications Network Planning". In: *International Conference on UK-China Emerging Technologies (UCET)*. 2020.

[26] E. I. Adegoke et al. "Characterizing the Indoor Industrial Channel at 3.5GHz for 5G". In: *Wireless Days (WD)*. 2019.

[27] Khandakar Ahmed et al. "Software Defined Networks in Industrial Automation". In: *Journal of Sensor and Actuator Networks* (2018).

[28] L. Ahumada et al. "Measurement and characterization of the temporal behavior of fixed wireless links". In: *IEEE Transactions on Vehicular Technology* (2005).

[29] Y. Ai, M. Cheffena, and Q. Li. "Power delay profile analysis and modeling of industrial indoor channels". In: *9th European Conference on Antennas and Propagation (EuCAP)*. 2015.

[30] J. Åkerberg, F. Reichenbach, and M. Björkman. "Enabling safety-critical wireless communication using WirelessHART and PROFIsafe". In: *15th IEEE International Conference on Emerging Technologies and Factory Automation (ETFA)*. 2010.

[31] I. Aktas et al. "LTE evolution - Latency reduction and reliability enhancements for wireless industrial automation". In: *IEEE International Symposium on Personal, Indoor and Mobile Radio Communications (PIMRC)*. 2017.

[32] M. Alhammadi et al. "Large-Scale Empirical Model for a 2.4 GHz Wireless Network in an Outdoor Environment". In: *Advances in Science and Engineering Technology International Conferences (ASET)*. 2019.

[33] Mustafa S Aljumaily. "Routing Protocols Performance in Mobile Ad-Hoc Networks Using Millimeter Wave". In: *arXiv preprint arXiv:1808.03168* (2018).

[34] Xueli An et al. "6G Network Architecture Vision". In: *Joint European Conference on Networks and Communications 6G Summit (EuCNC/6G Summit)*. 2021.

[35] James Arnold and Rob Alexander. "Testing autonomous robot control software using procedural content generation". In: *International Conference on Computer Safety, Reliability, and Security*. Springer. 2013.

[36] R Varun Arvind et al. "Industrial automation using wireless sensor networks". In: *Indian Journal of Science and Technology* (2016).

[37] Tomonori Asano, Hiroyuki Unoki, and Hiroaki Higaki. "LBSR: Routing protocol for MANETs with unidirectional links". In: *18th International Conference on Advanced Information Networking and Applications, (AINA)*. IEEE. 2004.

[38] S. A. Ashraf et al. "Ultra-reliable and low-latency communication for wireless factory automation: From LTE to 5G". In: *21st IEEE International Conference on Emerging Technologies and Factory Automation (ETFA)*. 2016.

[39] K. Ayush and N. K. Agarwal. "Real time visual SLAM using cloud computing". In: *Fourth International Conference on Computing, Communications and Networking Technologies (ICCCNT)*. 2013.

[40] Fan Bai, Narayanan Sadagopan, and Ahmed Helmy. "The IMPORTANT framework for analyzing the Impact of Mobility on Performance Of RouTing protocols for Adhoc NeTworks". In: *Ad hoc networks* (2003).

[41] A. Balatsoukas-Stimming, P. Giard, and A. Burg. "Comparison of Polar Decoders with Existing Low-Density Parity-Check and Turbo Decoders". In: *IEEE Wireless Communications and Networking Conference Workshops (WCNCW)*. 2017.

[42] Stefano Basagni. "Distributed clustering for ad hoc networks". In: *Proceedings Fourth International Symposium on Parallel Architectures, Algorithms, and Networks (I-SPAN)*. IEEE. 1999.

[43] A. J. Bayes. "Statistical Techniques for Simulation Models". In: *Australian Computer Journal* (1970).

[44] Philipp Becker. *Qos routing protocols for mobile ad-hoc networks-a survey*. Tech. rep. Technische Universität Kaiserslautern - Fachbereich Informatik, 2007.

[45] P. Benavidez et al. "Cloud-based realtime robotic Visual SLAM". In: *Annual IEEE Systems Conference (SysCon)*. 2015.

[46] Laura Bernado et al. "Time- and Frequency-Varying K-Factor of Non-Stationary Vehicular Channels for Safety-Relevant Scenarios". In: *IEEE Transactions on Intelligent Transportation Systems* (2015).

[47] Andrew C Berry. "The accuracy of the Gaussian approximation to the sum of independent variates". In: *Transactions of the american mathematical society* (1941).

[48] Leonardo Betancur et al. "A statistical channel model for on body Area networks in Ultra Wide Band Communications". In: *2009 IEEE LatinCom*. 2009.

[49] Christian Bettstetter, Hannes Hartenstein, and Xavier Pérez-Costa. "Stochastic properties of the random waypoint mobility model". In: *Wireless networks* (2004).

[50] E. Bjoernson, E. G. Larsson, and T. L. Marzetta. "Massive MIMO: ten myths and one critical question". In: *IEEE Communications Magazine* (2016).

[51] J. Blanchet and H. Lam. "Rare event simulation techniques". In: *Proceedings of the Winter Simulation Conference (WSC)*. 2011.

[52] C. Bockelmann et al. “Massive machine-type communications in 5G: physical and MAC-layer solutions”. In: *IEEE Communications Magazine* (2016).

[53] D.G. Brennen. “Linear diversity combining techniques”. In: *Proceedings of the IRE*. 1959.

[54] L. Buccheri et al. “Hybrid retransmission scheme for QoS-defined 5G ultra-reliable low-latency communications”. In: *IEEE Wireless Communications and Networking Conference (WCNC)*. 2018.

[55] R. Bultitude. “Measurement, characterization and modeling of indoor 800/900 MHz radio channels for digital communications”. In: *IEEE Communications Magazine* (1987).

[56] Bundesnetzagentur. *Verwaltungsvorschrift zu 3.7-3.8 GHz*. 2021.

[57] F. Burkhardt et al. “QuaDRiGa: A MIMO channel model for land mobile satellite”. In: *The 8th European Conference on Antennas and Propagation (EuCAP)*. 2014.

[58] Richard Candell et al. “Industrial wireless systems: Radio propagation measurements”. In: (2017).

[59] A Lagar Cavilla et al. “Simplified simulation models for indoor MANET evaluation are not robust”. In: *First Annual IEEE Communications Society Conference on Sensor and Ad Hoc Communications and Networks (SECON)*. IEEE. 2004.

[60] G. Cena, M. Cereia, and A. Valenzano. “Security aspects of safety networks”. In: *16th IEEE International Conference on Emerging Technologies and Factory Automation (ETFA)*. 2011.

[61] M. Centenaro et al. “Comparison of Collision-Free and Contention-Based Radio Access Protocols for the Internet of Things”. In: *IEEE Transactions on Communications* (2017).

[62] H. Chen et al. “Ultra-Reliable Low Latency Cellular Networks: Use Cases, Challenges and Approaches”. In: *IEEE Communications Magazine* (2018).

[63] K. Chen et al. “Ultra-Low Latency Mobile Networking”. In: *IEEE Network* (2019).

[64] L. Chen and W. B. Heinzelman. “QoS-aware routing based on bandwidth estimation for mobile ad hoc networks”. In: *IEEE Journal on selected areas in communications* (2005).

[65] Y. Chen, L. Cheng, and L. Wang. “Prioritized resource reservation for reducing random access delay in 5G URLLC”. In: *IEEE 28th Annual International Symposium on Personal, Indoor, and Mobile Radio Communications (PIMRC)*. 2017.

[66] Chia-Chin Chong. “SV Parameter Extraction: General Guidelines”. In: *IEEE 15-04-0283-00-004a, Standardization Comitee IEEE P802.15* (2019).

[67] Chia-Chin Chong and Su Khiong Yong. “A generic statistical-based UWB channel model for high-rise apartments”. In: *IEEE Transactions on Antennas and Propagation* (2005).

[68] Mo-Yuen Chow and Yodyium Tipsuwan. “Network-based control systems: a tutorial”. In: *27th Annual conference of the IEEE Industrial Electronics Society (IECON)*. 2001.

[69] T. Chrysikos, C. Papadakos, and S. Kotsopoulos. “Wireless channel measurements and modeling for an office topology at 3.5 GHz”. In: *Wireless Telecommunications Symposium (WTS)*. 2015.

[70] T. Chrysikos et al. “Channel measurement and characterization for a complex industrial and office topology at 2.4 GHz”. In: *11th International Conference on Software, Knowledge, Information Management and Applications (SKIMA)*. 2017.

[71] T. Chrysikos et al. “Measurement-based characterization of the 3.5 GHz channel for 5G-enabled IoT at complex industrial and office topologies”. In: *Wireless Telecommunications Symposium (WTS)*. 2018.

[72] J. Chuang. “The Effects of Time Delay Spread on Portable Radio Communications Channels with Digital Modulation”. In: *IEEE Journal on Selected Areas in Communications* (1987).

[73] A. De Gante, M. Aslan, and A. Matrawy. “Smart wireless sensor network management based on software-defined networking”. In: *27th Biennial Symposium on Communications (QBSC)*. 2014.

[74] Wout Debaenst et al. “RMS Delay Spread vs. Coherence Bandwidth from 5G Indoor Radio Channel Measurements at 3.5 GHz Band”. In: *Sensors* (2020).

[75] S. Dietrich et al. “Performance indicators and use case analysis for wireless networks in factory automation”. In: *22nd IEEE Emerging technologies and factory automation (ETFA)*. 2017.

[76] NTT DOCOMO. *Technical Journal*. Tech. rep. NTT DOCOMO, 2018.

[77] L. Dong et al. “Introduction on IMT-2020 5G Trials in China”. In: *IEEE Journal on selected areas in communication (JSAC)* (2017).

[78] S. E. Elayoubi et al. “5G service requirements and operational use cases: Analysis and METIS II vision”. In: *European Conference on Networks and Communications (EuCNC)*. 2016.

[79] S. Eldessoki, D. Wieruch, and B. Holfeld. “Impact of Waveforms on Coexistence of Mixed Numerologies in 5G URLLC Networks”. In: *21th International ITG Workshop on Smart Antennas (WSA)*. 2017.

[80] N. Enneya, M. El Koutbi, and A. Berqia. “Enhancing AODV Performance based on Statistical Mobility Quantification”. In: *2nd International Conference on Information Communication Technologies*. 2006.

[81] Ericsson. “The Industry Impact of 5G”. In: (2018).

[82] D. Etz et al. “Simplifying functional safety communication in modular, heterogeneous production lines”. In: *14th IEEE International Workshop on Factory Communication Systems (WFCS)*. 2018.

[83] Kevin Fall. “A delay-tolerant network architecture for challenged internets”. In: *Proceedings of the conference on Applications, technologies, architectures, and protocols for computer communications*. ACM. 2003.

[84] A. Fellan et al. “Enabling Communication Technologies for Automated Unmanned Vehicles in Industry 4.0”. In: *International Conference on ICT confergence (ICTC)*. 2018.

[85] AGCO - FENDT et al. *5G im Maschinen- und Anlagenabu - Use Case Remoteanwendungen*. Tech. rep. VDMA - German association for mechanical and plant engineering, 2019.

[86] Frank HP Fitzek and Patrick Seeling. “Why we should not talk about 6g”. In: *arXiv preprint arXiv:2003.02079* (2020).

[87] B.H. Fleury. “An uncertainty relation for WSS processes and its application to WSSUS systems”. In: *IEEE Transactions on Communications* (1996).

[88] Russell Ford et al. “Provisioning low latency, resilient mobile edge clouds for 5G”. In: *IEEE Conference on Computer Communications Workshops (INFOCOM WORKSHOPS)*. IEEE. 2017.

[89] B. Fourestie and S. Renou. “On the enhancement of Monte Carlo 3G network modelling tools for QoS prediction”. In: *IEEE 61st Vehicular Technology Conference*. 2005.

[90] P. Gaj, J. Jasperneite, and M. Felser. “Computer Communication Within Industrial Distributed Environment—a Survey”. In: *IEEE Transactions on Industrial Informatics* (2013).

[91] K. Ganesan et al. “Poster: A TDM approach for latency reduction of ultra-reliable low-latency data in 5G”. In: *IEEE Vehicular Networking Conference (VNC)*. 2016.

[92] Jens Gebert and Andreas Wich. “Alternating Transmission of Packets in Dual Connectivity for Periodic Deterministic Communication Utilising Survival Time”. In: *European Conference on Networks and Communications (EuCNC)*. 2020.

[93] A. Gelberger, N. Yemini, and R. Giladi. “Performance Analysis of Software-Defined Networking (SDN)”. In: *IEEE 21st International Symposium on Modelling, Analysis and Simulation of Computer and Telecommunication Systems*. 2013.

[94] M. Gidlund, T. Lennvall, and J. Akerberg. “Will 5G become yet another wireless technology for industrial automation?” In: *IEEE International Conference on Industrial Technology (ICIT)*. 2017.

[95] M. Giordani et al. “Toward 6G Networks: Use Cases and Technologies”. In: *IEEE Communications Magazine* (2020).

[96] Silvia Giordano. “Mobile Ad Hoc Networks”. In: *Handbook of Wireless Networks and Mobile Computing*. USA: John Wiley & Sons, Inc., 2002.

[97] github.com/c17r?tab=repositories. *Measurement Data NEP*. 2020.

[98] github.com/ChrSau/click_SDN_Implementation.git. *Soure code*. 2021.

[99] github.com/ChrSau/Procedural_Simulation_Of_AGV_MANET.git. *Repository of simulation tool*. 2021.

[100] github.com/elycz/PDP_Meas. *Measurement Data*. 2021.

[101] Carmelita Görg and Friedrich Schreiber. "The RESTART/LRE method for rare event simulation". In: *Proceedings of the 28th conference on Winter simulation*. 1996.

[102] HAHN GROUP, SEW-EURODRIVE, and Fraunhofer IIS. *5G im Maschinen- und Anlagenabu - Use Case Human Machine Interface*. Tech. rep. VDMA - German association for mechanical and plant engineering, 2019.

[103] KION GROUP/STILL, SEW-EURODRIVE, and Fraunhofer IIS. *5G im Maschinen- und Anlagenabu - Use Case Ortung und Kommunikation in der Logistik*. Tech. rep. VDMA - German association for mechanical and plant engineering, 2019.

[104] Armin Hadziaganovic et al. "The performance of openSAFETY protocol via IEEE 802.11 wireless communication". In: *26th IEEE International Conference on Emerging Technologies and Factory Automation (ETFA)*. 2021.

[105] Peter Hall, Joel L Horowitz, and Bing-Yi Jing. "On blocking rules for the bootstrap with dependent data". In: *Biometrika* (1995).

[106] K. Hansen. "Security attack analysis of safety systems". In: *14th IEEE Conference on Emerging Technologies Factory Automation (ETFA)*. 2009.

[107] Lajos Hanzo and Rahim Tafazolli. "A survey of QoS routing solutions for mobile ad hoc networks". In: *IEEE Communications Surveys & Tutorials* (2007).

[108] R. He et al. "Channel measurements and modeling for 5G communication systems at 3.5 GHz band". In: *URSI Asia-Pacific Radio Science Conference (URSI AP-RASC)*. 2016.

[109] D. Henneke, L. Wisniewski, and J. Jasperneite. "Analysis of realizing a future industrial network by means of Software-Defined Networking (SDN)". In: *IEEE World Conference on Factory Communication Systems (WFCS)*. 2016.

[110] J. P. Hespanha, P. Naghshtabrizi, and Y. Xu. "A Survey of Recent Results in Networked Control Systems". In: *Proceedings of the IEEE* (2007).

[111] Peter Adam Hoeher. *Grundlagen der digitalen Informationsuebertragung*. Springer Fachmedien Wiesbaden, 2013.

[112] B. Holfeld et al. "Wireless Communication for Factory Automation: an opportunity for LTE and 5G systems". In: *IEEE Communications Magazine* (2016).

[113] Rui Hou et al. "A brief survey of optical wireless communication". In: *Proc. Australas. Symp. Parallel Distrib. Comput.(AusPDC 15)*. 2015.

[114] Wei-jen Hsu and Ahmed Helmy. "On Nodal Encounter Patterns in Wireless LAN Traces". In: *IEEE Transactions on Mobile Computing* (2010).

[115] *IEC 61784-3 Profiles for functional safe communications in industrial networks*. IEC.

[116] M. Iwabuchi et al. "5G Field Experimental Trials on URLLC Using New Frame Structure". In: *IEEE Globecom Workshops (GC Workshops)*. 2017.

[117] M. Iwabuchi et al. "Evaluation of Coverage and Mobility for URLLC via Outdoor Experimental Trials". In: *IEEE Vehicluar Technology Conference Spring (VTC Spring)*. 2018.

[118] S. Jaeckel et al. "Industrial Indoor Measurements from 2-6 GHz for the 3GPP-NR and QuaDRiGa Channel Model". In: *IEEE 90th Vehicular Technology Conference (VTC2019-Fall)*. 2019.

[119] Elnaz Alizadeh Jarchlo et al. "To mesh or not to mesh: flexible wireless indoor communication among mobile robots in industrial environments". In: *15th AdHoc-Now*. 2016.

[120] C. Jegourel, J. Wang, and J. Sun. "Importance Sampling of Interval Markov Chains". In: *48th Annual IEEE/IFIP International Conference on Dependable Systems and Networks (DSN)*. 2018.

[121] H. Ji et al. "Ultra-Reliable and Low-Latency Communications in 5G Downlink: Physical Layer Aspects". In: *IEEE Wireless Communications* (2018).

[122] N. A. Johansson et al. "Radio access for ultra-reliable and low-latency 5G communications". In: *IEEE International Conference on Communication Workshop (ICCW)*. 2015.

[123] David B Johnson, David A Maltz, Josh Broch, et al. "DSR: The dynamic source routing protocol for multi-hop wireless ad hoc networks". In: *Ad hoc networking* (2001).

[124] Philo Juang et al. "Energy-efficient computing for wildlife tracking: Design tradeoffs and early experiences with ZebraNet". In: *ACM SIGARCH Computer Architecture News* (2002).

[125] R. Jurdi, S. R. Khosravirad, and H. Viswanathan. "Variable-rate ultra-reliable and low-latency communication for industrial automation". In: *52nd Annual Conference on Information Sciences and Systems (CISS)*. 2018.

[126] H. Kahn and T. E. Harris. "Estimation of Particle Transmission by Random Sampling". In: *National Bureau of Standards applied mathematics series*. 1951.

[127] J. Karedal et al. "A Measurement-Based Statistical Model for Industrial Ultra-Wideband Channels". In: *IEEE Transactions on Wireless Communications* (2007).

[128] Johan Karedal et al. "Statistical analysis of the UWB channel in an industrial environment". In: *VTC*. 2004.

[129] B. Kehoe et al. "A Survey of Research on Cloud Robotics and Automation". In: *IEEE Transactions on Automation Science and Engineering* (2015).

[130] K. Khaled and L. Talbi. "Case study of radio coverage in complex indoor environments for 5G communications". In: *IEEE International Conference on Wireless for Space and Extreme Environments (WiSEE)*. 2019.

[131] Y. Khamayseh, O. M. Darwish, and S. A. Wedian. "MA-AODV: Mobility Aware Routing Protocols for Mobile Ad Hoc Networks". In: *Fourth International Conference on Systems and Networks Communications*. 2009.

[132] E. Khorov, A. Krasilov, and A. Malyshev. "Radio resource and traffic management for ultra-reliable low latency communications". In: *IEEE Wireless Communications and Networking Conference (WCNC)*. 2018.

[133] E. Khorov, A. Krasilov, and A. Malyshev. "Radio resource scheduling for low-latency communications in LTE and beyond". In: *IEEE/ACM 25th International Symposium on Quality of Service (IWQoS)*. 2017.

[134] Evgeny Khorov et al. "A Tutorial on IEEE 802.11ax High Efficiency WLANs". In: *IEEE Communications Surveys Tutorials* (2019).

[135] Burka Kizilkaya et al. "Age Of Control Process For Real-Time Wireless Control". In: *IEEE Annual International Symposium on Personal, Indoor, and Mobile Radio Communications (PIMRC)*. 2021.

[136] Snorre Kjesbu and Torkil Brunsvik. "Radiowave propagation in industrial environments". In: *26th Annual Conference of the IEEE Industrial Electronics Society (IECON)*. IEEE. 2000.

[137] H. I. Kobo, A. M. Abu-Mahfouz, and G. P. Hancke. "A Survey on Software-Defined Wireless Sensor Networks: Challenges and Design Requirements". In: *IEEE Access* (2017).

[138] Eddie Kohler et al. "The Click Modular Router". In: *ACM Trans. Comput. Syst.* (2000).

[139] Vinay Kolar et al. "Measurement and Analysis of Link Quality in Wireless Networks: An Application Perspective". In: *IEEE Conference on Computer Communications Workshops (INFOCOM)*. IEEE, 2010.

[140] D. Kong et al. "Ricean Factor Estimation and Performance Analysis". In: *International Forum on Computer Science-Technology and Applications*. 2009.

[141] J. O. Krah and A. Basic. "Lean and Fast Fieldbus based Safety Functionality for Drives in Automation". In: *International Exhibition and Conference for Power Electronics, Intelligent Motion, Renewable Energy and Energy Management (PCIM)*. 2018.

[142] Hans R. Kunsch. "The Jackknife and the Bootstrap for General Stationary Observations". In: *The Annals of Statistics* (1989).

[143] S. N. Lahiri. *Resampling Methods for Dependent Data*. Springer New York, 2003.

[144] Leslie Lamport. "Time, Clocks, and the Ordering of Events in a Distributed System". In: *Communications of the ACM* (1978).

[145] Trung-Kien Le, Umer Salim, and Florian Kaltenberger. "An Overview of Physical Layer Design for Ultra-Reliable Low-Latency Communications in 3GPP Releases 15, 16, and 17". In: *IEEE Access* (2021).

[146] J. Lianghai et al. "Applying Multiradio Access Technologies for Reliability Enhancement in Vehicle-to-Everything Communication". In: *IEEE Access* (2018).

[147] Q. Liao et al. "Resource Scheduling for Mixed Traffic Types with Scalable TTI in Dynamic TDD Systems". In: *IEEE Globecom Workshops (GC Workshops)*. 2016.

[148] J.P. Linnartz et al. "ELIoT: New Features in LiFi for Next-Generation IoT". In: *Joint European Conference on Networks and Communications 6G Summit (EuCNC/6G Summit)*. 2021.

[149] Regina Y Liu, Kesar Singh, et al. "Moving blocks jackknife and bootstrap capture weak dependence". In: *Exploring the limits of bootstrap* (1992).

[150] I. Lokshina. "Algorithms to accelerate rare event simulation with Markov chain modeling in wireless telecommunications networks". In: *Wireless Telecommunications Symposium (WTS)*. 2011.

[151] I. Lokshina, S. Oneonta, and E. Schiele. "Buffer overflow simulation in self-similar queuing networks with finite buffer capacity accelerated using RESTART/LRE". In: *Wireless Telecommunications Symposium (WTS)*. 2015.

[152] I. Lokshina, T. Wendt, and C. Lanting. "Accelerated buffer overflow simulation in self-similar queuing networks with long-range dependent processes and finite buffer capacity". In: *3rd International Symposium on Wireless Systems within the Conferences on Intelligent Data Acquisition and Advanced Computing Systems (IDAACS-SWS)*. 2016.

[153] M. C. Lucas-Estan et al. "An Experimental Evaluation of Redundancy in Industrial Wireless Communications". In: *23rd IEEE International Conference on Emerging Technologies and Factory Automation (ETFA)*. 2018.

[154] E. Lyczkowski et al. "Wireless Communication in Industrial Applications". In: *24th IEEE International Conference on Emerging Technologies and Factory Automation (ETFA)*. 2019.

[155] Eike Lyczkowski et al. "Avoiding keep-alive messages by exposing 5G channel state information to applications". In: *26th IEEE International Conference on Emerging Technologies and Factory Automation (ETFA)*. 2021.

[156] Eike Lyczkowski et al. "Performance of a 5G NPN in industry: statistical analysis and application to black channel protocols". In: *26th IEEE International Conference on Emerging Technologies and Factory Automation (ETFA)*. 2021.

[157] Eike Lyczkowski et al. "Performance of private LTE on the factory floor". In: *International Conference on Communications Workshops (ICC Workshops)*. 2020.

[158] Eike Lyczkowski et al. “Power decay behavior of the Saleh-Valenzuela model for industrial environments from 2 to 6 GHz”. In: *IEEE Wireless Communications and Networking Conference (WCNC)*. 2022.

[159] Eike Lyczkowski et al. “Power delay profile analysis of industrial channels at 2.1, 2.6, 3.8 and 5.1 GHz”. In: *IEEE Annual International Symposium on Personal, Indoor, and Mobile Radio Communications (PIMRC)*. 2021.

[160] Eike Lyczkowski et al. “SDN controlled visible light communication clusters for AGVs”. In: *European Conference on Networks and Communications (EuCNC)*. 2021.

[161] C. Mannweiler et al. “Cross-domain 5G network management for seamless industrial communications”. In: *IEEE IFIP Network Operations and Management Symposium (NOMS)*. 2016.

[162] John G Markoulidakis, George L Lyberopoulos, and Miltiades E Anagnostou. “Traffic model for third generation cellular mobile telecommunication systems”. In: *Wireless Networks* (1998).

[163] Marsch et al., eds. *5G system design architectural and functional considerations and long term research*. WILEY, 2018.

[164] Shuji Maruyama et al. “On location of relay facilities to improve connectivity of multihop wireless networks”. In: *The Joint Conference of the 10th Asia-Pacific Conference on Communications and the 5th International Symposium on Multi-Dimensional Mobile Communications Proceeding (APCC/MDMC)*. IEEE. 2004.

[165] Arjan Meijerink and Andreas F. Molisch. “On the Physical Interpretation of the Saleh–Valenzuela Model and the Definition of Its Power Delay Profiles”. In: *IEEE Transactions on Antennas and Propagation* (2014).

[166] Agon Memedi and Falko Dressler. “Vehicular Visible Light Communications: A Survey”. In: *IEEE Communications Surveys Tutorials* (2021).

[167] R. Molina-Masegosa and J. Gozalvez. “LTE-V for Sidelink 5G V2X Vehicular Communications: A New 5G Technology for Short-Range Vehicle-to-Everything Communications”. In: *IEEE Vehicular Technology Magazine* (2017).

[168] Andreas F Molisch et al. “A comprehensive model for ultrawideband propagation channels”. In: *IEEE Global Communication Conference (GLOBECOM)*.

[169] Sungwook Moon and Ahmed Helmy. “Understanding periodicity and regularity of nodal encounters in mobile networks: A spectral analysis”. In: *CoRR* (2010).

[170] N. Moraitis et al. “Delay spread measurements and characterization in a special propagation environment for PCS microcells”. In: *The 13th IEEE International Symposium on Personal, Indoor and Mobile Radio Communications (PIMRC)*. 2002.

[171] Norbert Th Müller. “An analysis of the LRE-Algorithm using Sojourn times.” In: *ESM*. Citeseer. 2000.

[172] H. A. Munz and J. Ansari. "An empirical study on using D2D relaying in 5G for factory automation". In: *IEEE Wireless Communications and Networking Conference Workshops (WCNCW)*. 2018.

[173] A. Neumann et al. "Towards integration of Industrial Ethernet with 5G mobile networks". In: *14th IEEE International Workshop on Factory Communication Systems (WFCS)*. 2018.

[174] Robert G. Newcombe. "Two-sided confidence intervals for the single proportion: comparison of seven methods". In: *Statistics in Medicine* (1998).

[175] NGMN. *NGMN 5G White Paper*. Tech. rep. NGMN, 2015.

[176] P. Park et al. "Wireless Network Design for Control Systems: A Survey". In: *IEEE Communications Surveys Tutorials* (2018).

[177] I. Parvez et al. "A Survey on Low Latency Towards 5G: RAN, Core Network and Caching Solutions". In: *IEEE Communications Surveys Tutorials* (2018).

[178] P. H. Pathak et al. "Visible Light Communication, Networking, and Sensing: A Survey, Potential and Challenges". In: *IEEE Communications Surveys Tutorials* (2015).

[179] K. I. Pedersen et al. "A flexible 5G frame structure design for frequency-division duplex cases". In: *IEEE Communications Magazine* (2016).

[180] K. I. Pedersen et al. "Punctured Scheduling for Critical Low Latency Data on a Shared Channel with Mobile Broadband". In: *IEEE 86th Vehicular Technology Conference (VTC-Fall)*. 2017.

[181] Charles Perkins, Elizabeth Belding-Royer, and Samir Das. *RFC3561: Ad hoc on-demand distance vector (AODV) routing*. 2003.

[182] Giovanni Peserico et al. "Wi-Fi based functional safety: an assessment of the fail safe over ethercat (FSoE) protocol". In: *26th IEEE International Conference on Emerging Technologies and Factory Automation (ETFA)*. 2021.

[183] G. Pocovi et al. "Achieving Ultra-Reliable Low-Latency Communications: Challenges and Envisioned System Enhancements". In: *IEEE Network* (2018).

[184] G. Pocovi et al. "MAC layer enhancements for ultra-reliable low-latency communications in cellular networks". In: *IEEE International Conference on Communications Workshops (ICC Workshops)*. 2017.

[185] Guillermo Pocovi et al. "Signal Quality Outage Analysis for Ultra-Reliable Communications in Cellular Networks". In: *IEEE Globecom Workshops (GC Wkshps)*. 2015.

[186] A. (Ed.) Pouttu. *6G White Paper on Validation and Trials for Verticals towards 2030's [White paper]*. Tech. rep. 2020.

[187] C. Preschern et al. “Software-Based Remote Attestation for Safety-Critical Systems”. In: *IEEE Sixth International Conference on Software Testing, Verification and Validation Workshops*. 2013.

[188] G Purushotham. “Mobile Relay arrangement in Wireless Sensor Networks”. In: *International Journal of Scientific Research in Computer Science, Engineering and Information Technology* (2018).

[189] Vu Khanh Quy et al. “Survey of Recent Routing Metrics and Protocols for Mobile Ad-Hoc Networks.” In: *J. Commun.* (2019).

[190] Barath Raghavan et al. “Software-defined internet architecture: decoupling architecture from infrastructure”. In: *Proceedings of the 11th ACM Workshop on Hot Topics in Networks*. 2012.

[191] J. Rao and S. Vrzic. “Packet duplication for URLLC in 5G dual connectivity architecture”. In: *IEEE Wireless Communications and Networking Conference (WCNC)*. 2018.

[192] J. Rao and S. Vrzic. “Packet Duplication for URLLC in 5G: Architectural Enhancements and Performance Analysis”. In: *IEEE Network* (2018).

[193] *Regelungstechnik 2*. Springer Berlin Heidelberg, 2008.

[194] M. Rentschler and P. Laukemann. “Towards a reliable parallel redundant WLAN black channel”. In: *9th IEEE International Workshop on Factory Communication Systems*. 2012.

[195] Justus Rischke et al. “5G Campus Networks: A First Measurement Study”. In: *IEEE Access* (2021).

[196] Gerado Rubino and Bruno Tuffin, eds. *Rare Event Simulation using Monte Carlo Methods*. John WIley & Sohns, 2009.

[197] A.A.M. Saleh and R. Valenzuela. “A Statistical Model for Indoor Multipath Propagation”. In: *IEEE Journal on Selected Areas in Communications* (1987).

[198] Malla Reddy Sama et al. “Why is Application Reliability an Issue for an Ultra-Reliable 6G Network?” In: *Joint European Conference on Networks and Communications 6G Summit (EuCNC/6G Summit)*. 2021.

[199] Christian Sauer, Eike Lyczkowski, and Marco Schmidt. “Mobility Models for the Industrial Peer-to-Peer Context Based on Empirical Investigation”. In: *IEEE Annual International Symposium on Personal, Indoor, and Mobile Radio Communications (PIMRC)*. 2021.

[200] Christian Sauer, Marco Schmidt, and Eike Lyczkowski. “On Ad Hoc Communication in Industrial Environments”. In: *Applied Sciences* (2020).

[201] Christian Sauer, Marco Schmidt, and Maja Sliskovic. “Advanced Models for the Simulation of AGV Communication in Industrial Environments: Model proposal and Demonstration”. In: *Proceedings of the 10th ACM Symposium on Design and Analysis of Intelligent Vehicular Networks and Applications*. 2020.

[202] Christian Sauer, Maja Sliskovic, and Marco Schmidt. “Flooding-Based Network Monitoring for Mobile Wireless Networks”. In: *International Conference on Communication and Network Protocol*. 2019.

[203] Christian Sauer et al. “Real-time Alarm Dissemination in Mobile Industrial Networks”. In: *In Proceedings of IEEE International Conference on Industrial Technology (ICIT)*. 2021.

[204] Christian Sauer et al. “Testing AGV Mobility Control Method for MANET Coverage Optimization using Procedural Generation”. In: *ACM 24th International Conference on Modeling, Analysis and Simulation of Wireless and Mobile Systems (MSWiM)*. 2021.

[205] S. Saur and M. Centenaro. “Radio Access Protocols with Multi-User Detection for URLLC in 5G”. In: *23th European Wireless Conference*. 2017.

[206] Hirokazu Sawada et al. “Impulse response model and parameters for indoor channel modeling at 60GHz”. In: *IEEE Vehicular Technology Conference (VTC)*. 2010.

[207] M. Schmieder et al. “Measurement and Characterization of an Indoor Industrial Environment at 3.7 and 28 GHz”. In: *14th European Conference on Antennas and Propagation (EuCAP)*. 2020.

[208] F Schreiber and C Gorg. “Stochastic simulation: A simplified LRE-algorithm for discrete random sequences”. In: *AEU-Archiv fuer Elektronik und Uebertragungstechnik - International Journal of Electonics and Communications* (1996).

[209] Friedrich Schreiber. “Effective control of simulation runs by a new evaluation algorithm for correlated random sequences”. In: *AEU. Archiv für Elektronik und T̈bertragungstechnik* (1988).

[210] Yozo Shoji et al. “A modified SV-model suitable for line-of-sight desktop usage of millimeter-wave WPAN systems”. In: *IEEE Transactions on Antennas and Propagation* (2009).

[211] SICK and Fraunhofer IIS. *5G im Maschinen- und Anlagenabu - Use Case Mobile Bedienpanels mit Nothalt*. Tech. rep. VDMA - German association for mechanical and plant engineering, 2019.

[212] B. Singh et al. “Contention-Based Access for Ultra-Reliable Low Latency Uplink Transmissions”. In: *IEEE Wireless Communications Letters* (2018).

[213] P. Skarin et al. “Towards Mission-Critical Control at the Edge and Over 5G”. In: *2018 IEEE EDGE*. 2018.

[214] B. Soret et al. “Fundamental tradeoffs among reliability, latency and throughput in cellular networks”. In: *IEEE Globecom Workshops (GC Workshops)*. 2014.

[215] Peter Sossalla et al. “Evaluating the Advantages of Remote SLAM on an Edge Cloud”. In: *26th IEEE International Conference on Emerging Technologies and Factory Automation (ETFA)*. 2021.

[216] A. I. Sulyman et al. “Directional Radio Propagation Path Loss Models for Millimeter-Wave Wireless Networks in the 28-, 60-, and 73-GHz Bands”. In: *IEEE Transactions on Wireless Communications* (2016).

[217] S. Sun et al. “Propagation Path Loss Models for 5G Urban Micro- and Macro-Cellular Scenarios”. In: *IEEE 83rd Vehicular Technology Conference (VTC Spring)*. 2016.

[218] Gordon J. Sutton et al. “Enabling Technologies for Ultra-Reliable and Low Latency Communications: From PHY and MAC Layer Perspectives”. In: *IEEE Communications Surveys and Tutorials* (2019).

[219] M. Sybis et al. “Channel Coding for Ultra-Reliable Low-Latency Communication in 5G Systems”. In: *IEEE 84th Vehicular Technology Conference (VTC-Fall)*. 2016.

[220] T. (Ed.) Taleb. *White paper on 6G networking [White paper] - 6G research visions, no. 6)*. Tech. rep. University of Oulu, 2020.

[221] E. Tanghe et al. “The industrial indoor channel: large-scale and temporal fading at 900, 2400, and 5200 MHz”. In: *IEEE Transactions on Wireless Communications* (2008).

[222] I. Tejado, B. M. Vinagre, and J. I. Suarez. “Effects of a communication network on the longitudinal and lateral control of an AGV”. In: *IEEE International Symposium on Industrial Electronics*. Only included in bib, to have a reference for the fact, that an AGV consists of the four fundamental components: vehicle, localization and guidance, communication and control system. 2008.

[223] C. Tepedelenlioglu, A. Abdi, and G.B. Giannakis. “The Ricean K factor: estimation and performance analysis”. In: *IEEE Transactions on Wireless Communications* (2003).

[224] Fabrice Theoleyre, Rabih Tout, and Fabrice Valois. “New metrics to evaluate mobility models properties”. In: *2nd International Symposium on Wireless Pervasive Computing*. IEEE. 2007.

[225] Yodyium Tipsuwan and Mo-Yuen Chow. “Control methodologies in networked control systems”. In: *Control Engineering Practice* (2003). Special Section on Control Methods for Telecommunication.

[226] David Tse and Pramod Viswanath. *Fundamentals of wireless communication*. Cambridge university press, 2005.

[227] George L Turin. “Communication through noisy, random-multipath channels”. PhD thesis. Massachusetts Institute of Technology, 1956.

[228] VDA and VDMA. *VDA5050 V1.1 AGV communication interface*. Tech. rep. VDA and VDMA, 2020.

[229] VDMA and Fraunhofer IIS. *5G im Maschinen- und Anlagenabu*. Tech. rep. VDMA - German association for mechanical and plant engineering, 2019.

[230] I. Veza, M. Mladineo, and N. Gjeldum. “Managing Innovative Production Network of Smart Factories”. In: *IFAC-PapersOnLine* (2015).

[231] Manuel Villen-Altamirano and Jose Villen-Altamirano. “RESTART: A method for accelerating rare event simulations”. In: (1991).

[232] Manuel Villen-Altamirano and Jose Villen-Altamirano. “RESTART: a straightforward method for fast simulation of rare events”. In: *Winter Simulation Conference*. 1995.

[233] José Villén-Altamirano. “RESTART vs Splitting: A comparative study”. In: *Performance Evaluation* (2018).

[234] C. Wang et al. “A Survey of 5G Channel Measurements and Models”. In: *IEEE Communications Surveys Tutorials* (2018).

[235] Jian Wang et al. “Spectral Efficiency Improvement with 5G Technologies: Results from Field Tests”. In: *IEEE Journal on Selected Areas in Communication (JSAC)* (2017).

[236] P. Wijesinghe, U. Gunawardana, and R. Liyanapathirana. “Combined Flat Histogram Monte Carlo Method for Efficient Simulation of Communication Systems”. In: *IEEE Communications Letters* (2012).

[237] M. Wollschlaeger, T. Sauter, and J. Jasperneite. “The Future of Industrial Communication: Automation Networks in the Era of the Internet of Things and Industry 4.0”. In: *IEEE Industrial Electronics Magazine* (2017).

[238] Ong Hwee Woon and Sivanand Krishnan. “Identification of clusters in UWB channel modeling”. In: *IEEE Vehicular Technology Conference*. IEEE. 2006.

[239] Z. Wu, F. Zhao, and X. Liu. “Signal space diversity aided dynamic multiplexing for eMBB and URLLC traffics”. In: *3rd IEEE International Conference on Computer and Communications (ICCC)*. 2017.

[240] Q. Xue and A. Ganz. “Ad hoc QoS on-demand routing (AQOR) in mobile ad hoc networks”. In: *Journal of parallel and distributed computing* (2003).

[241] Wei Yang et al. “Quasi-Static Multiple-Antenna Fading Channels at Finite Blocklength”. In: *IEEE Transactions on Information Theory* (2014).

[242] Jennifer Yick, Biswanath Mukherjee, and Dipak Ghosal. “Wireless sensor network survey”. In: *Computer networks* (2008).

[243] Jane Yang Yu and Peter Han Joo Chong. “A survey of clustering schemes for mobile ad hoc networks”. In: *IEEE Communications Surveys & Tutorials* (2005).

[244] M. Zhan et al. “Channel Coding for High Performance Wireless Control in Critical Applications: Survey and Analysis”. In: *IEEE Access* (2018).

[245] M. Zhang and K. Yu. “Wireless Communication Technologies in Automated Guided Vehicles: Survey and Analysis”. In: *Annual Conference of the IEEE Industrial Electronics Society (IECON)*. 2018.

[246] Anatolii Zolotukhin, Sergei Nagaev, and Vladimir Chebotarev. “On a bound of the absolute constant in the Berry–Esseen inequality for i.i.d. Bernoulli random variables”. In: *Modern Stochastics: Theory and Applications* (2018).